Synthesis of Zeolite Y using novel material and method for catalytic application

A Thesis submitted to Gujarat Technological University

For the award of

Doctor of Philosophy

in

Chemical Engineering

by

Dolly Rajnikant Gandhi

(Enrollment No: 159997105005)

Under the supervision of

Co-Supervisor
Dr. Rajib Bandyopadhyay

Supervisor
Dr. Bhavna Soni

GUJARAT TECHNOLOGICAL UNIVERSITY

AHMEDABAD

[OCTOBER 2022]

DECLARATION

I declare that the thesis entitled "Synthesis of Zeolite Y using novel material and method for catalytic application" submitted by me for the degree of Doctor of philosophy is the record of research work carried out by me during the period from June 2015 to October 2022 under the supervision of Dr. Bhavna Soni and Dr. Rajib Bandyopadhyay and this has not formed the basis for the award of any degree, diploma, associateship, fellowship, titles in this or any other University or other institution of higher learning.

I further declare that the material obtained from other sources has been duly acknowledged in the thesis. I shall be solely responsible for any plagiarism or other irregularities, if noticed in the thesis.

Signature of the Research Scholar: Date: 13/10/2022

Name of Research Scholar: Dolly Rajnikant Gandhi

Place: Ahmedabad.

CERTIFICATE

I certify that the work incorporated in the thesis "Synthesis of Zeolite Y using novel material and method for catalytic application" submitted by Ms. Dolly Rajnikant Gandhi was carried out by the candidate under my supervision/guidance. To the best of my knowledge: (i) the candidate has not submitted the same research work to any other institution for any degree/diploma, associateship, fellowship or other similar titles (ii) the thesis submitted is a record of original research work done by the Research Scholar during the period of study under my supervision, and (iii) the thesis represents independent research work on the part of the Research Scholar.

Signature of Co Supervisor: Date: 13/10/2022

Name of Supervisor: Dr. Rajib Bandyopadhyay

Place: Ahmedabad.

Signature of Supervisor: Date: 13/10/2022

Name of Supervisor: Dr. Bhavna Soni

Place: Ahmedabad.

Course-work Completion Certificate

This is to certify that Ms. Dolly Rajnikant Gandhi, Enrolment No. 159997105005 is a PhD scholar enrolled for PhD program in the branch Chemical Engineering of Gujarat Technological University, Ahmedabad.

(Please tick the relevant option(s))

☐ He has been exempted from the course-work (successfully completed during M.Phil Course)

☐ He has been exempted from Research Methodology Course only (successfully completed during M.Phil Course)

☑ She has successfully completed the PhD course work for the partial requirement for the award of PhD Degree. His/ Her performance in the course work is as follows:

Grade Obtained in Research Methodology	Grade Obtained in Self Study Course (Core Subject)
(PH001)	(PH002)
BC	AA

Co Supervisor's Sign

(Dr. Rajib Bandyopadhyay)

Supervisor's Sign

(Dr. Bhavna Soni)

Originality Report Certificate

It is certified that PhD Thesis titled "Synthesis of Zeolite Y using novel material and method for catalytic application" by Dolly Rajnikant Gandhi has been examined by us. We undertake the following:

a. Thesis has significant new work / knowledge as compared already published or is under consideration to be published elsewhere. No sentence, equation, diagram, table, paragraph or section has been copied verbatim from previous work unless it is placed under quotation marks and duly referenced.

b. The work presented is original and own work of the author (i.e. there is no plagiarism). No ideas, processes, results or words of others have been presented as author own work.

c. There is no fabrication of data or results which have been compiled / analysed.

d. There is no falsification by manipulating research materials, equipment or processes, or changing or omitting data or results such that the research is not accurately represented in the research record.

e. The thesis has been checked using https://www.urkund.com (copy of originality report attached) and found within limits as per GTU Plagiarism Policy and instructions issued from time to time (i.e. permitted similarity index <=10%).

Signature of the Research Scholar: Date: 13/10/2022

Name of Research Scholar: Dolly Rajnikant Gandhi

Place: Ahmedabad

Signature of Co Supervisor: Date: 13/10/2022

Name of Co Supervisor: Dr. Rajib Bandyopadhyay

Place: Ahmedabad

Signature of Supervisor: Date: 13/10/2022

Name of Supervisor: Dr. Bhavna Soni

Place: Ahmedabad

Copy of Originality Report

Curigional

Document Information

Analyzed document	Dolly Gandhi_ PhD Thesis.pdf (D132172606)
Submitted	2022-03-31T15:54:00.0000000
Submitted by	M M Sharma
Submitter email	mec01.owner@gtu.edu.in
Similarity	1%
Analysis address	mec.01.owner.gtu@analysis.urkund.com

Sources included in the report

W	URL: https://www.research.manchester.ac.uk/portal/files/54507037/FULL_TEXT.PDF Fetched: 2021-11-08T05:57:57.0930000	11
W	URL: https://www.researchgate.net/publication/322254674_Synthetic_zeolites_-_structure_clasification_current_trend_in_zeolite_synthesis_Review Fetched: 2021-09-21T13:36:32.9800000	2
W	URL: https://vndoc.com/al-h2so4-al2-so4-3-so2-h2o-237427 Fetched: 2022-01-09T10:41:13.8600000	1
W	URL: http://www.iosj.net/iosj/?func=fulltext&aid=102642 Fetched: 2022-03-31T15:54:00.0000000	1

PhD THESIS Non-Exclusive License to GUJARAT TECHNOLOGICAL UNIVERSITY

In consideration of being a Research Scholar at Gujarat Technological University, and in the interests of the facilitation of research at the University and elsewhere, I, (Dolly Rajnikant Gandhi) having (Enrollment No.) 159997105005 hereby grant a non-exclusive, royalty free and perpetual license to the University on the following terms:

a) The University is permitted to archive, reproduce and distribute my thesis, in whole or in part, and/or my abstract, in whole or in part (referred to collectively as the "Work") anywhere in the world, for non-commercial purposes, in all forms of media;

b) The University is permitted to authorize, sub-lease, sub-contract or procure any of the acts mentioned in paragraph (a);

c) The University is authorized to submit the Work at any National / International Library, under the authority of their "Thesis Non-Exclusive License";

d) The Universal Copyright Notice (©) shall appear on all copies made under the authority of this license;

e) I undertake to submit my thesis, through my University, to any Library and Archives. Any abstract submitted with the thesis will be considered to form part of the thesis.

f) I represent that my thesis is my original work, does not infringe any rights of others, including privacy rights, and that I have the right to make the grant conferred by this non-exclusive license.

g) If third party copyrighted material was included in my thesis for which, under the terms of the Copyright Act, written permission from the copyright owners is required, I have obtained such permission from the copyright owners to do the acts mentioned in paragraph (a) above for the full term of copyright protection.

h) I understand that the responsibility for the matter as mentioned in the paragraph (g) rests with the authors / me solely. In no case shall GTU have any liability for any acts / omissions / errors / copyright infringement from the publication of the said thesis or otherwise.

i) I retain copyright ownership and moral rights in my thesis, and may deal with the copyright in my thesis, in any way consistent with rights granted by me to my University in this non-exclusive license.

j) GTU logo shall not be used /printed in the book (in any manner whatsoever) being published or any promotional or marketing materials or any such similar documents.

k) The following statement shall be included appropriately and displayed prominently in the book or any material being published anywhere: "The content of the published work is part of the thesis submitted in partial fulfilment for the award of the degree of Ph.D. in Chemical Engineering of the Gujarat Technological University".

l) I further promise to inform any person to whom I may hereafter assign or license my copyright in my thesis of the rights granted by me to my University in this nonexclusive license. I shall keep GTU indemnified from any and all claims from the Publisher(s) or any third parties at all times resulting or arising from the publishing or use or intended use of the book / such similar document or its contents.

m) I am aware of and agree to accept the conditions and regulations of Ph.D. including all policy matters related to authorship and plagiarism.

Signature of the Research Scholar:

Name of Research Scholar: Dolly Rajnikant Gandhi

Date: 13/10/2022 Place: Ahmedabad

Recommendation of the Co-Supervisor: Recommended

Signature of Co Supervisor:

Name of Co Supervisor: Dr. Rajib Bandyopadhyay

Date: 13/10/2022 Place: Ahmedabad.

Recommendation of the Supervisor: Recommended

Signature of Supervisor:

Name of Supervisor: Dr. Bhavna Soni

Date: 13/10/2022 Place: Ahmedabad

Thesis Approval Form

The viva-voce of the PhD Thesis submitted by Ms. Dolly Rajnikant Gandhi, Enrolment No. 159997105005 entitled "Synthesis of Zeolite Y using novel material and method for catalytic application" was conducted on 13/10/2022 at Gujarat Technological University.

(Please tick the relevant option(s))

☑ The performance of the candidate was satisfactory. We recommend that he/she be awarded the PhD degree.

☐ Any further modifications in research work recommended by the panel after 3 months from the date of first viva-voce upon request of the Supervisor or request of Independent Research Scholar after which viva-voce can be re-conducted by the same panel again.

☐ The performance of the candidate was unsatisfactory. We recommend that he/she should not be awarded the PhD degree.

Dr. Bhavna Soni
(Supervisor)

Dr. Rajib Bandyopadhyay
(Co Supervisor)

Dr. Deepak Chandra Sau
(External Examiner 1)

Dr. Pragnesh N. Dave
(External Examiner 2)

x

ABSTRACT

Zeolite Y is crystalline and porous material which possesses essential structural properties suitable for application as adsorbents, ion-exchangers, catalysts and components of catalyst. Traditional synthesis of zeolite Y uses hydrothermal conditions, organic templates, high pressure conditions which are inherently inefficient and generate wastes. In this work two novel environmentally friendly synthesis techniques are attempted. First a novel material, hitherto not applied, Kaolin clay from Kachchh region of Gujarat is used as indigenous and inexpensive source of silica and alumina to synthesize zeolite Y by hydrothermal method. The synthesis route comprised of the following steps: sulphuric acid treatment at 110°C (4h) for impurity removal followed by calcination at 600°C for 4h, thermal activation of kaolin into metakaolin by NaOH fusion at 850°C (8h); aging of reaction mixtures at 50°C (24h); crystallization (48h) followed by washing and drying. In the second approach, a novel but facile synthesis method by using chemical route using ultrasonic technique is demonstrated. In this method, the precursor gel was sonicated with ultrasonic processor (20 kHz, 500 W) for 90 min and treated hydrothermally without stirring at 100°C for 90 min followed by washing, filtration and drying. The formations of synthesized zeolites Y were confirmed by multiple characterization techniques. Detailed structural examination indicated a porous structure having majority of micropores and remaining mesopores. Comparison with a reference zeolite Y prepared by standard method and a commercial zeolite Y procured from Zeolyst International was also carried out. The synthesized zeolite Y was applied as a catalyst for esterification of succinic acid with ethanol to form valuable esters. The results indicated good conversion rate and selectivity at moderate reaction conditions. This work demonstrated an effective way of preparing environmentally benign and porous zeolite Y having required structural properties suitable for catalytic applications.

GRAPHICAL ABSTRACT

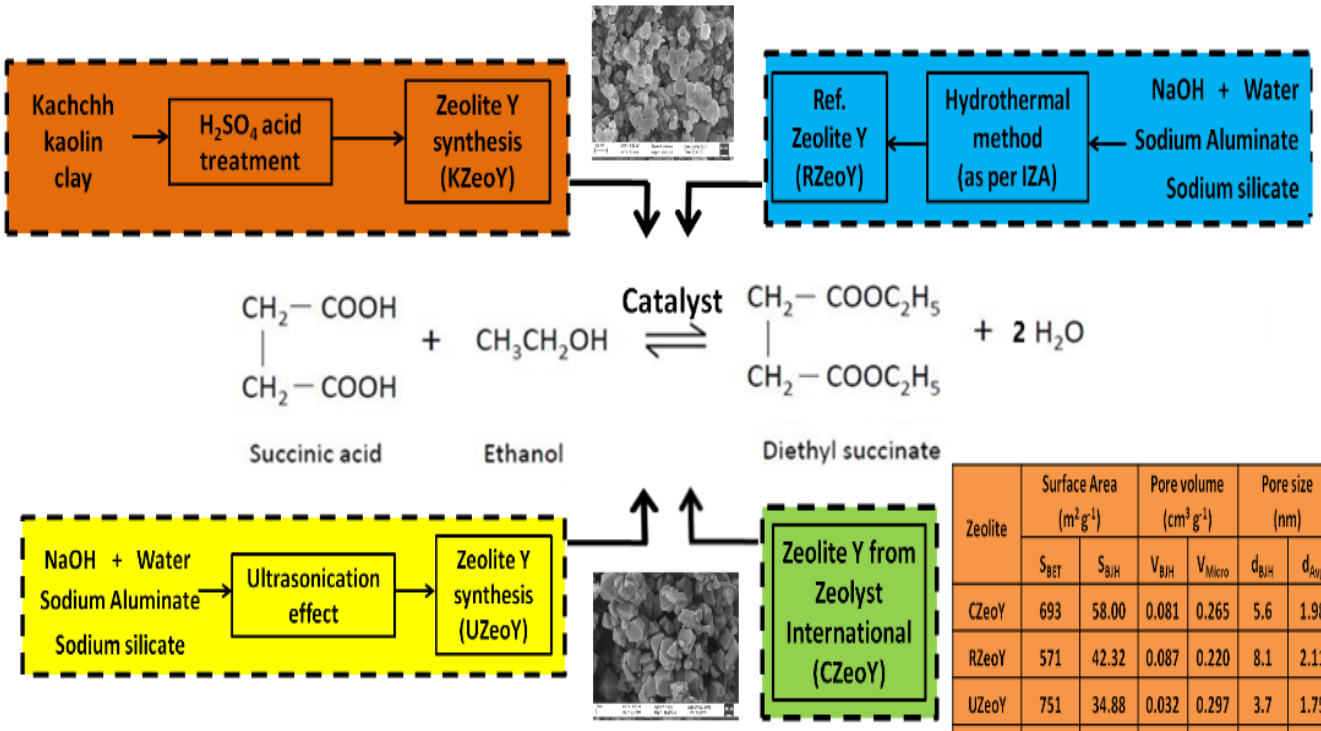

Zeolite	Surface Area ($m^2 g^{-1}$)		Pore volume ($cm^3 g^{-1}$)		Pore size (nm)	
	S_{BET}	S_{BJH}	V_{BJH}	V_{Micro}	d_{BJH}	d_{Avg}
CZeoY	693	58.00	0.081	0.265	5.6	1.98
RZeoY	571	42.32	0.087	0.220	8.1	2.11
UZeoY	751	34.88	0.032	0.297	3.7	1.75
KZeoY	320	33.52	0.080	0.136	9.6	2.89

Acknowledgement

I express my sincere appreciation to those who have contributed to this thesis and supported me in one way or the other during this amazing journey. Without them, this research work would not have been possible. I express my sincere gratitude to all, and take this opportunity to particularly mention few of their names here.

First and foremost, I would like to express my sincere gratitude to my research supervisor Dr. Bhavna Soni, Professor and Head, Department of Chemical Engineering, SAL College of Engineering, Ahmedabad. Her continuous guidance, motivation, inspiration and care throughout my research period were overwhelming. With her wholehearted support and continuous encouragement, the work was not only completed successfully within time but also with complete satisfaction. Secondly, I would like to express my genuine gratefulness to Dr. Rajib Bandyopadhyay, Professor, Department of Chemistry, School of Technology, Pandit Deendayal Energy University, Gandhinagar for guiding me throughout my experimental work. He obliged by allowing to perform some of the crucial work at his laboratory. His valuable technical guidance and moral support always encouraged me to do something which is really valuable.

My sincere and deep appreciation also goes to Dr. Ranjan Sengupta, Retd. Professor, The Maharaja Sayajirao University of Baroda who was a member of my doctoral progress committee (DPC). Being a very senior and respectable faculty member, his continuous encouragement helped me a lot towards completion of the research work. He gave his valuable suggestions generously and took keen interest in my research work. My sincere and deep gratitude also goes to Dr. Jagannath Das, Retd. Vice President, Reliance Industries, Vadodara who was my other DPC member for always being supportive and providing encouragement. He was always eager to know about the developments and progress in my research work. His technical guidance, thoughtful feedback and insightful comments toward improving my research work were very helpful. Despite of their busy schedule, both the

members always remained present in the DPC meeting and ensured that I could present my work freely without any stress.

I am sincerely grateful to Dr. Nilay Bhuptani, Principal of Vishwkarma Government Engineering College, Chandkheda, Ahmedabad who gave me this golden opportunity and permission for pursuing this Ph.D programme under Gujarat Technological University, Ahmedabad and also providing me necessary support to carry out my research work. I also thank Dr. N. M. Patel, Professor and Prof. S. B. Thakore, Associate Professor in Chemical Engineering for their support in doing the thesis. I also wish to thank all faculty members of chemical department of Vishwakarma Government College of Engineering, Chandkheda, Ahmedabad for encouraging and helping me throughout.

I would like to specially thank the valuable contribution of Mr. B. K. Patel and Mr. Amit Dave of M/s Gujarat Multi gas base Chemicals (P) Ltd., Mehsana, Mr. Jayesh Patel of Your Micron LLP, Morbi, Mr. Vinay Dangar and Dr. Reddy of Gunjan Minerals Pvt. Ltd., Bhuj, Mr. Aroh Shrivastava of Institute of Plasma Research, Gandhinagar, and Mr. Arun Basrur of Süd-Chemie India Pvt. Ltd., Vadodara for providing vital support in completing the research work. The unconditional support from their side with the sole purpose of supporting quality research work without asking anything in return is really commendable.

I am particularly thankful to my students Dhaval, Binit, Vaibhav, Vatsal, Kuldeep and Punit for their untiring effort and hard work towards making this research work successful. Last but not the least; I would like to say a heartfelt thanks to my family and friends for their unconditional support and love for me.

Dolly Rajnikant Gandhi

Date: 13/10/2022 Place: Ahmedabad

Dedicated to my parents

Table of Content

#	**Abstract …….. ……..…**			XI
#	**Graphical Abstract ……..…..**			XII
#	**Acknowledgement ……..**			XIII
#	**List of abbreviation ……**			XVIII
#	**List of symbols ……**			XIX
#	**List of figures ……**			XX
#	**List of tables ……**			XXII
#	**List of appendices ……**			XXIII
1.	**Introduction ……**			1
	1.1	About zeolite		1
	1.2	Definition of the problem		4
	1.3	Objectives and Scope of research work		4
	1.4	Presentation and layout of the thesis		5
2	**Literature Review**			6
	2.1	About Zeolites		6
		2.1.1	Brief history of Zeolites	7
		2.1.2	Zeolite structure and properties	7
		2.1.3	Zeolite application	12
		2.1.4	Zeolite synthesis	14
		2.1.5	Method for Zeolite synthesis	15
		2.1.6	Zeolite synthesis raw materials	22
		2.1.7	Zeolite characterization	23
	2.2	Zeolite Y structure and properties		28
		2.2.1	Zeolite Y synthesis	29
		2.2.2	Zeolite Y synthesis from Kaolin	31
		2.2.3	Zeolite Y synthesis from Bentonite	32
		2.2.4	Application of Zeolite Y as catalyst	35
	2.3	Esterification reaction		35
		2.3.1	Esterification of succinic acid with ethanol	37
	2.4	Research gap and challenges		38
3	**Materials and methods**			40
	3.1	Materials used		41
		3.1.1	Equipments and instruments	41
		3.1.2	Glass wares/plastic wares	41
		3.1.3	Chemicals	41
	3.2	Experimental		42
		3.2.1	Synthesis of Reference Zeolite Y (RZeoY) by conventional method	42
		3.2.2	Synthesis of Zeolite Y by using Kachchh clay	44

			3.2.2.1	Clay treatment of kaolin clay	44
			3.2.2.2	Clay treatment of Bentonite clay	46
			3.2.2.3	Synthesis of Zeolite Y from clay	47
		3.2.3	Synthesis of Zeolite Y by using ultrasonication		51
		3.2.4	Ion exchange by NH_4NO_3 - Catalyst activation		52
		3.2.5	Esterification reaction		53
	3.3	Analytical methodologies			55
		3.3.1	X-Ray Diffraction		55
		3.3.2	Infrared Spectroscopy		56
		3.3.3	Thermal Analysis		56
		3.3.4	X-ray fluorescence (XRF)		58
		3.3.5	N_2-adsorption-desorption		58
		3.3.6	Electron Microscopy		59
4	**Result and Discussion**				61
	4.1	Characterization of reference Zeolite Y (RZeoY)			61
	4.2	Clay Treatment			62
		4.2.1	Kaolin clay		62
		4.2.2	Bentonite clay		70
		4.2.3	Environment impact assessment		79
	4.3	Synthesis of Zeolite Y from clay			80
		4.3.1	Kaolin clay to Zeolite Y (KZeoY)		80
	4.4	Zeolite Y synthesized by ultrasonic method (UZeoY)			87
	4.5	Application in esterification reaction			91
		4.5.1	Ion exchange by NH_4NO_3 - catalyst activation		91
		4.5.2	Esterification reaction		92
			4.5.2.1	Kaolin clay	93
			4.5.2.2	Bentonite clay	94
			4.5.2.3	Zeolite Y from kaolin (KZeoY)	95
			4.5.2.4	Ultrasonic Zeolite Y (UZeoY)	97
		4.5.3	Kinetic and rate constant study		99
5	**Conclusion and future scope**				102
	5.1	Major conclusions			102
	5.2	Original contribution by the thesis			106
	5.3	Future scope of work			106
	References				108
	Research Publications				127
	Appendix				128
	A	Crystallinity and Lattice parameter calculation			129
	B	Sample Batch calculation			136
	C	Research Publications & Conferences			148

List of Abbreviation

Abbreviation	Meaning
FCC	Fluid catalytic cracking
HC	Hydrocarbon cracking
FAU	Faujasite
RHA	Rice husk ash
BFS	Blast furnace slag
AAS	Atomic absorption spectrometry
XRD	X-ray diffraction
FTIR	Fourier transform infrared spectrometry
SEM	Scanning Electron Microscopy
TGA	Thermogravimetric Analysis
DTG	Difference Thermogravimetry
DTA	Differential Thermal Analysis
DSC	Differential scanning calorimetry
BET	Brunauer-Emmett-Teller
RE	Rare earth
RPM	Revolutions per minute
AR	Analytical reagent
RZeoY	Reference zeolite Y
CZeoY	Commercial zeolite Y
UZeoY	Ultrasonic zeolite Y
KZeoY	Zeolite Y from kaolin clay
MES	Monoethyl succinate/MES
DES	Diethyl succinate/DES
SSA	Specific surface area
SA	Succinic acid

List of Symbols

Symbol	Unit	Meaning
S	$m^2 g^{-1}$	Specific surface area
V	$cm^3 g^{-1}$	Pore volume
d	nm	Pore diameter
a	Å	Lattice parameter
K	s^{-1}	Rate constant

List of Figures

Figure No.	Title	Page no.
Fig. 2.1	Chemical structure of zeolite	8
Fig. 2.2	Primary building unit of zeolite structure	8
Fig. 2.3	Brønsted and Lewis acid sites in zeolites	10
Fig. 2.4	(a) Reactant selectivity, (b) Product selectivity and (c) Restricted Transition-State selectivity	11
Fig. 2.5	Synthesis of Zeolite	15
Fig. 2.6	Characterization techniques applied for the structural and compositional analysis of zeolites	28
Fig. 2.7	(a) The structure of Zeolite Y (b) The double ring, sodalite and super cage of zeolite Y	29
Fig. 3.1	Experimental approach	40
Fig. 3.2	Schematic diagram of Synthesis of Reference Zeolite Y	43
Fig. 3.3	Sample of (a) kaolin Clay (b) Bentonite Clay	44
Fig. 3.4	Flow diagram representing clay treatment	44
Fig. 3.5	Acid treatment of kaolin clay	45
Fig. 3.6	Acid treatment of Bentonite clay	47
Fig. 3.7	Synthesis of Zeolite Y from Kaolin clay (KZeoY)	48
Fig. 3.8	Experimental steps of synthesis of Zeolite Y from Kaolin clay (KZeoY).	49
Fig. 3.9	Synthesis of Zeolite Y from Bentonite clay	50
Fig. 3.10	Experimental steps of synthesis of Zeolite Y from Bentonite clay	51
Fig. 3.11	Synthesis of Zeolite Y by using ultrasonication	52
Fig. 3.12	Schematic diagram of ammonium nitrate ion exchange of all synthesized Zeolite Y	53
Fig. 3.13	Schematic diagram of esterification reaction	54
Fig. 3.14	Esterification reaction experimental set up	54
Fig. 3.15	Rigaku Miniflex instrument for XRD pattern	56
Fig. 3.16	Fourier transform infrared spectroscope (ATR-FTIR, VERTEX 80, Bruker Corp., Germany)	57
Fig. 3.17	Dispersive XRF spectrometer EDX-7000 (SHIMADZU Corporation, Japan)	58
Fig. 3.18	Surface area analyzer TriStar II 3020 (Micromeritics Instruments Corporation, US)	59
Fig. 3.19	Scanning electron microscope (ZEISS Gemini Sigma)	60
Fig. 4.1	XRD and N_2 adsorption-desorption isotherms of RZeoY and CZeoY	61
Fig. 4.2	SEM images of (a) RZeoY and (b) CZeoY	62
Fig. 4.3	FTIR analysis of (a) raw kaolin clay (blue) (b) 7M H_2SO_4 treated kaolin clay (pink) (c) 10M H_2SO_4 treated kaolin clay (red).	65
Fig. 4.4	SEM images of (a) raw kaolin clay (b) 7M H_2SO_4 treated kaolin clay (c) 10M H_2SO_4 treated kaolin clay.	65

Fig. 4.5	(a) TGA of raw kaolin and H_2SO_4 treated kaolin clay (b) DTA of raw kaolin and H_2SO_4 treated kaolin clay.	67
Fig. 4.6	XRD analysis of (a) raw kaolin clay (blue) (b) 7M H_2SO_4 treated kaolin clay (red) (c) 10M H_2SO_4 treated kaolin clay (black).	68
Fig.4.7	N_2 adsorption isotherm of (a) raw kaolin clay (orange) (b) 7M H_2SO_4 treated kaolin clay (blue) (c) 10M H_2SO_4 treated kaolin clay (green).	69
Fig. 4.8	FTIR analysis of (a) raw Bentonite clay (blue) (b) bentonite clay treated by 5M H_2SO_4 (black) (c) bentonite clay treated by 10M H_2SO_4 (red).	73
Fig. 4.9	DTA of (a) raw Bentonite clay (black) (b) bentonite clay treated by 5M H_2SO_4 (red) (c) bentonite clay treated by 10M H_2SO_4 (blue).	74
Fig. 4.10	XRD analysis of raw bentonite clay, treated by 5M and 10M H_2SO_4, M-Montmorillonite-bentonite, Q-Quartz, G-Gypsum	76
Fig. 4.11	SEM micrographs (500×) of (a) raw bentonite clay (b) bentonite clay treated by 5M H_2SO_4 (c) bentonite clay treated by 10M H_2SO_4.	77
Fig. 4.12	SEM micrographs (5000×) of acid treated bentonite clay revealing highly porous structure caused due to acid treatment using 5M H_2SO_4 followed by calcination	77
Fig. 4.13	Comparison of the XRD patterns of (a) raw kaolin clay (b) synthesized zeolite Y (KZeoY) from kaolin clay and reference zeolite Y (RZeoY).	82
Fig. 4.14	SEM images of (a) raw kaolin clay (b) KZeoY (c) RZeoY	85
Fig. 4.15	(a) N_2 adsorption-desorption isotherms (b) Pore volume distribution of KZeoY and RZeoY	86
Fig.4.16	XRD of samples of bentonite base synthesized Y for different crystallization time (a) 72 h (b) 84 h and (c) 96 h	87
Fig. 4.17	XRD of synthesized UZeoY, RZeoY and CZeoY	88
Fig. 4.18	SEM images of (a) CZeoY and (b) UZeoY	90
Fig. 4.19	(a) N_2 adsorption-desorption isotherms and (b) Pore volume distribution of UZeoY and comparison with references	91
Fig. 4.20	Conversion of Succinic acid with time for all Zeolites	95
Fig. 4.21	Catalytic activity of Y zeolites [(a) RZeoY and (b) KZeoY] with time on stream	97
Fig. 4.22	Catalytic activity of Y zeolites [(a) RZeoY and (b) UZeoY] with time on stream	99
Fig. 4.23	Plot of the conversion of succinic acid with time for (a) KZeoY and (b) UZeoY	101

List of Tables

Table No.	Title	Page no.
Table 2.1	Comparison of the various methods of zeolite synthesis	19
Table 2.2	Effect of ultrasonication on synthesis/modification of Zeolite Y and other zeolites.	22
Table 2.3	Analysis of kaolin clay obtained from various regions	30
Table 2.4	A brief overview of acid treatment of kaolin clay	31
Table 2.5	Overview of the physico-chemical changes of raw Bentonite clay before and after H_2SO_4 treatment	34
Table 2.6	Esterification reactions using zeolite Y as catalyst	36
Table 4.1	Textural properties of RZeoY and CZeoY	62
Table 4.2	XRF analysis of raw and H_2SO_4 (7M and 10M) treated kaolin clay	63
Table 4.3	Textural properties of raw and acid treated kaolin clay	69
Table 4.4	XRF analysis of raw Bentonite (RB) clay and after acid treatment using 5M and 10M H_2SO_4	72
Table 4.5	Textural properties of raw Bentonite clay and after acid treatment using 5M and 10M H_2SO_4.	79
Table 4.6	Composition of raw kaolin clay and synthesized zeolite Y (KZeoY) with respect to reference zeolite Y (RZeoY)	81
Table 4.7	Crystallinity calculation of synthesized zeolite Y (KZeoY)	83
Table 4.8	Lattice parameter calculation	83
Table 4.9	Textural properties of raw kaolin clay and synthesized zeolite Y	86
Table 4.10	Lattice parameter of UZeoY	89
Table 4.11	Crystallinity calculation of UZeoY	89
Table 4.12	Textural properties of synthesized UZeoY, CZeoY and RZeoY	91
Table 4.13	Na_2O content of zeolites before and after activation by ion exchange	92
Table 4.14	Esterification of succinic acid with ethanol using H form of synthesized zeolites from kaolin clay as catalyst.	96
Table 4.15	Comparison of the performance of reported catalysts in the esterification of succinic acid with ethanol.	97
Table 4.16	Esterification of succinic acid with ethanol using H form of synthesized zeolites as catalyst.	99
Table 4.17	Rate constant, K for the all the zeolites	101

List of Appendices

Appendix No.	Title	Page no.
Appendix A	Crystallinity and Lattice parameter calculation	129
Appendix B	Sample Batch calculation	136
Appendix C	Research Publications & Conferences	148

CHAPTER - 1

Introduction

1.1 About zeolite

It is more than a century since zeolites were first discovered but the interest in research of zeolite materials is still growing. Zeolites have become popular due to its diverse applicability in the field of agriculture and animal husbandry, medicine, chemical industry, biotechnology, construction industry, petroleum industry, water processing, etc. They have also found space in the development of new technologies which contribute to sustainable development. Due to their specific properties which are also tunable, high thermal and hydrothermal stability, as well as environmental acceptability, zeolites are formidable alternatives to similar materials that have their own set of issues and are often economically and environmentally unacceptable. Since their discovery the demand for zeolites has grown to the extent that they are almost vital and irreplaceable in some applications. Zeolites are used both individually and in combination with other micro- and nanoporous materials as catalysts, adsorbents, and ion exchangers with high capacity and selectivity. The global zeolites market size is estimated to be USD 12.1 billion in 2021 and is projected to reach USD 14.1 billion by 2026, at a CAGR of 3.1% between 2021 and 2026 [1]. Some of the leading companies in the zeolites market include Albemarle Corporation (US), BASF SE (Germany), Honeywell International Inc. (US), Clariant (Switzerland), Huiying Chemical Industry (Xiamen) Co., Ltd. (China), Chemiewerk Bad Köstritz GmbH (Germany), NALCO India (India) among others. Out of all, the catalyst segment is estimated to account for the largest share of the overall zeolites market, in terms of value, in 2020.

Zeolites are inorganic crystalline aluminosilicates built from TO_4 tetrahedra (T = Si and Al) with a network of pores that are considered valuable for application as catalysts and adsorbents. Though zolites are available in natural form, they suffer from inherent disadvantages like presence of impurities, inconsistent pore size and low cation exchange capacity. Hence, they are not preferred for critical catalytic application where product consistency is important. Compared to natural zeolites, synthetic zeolites are favored as

catalysts owing to purity of crystalline products and uniformity of particle sizes [2,3]. Synthetic zeolites possess excellent properties like high surface area, porosity in both micro and meso form, shape selectivity, high ion- exchange capacity, strong Brønsted acidity and high thermal and hydrothermal stability [2,4]. This makes them suitable for numerous industrial applications, such as catalysts [5–8], membrane separations [9–12], adsorbents [13–15], ion exchange etc. Zeolites are the most important inorganic material used in the production of oil & gas in the petrochemical and oil refining industries [16]. Demand for zeolites as catalysts in fluid catalytic cracking (FCC) and hydrocarbon cracking (HC) applications is continuously growing**.** The principle raw materials used for the synthesis of the zeolites are different sources of silica and alumina, which are usually composed of sodium silicates, sodium aluminate, aluminium salts or colloidal silica. However, the traditional methods for synthesizing zeolites normally engage chemical reagents as starting materials or crystallization from a gel or clear solution under hydrothermal conditions. Though the process is simple and widely applied, still it suffers from the disadvantages of high cost, waste generation and not considered environment friendly. Therefore, many attempts are underway for economical synthesis of zeolites and at the same time being environmentally benign i.e. green synthesis. Consequently natural aluminosilicate and silicate minerals have been explored as silica and/or alumina source because they are cost-effective precursors and can lead to reduction of the synthesis costs. Vast natural reserves make them abundantly available and help in reducing the generation of hazardous wastes, saving energy, and great potential in altering the properties of the resulting zeolites. Zeolites has been successfully synthesized from natural minerals such as kaolinite [17–20], bentonite [21], montmorrilonite [22,23] and other precursors. Several industrial solid wastes have also been successfully utilized as a silica source which serves dual benefits of waste utilization and an inexpensive raw material. Several such industrial waste like fly ash [24,25], rice husk ash [26,27] and blast furnace slag [28] etc. have been successfully used for zeolite synthesis. However, uncertainty in their supplies and presence of impurities somehow limit their application. Among the zeolites, zeolite Y which falls under the faujasite class of zeolites has gained importance as a catalyst. Zeolite Y has faujasite (FAU) framework structure, having a complex network of interconnected micropores. Due to the porous structure with large void space and interconnectivity, large sized molecules can easily access the interior active sites resulting in

high reaction rates and enhanced selectivity. These zeolites find important strategic applications in the petroleum refining and petrochemical industry. However, the inherent costly nature of synthetic zeolite Y raises the need of scouting for cheap raw materials and simple process conditions. The most important parameter which affects zeolite synthesis is the temperature and pressure applied during the hydrothermal process. Apart from that a host of other variables, such as batch composition, reactant sources, Si/Al ratio, alkalinity, inorganic cations, ageing, stirring, organic templates, solvents, water content, temperature, and seeding. As a result the process conditions employed by various researchers are quite diverse in nature. Finding the parameters helpful for obtaining the optimal properties of synthetic zeolite for their technological application is of utmost priority in scientific research.

Kachchh district in Gujarat of India is a mineral rich region having a vast reserve of Lignite, Gypsum, Bauxite, Bentonite and other minerals. Among the naturally occurring minerals found in Bhuj, Kachchh belt; kaolin clay which predominantly consists of kaolinite ($Al_2Si_2O_5(OH)_4$) is industrially important because of its vital properties and being inexpensive. Kaolin clay is commercially valued for its whiteness and fine particle size and used in raw form in cement industry and post processing as filler in paper, rubber and plastic; extender and flattening agent in paints; constituent in ceramics and numerous other applications [29]. Presence of silica along with crystalline mesoporous structure makes it suitable for use as a base material for preparation of catalyst that can be applied in various types of reactions and other potential applications as adsorbents, separation media/hosts for bulky molecules for advanced materials applications [2]. The abundant availability and low cost of kaolin clay in the Kachchh district of Gujarat makes it potential and untapped raw material for synthesis of zeolites. High silica-alumina ratio along with high surface area makes the activated kaolin clay suitable for application predominantly as adsorbents [13,30,31] and catalysts [32–36]. As a catalyst they are easy to handle, non-corrosive, economical, recoverable and reusable without losing catalytic activity [37].

Application of hydrothermal synthesis technique using natural clay as a sustainable silica-alumina source has gained tremendous acceptance among researchers due to its several advantages like high reactivity of reactants, low energy consumption, low air pollution, easy of control and formation of metastable phases among others [38]. Subcritical synthesis involves moderate temperature (100–240°C) and pressure conditions adding to ease of

synthesis. Also it is a step towards green synthesis that replaces the use of toxic organic templates. In order to further improve the yield and efficiency of the process, sonochemical based synthesis using ultrasonic irradiation offers a better alternative which particularly helps in the crystallization step. It provides faster crystal growth rate simultaneously providing better control over the nucleation process that also improves particle size distribution and morphology [39]. Also, the sonochemical synthesis is simple, fast, and does not need any complicated facilities. Hence, ultrasonic assisted hydrothermal synthesis has been widely accepted of late and is considered as a big step further toward green synthesis [40–42] .

1.2 Definition of the problem

Since, kaolin clay originates from various sources; their composition varies with geographical location and the chemical composition and crystalline phases vary with the geological layer of the soil. The protocol for synthesis of zeolite Y from kaolin clay is not standardized. The main steps of zeolite Y synthesis from kaolin clay include: initial physico-chemical treatment for impurity removal (metal oxides along with some amount of dealumination) which is done by acid or alkaline treatment followed by calcination at high temperature; addition of external silica and/or dealumination depending on the silica-alumina ratio; activation of kaolin at high temperature to get metakaolin; ageing of reaction mixtures at ambient temperature (gel formation) followed by crystallization. The process variables like acid concentration, time required for activation, ageing, crystallization and temperature required for activation, crystallization needs to be determined and adjusted with respect to the clay composition. Consequently the SiO_2/Al_2O_3 ratio and the surface properties like pore size, pore volume and surface area of the synthesized zeolite can be tuned considerably to provide the required properties suitable for catalytic and other applications.

1.3 Objectives and Scope of research work

Based on the preceding background the objectives and scopes of the present research are appended below:

- Synthesis of zeolite Y by using novel material.
- Synthesis of zeolite Y by using a novel method.
- Confirmation of formation of zeolite Y by multiple characterization techniques.
- Application of synthesized zeolite Y as a catalyst.

1.4 Presentation and layout of the thesis

This thesis contains five chapters with appropriate sections, subsections, references, appendices and the list of research publications. The first chapter of this thesis deals with the introduction and significance of the zeolites in chemical reaction engineering along with its advantages and limitations in comparison to conventional catalysts. It also describes the definition of problem and objectives of the present research work. The motivation of selecting the novel materials and novel path in zeolite synthesis has been explained. In the second chapter, an overview of zeolites containing brief history, structure, properties, application and characterization techniques are presented. All the methods of zeolite synthesis are discussed with a focus on modern methods incorporating microwave and ultrasonic. The various raw materials which can be used for zeolite synthesis is also discussed. A detailed literature survey has been carried out on zeolite Y synthesis from various clay with a special focus on kaolin and bentonite clay. A detailed outline on application of zeolite Y as a catalyst in esterification reaction is also presented. The research gap along with the various challenges has been identified. The third chapter describes the experimental setup in detail along with the raw materials used and process conditions while performing the experiments. The methodologies of performing the experiments are explained. The specifications of different chemicals and measurement devices used to carry out the present research work are provided. Characterization techniques that are used to determine the structural and compositional analysis of the synthesized and reference zeolites are elucidated. The fourth chapter discusses the experimental results obtained using different types of raw materials and process conditions towards synthesizing zeolites. The chapter also tries to give a detailed explanation of the possible phenomenon happening inside the zeolite structure that decides its success when applied as a catalyst in reaction. Also the effect of various external parameters like acid concentration, crystallization time, etc. has been studied in depth. Performance evaluation of the synthesized zeolite as a catalyst in esterification reaction was performed. Chapter 5 summarizes the findings and the major conclusions that have been drawn from this investigation. The future scope in this area of research work is also provided along with recommendations for further study.

CHAPTER - 2

Literature Review

2.1 About Zeolites

Zeolites are crystalline aluminosilicate materials supported by tetrahedral SiO_4 and AlO_4 elementary building blocks that give rise to a three-dimensional network. They are found naturally (e.g., clinoptilolite, mordenite and garronite), and can also be synthesized from various raw materials (e.g., zeolite A, P, X and Y). Currently, there are over two hundred types of zeolites available. As natural zeolites possess inherent disadvantages like presence of impurities, inconsistent pore size and low cation exchange capacity, they are not preferred for critical catalytic application where product consistency is important. Synthetic zeolites offer more benefits than natural zeolite [43]. Compared to natural zeolites, synthetic zeolites are favored as catalysts owing to high purity of the crystalline products and uniformity in the particle size [3]. Out of all the zeolites, zeolite Y which falls under the faujasite class of zeolites has gained importance as a catalyst. Zeolite Y has faujasite (FAU) framework structure, having an internally connected complex network of micropores. The pores, which are formed by 12 Si or Al atoms which are linked through O atoms forming a tetrahedral structure. The pores have a moderately large diameter of 7.4 Å forming a porous structure. 10 sodalite cages surround the inner cavity with a diameter of 12 Å. The unit cell of the zeolite has a cubic structure having high thermal stability and good Bronsted acidity [44,45]. Due to the porous structure with large void space and interconnectivity, large sized molecules can easily access the interior active sites resulting in high reaction rates and enhanced selectivity. The catalytic activity depends on the strong network of macropores and mesopores for mass transfer from the surface of the crystal to the internal mesopores for subsequent diffusion into the micropores where reaction occurs [46,47]. However, to synthesize zeolite Y with proper hierarchical structure with required mesoporosity simultaneously maintaining its crystallinity is still a challenge [48]. Hence, this hierarchical structure is generated synthetically by various forms of acid treatment or a combination of acid and base treatment. Zeolites find important strategic applications in the petroleum refining and petrochemical industry [49–52].

2.1.1 Brief history of Zeolites

Zeolites has a long history and the first zeolite mineral was discovered in 1756 [53]. Zeolites originated due to chemical reactions within the volcanic magma and were found in the cavities inside rocks. Swedish mineralogist Axel F. Cronstedt derived the term “zeolite” from two classical Greek words “zeo” meaning “to boil” and “lithos” meaning “a stone” [54]. Over the years more fundamental properties of zeolites were established. Damour in 1840 reported that zeolites had experienced reversible dehydration without any major change in the transparency of the crystal form. In 1858 Eichhorn observed the reversibility of ion exchange on zeolite minerals. Taylor and Pauling in 1930 established the crystal structure of the zeolites and also provided evidence of the existence of cavities in these structures. After a couple of years in 1932 McBa5in coined the term “molecular sieve” to describe the porous solid material structure, and the capability of zeolite structure to work as sieves on a molecular scale [2]. In 1945 Barrer, who is considered the father of zeolite science in the United Kingdom, reported the first classification of zeolite minerals based on the size and the rate of molecules absorbed. In the early 1950s, Milton and Breck discovered the commercially important synthetic zeolites A, P, X and Y which were synthesized from readily available raw materials. At that juncture, only aluminium-rich zeolites could be synthesized. In 1967, Wadlinger and his co-workers introduced the silica rich forms of zeolite beta (BEA) [55]. Till date over 200 zeolite framework types having a range of physical and chemical properties have been synthesized, and 176 of these are listed in the 6th edition of the Atlas of Zeolite Framework Types [56]. These zeolites are applied in a wide range of industrial processes as adsorbents, ion-exchangers, catalysts and components of catalyst.

2.1.2 Zeolite structure and properties

Zeolites are crystalline, porous polyaluminosilicate. The general crystallographic unit cell formula of a zeolite is given as: $M_{x/m}\,[(AlO_2)_x\,(SiO_2)_y]$. z H_2O where the non-system metal cation is M with charge m, the quantity of water particles is z and x and y are whole numbers to such an extent that $y/x \geq 1$ [54]. The square sections demonstrate the anionic aluminosilicates system. Their structure is made up of polyaluminosilicate that has a three-dimensional framework of SiO_4 and AlO_4 tetrahedra connected to one another by sharing oxygen elements(Fig. 2.1and 2.2). The structure contains channels or interconnected voids

that have microporosity and macroporosity. These channels and voids are occupied by water atoms and the cations; and additionally, soluble base or antacid earth metal particles which are mobile and adjust the negative charge of the structure [54,57]. All these tetrahedrally coordinated atoms are generally called the T-atoms (T=Si, Al, etc.). Common building blocks of zeolite structures consist of 3, 4, 5, and 6 membered rings (n-MR). Each n-MR consists of n T atoms linked in a ring by O ions and thus actually has 2n atoms; thus a 6-MR has 12 total atoms. The structures are arranged such that they form larger rings that represent the molecular pores – commonly 8-, 10- and 12-MR [58], although structures with 9-, 14-, 18-, and 20-MR pores are known. When a trivalent atom is present in the zeolite framework, a negative charge is created in the lattice, which is compensated by cations like sodium, potassium, etc. Brönsted acid sites are developed when the cation is exchanged by a proton. The proton is attached to the oxygen atom bridging the silicon and aluminium atoms, resulting in the acidic hydroxyl group which is the site responsible for the Brönsted acidity of zeolites. The acid sites of zeolites, in combination with their well-defined pore architecture, make zeolites suitable as a shape selective solid acid catalyst. Therefore, the synthesis of zeolites with new structures is one of the main topics in zeolite research.

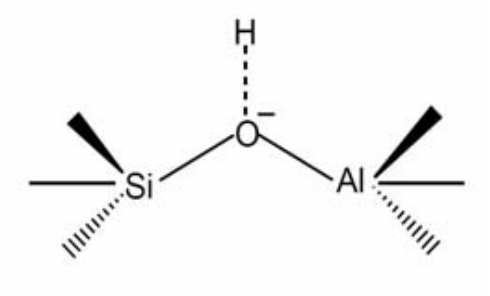

Fig. 2.1. Chemical structure of zeolite [59]

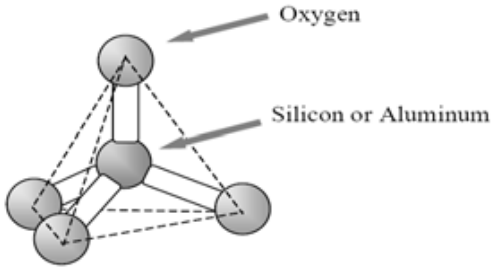

Fig. 2.2. Primary building unit of zeolite structure[60]

Zeolites can be categorized based on their chemical composition [61]. Depending on the silica-alumina ratio, zeolites are mainly classified as low silica (1 – 1.5; e.g. sodalite, X, Y), intermediate silica (2-5; e.g. mordenite, omega, FAU), high silica (5 and above; e.g. MCM-22, ZSM-5, EU-1) and pure silica zeolites (silicalites). Similarly, zeolites are also categorized based on their pore diameter and ring size. The pore diameter of zeolite is dependent on the

number of tetrahedra present in the ring aperture. Depending on the pore openings, zeolites are generally classified into small pore (6 or 8-member ring; e.g. MTN, NU-1, Chabazite, Erionite, etc.), medium pore (10-member ring; e.g. Ferrierite, ZSM-5, MCM-22, ZSM-11, ZSM-50,Stilbite etc.) and large pore (12-member ring; e.g. Cancrinite, Linde X,Y,L, Mardenite, Beta etc.). ZSM 5, MCM-22 and mordenite with 10 and 8 rings respectively have pore diameters in the range of 3-5Å. Conversely, MCM-22, faujasite X and Y have 12 rings with larger pore diameter of 7-8Å. Aluminophosphates (ALPOs) have a significantly extended range of pore sizes. ALPOs containing 12 rings have a pore diameter of 10 Å while 18 ring ALPOs have a pore diameter of 10-15Å.

Zeolites have some essential properties that make them suitable for several and widespread applications. Ion exchange is an important intrinsic property of most zeolites. Zeolites are mineral in origin, comprising silicon, aluminium, alkali and alkaline earth elements. Water is also an important component in zeolites. The zeolite framework has an intrinsic ability to exchange cations, which arises due to isomorphous replacement. In zeolites, always the isomorphous replacement is of the tetravalent framework cation *(i.e.,* silicon) by a cation of lower charge (normally aluminium). As a result of this substitution a net negative charge arises on the framework of the zeolite which has to be neutralized by the presence of cations within the pores. These cations may be any of the metals or metal complexes, or alkyl ammonium cations. It is the diversity in nature and extent of exchange of different cationic species that take place in zeolites which gives rise to the richness of the chemistry. As a result the phenomenon has given rise to direct applications, or the phenomenon is used indirectly, as a means of "tailoring" zeolite structure and hence properties when these materials are used in other applications, such as in catalysis or gas sorption.

The other important property is acidity. Zeolites have two prime acidities; Lewis sites and Bronsted sites as shown in Fig. 2.3. Substances that can donate protons (H+) are called Bronsted acids and which can accept electron pairs are called Lewis acids. The catalytic activity of the zeolites is dependent on the structure, concentration, strength and accessibility of the acid sites and their interaction with the adsorbed molecules [63]. The nature, density, and strength of these sites can be modified by various post-synthesis treatments to make them

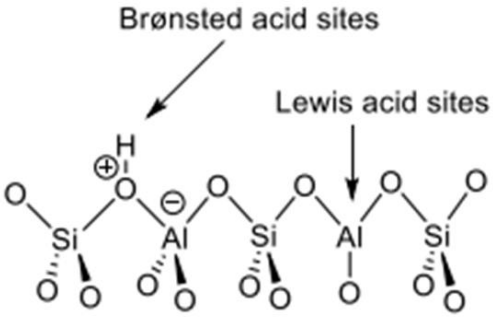

Fig. 2.3. Brønsted and Lewis acid sites in zeolites [62]

more powerful in the field of catalysis [64]. For example, alkylation of toluene with methanol over H-ZSM-5 (strong acid sites) in the gas phase is around 50 times faster than that of chlorobenzene [63]. Zeolite acidity is linked with the presence of silica and alumina content in which lesser alumina gives higher acidity and vice versa. Such kind of acidity dependence is observed in desilication and dealumination treatment. For instance, desilication of a zeolitic precursor makes the transformation of Bronsted sites into Lewis sites [64]. On the other hand, dealumination makes them lesser in acid site density while it increases the strength of acid sites and modifies zeolites porosity [65]. Such acid sites play a major role in the field of hydrocarbon reactions catalysis making them irreplaceable.

Another important property of zeolites is shape selectivity which makes them highly popular as a catalyst. A catalytic reaction that depends upon the pore structure of the catalyst and on the size of the reactant and the product molecules is called shape-selective catalysis. For example, catalysis by zeolites is a shape-selective catalysis (Fig. 2.4). If most catalytic sites are inside this pore structure and pores are small, the chance of reactant molecules and the probability of forming product molecules are determined mostly by molecular dimension and shape. Reactant selectivity observed when only one type of reactant molecule could pass through the catalyst pores (Fig. 2.4(a)). For example, the transformation of n-alkanes of light gasoline into propane and n-butane where the linear n-alkanes can enter the pores of the zeolite catalysts and be transformed, whereas the branched alkanes are not able to enter the pores and so does not react [66]. Product selectivity (Fig. 2.4(b)) observed when, among all the product molecules formed within the pores, only those molecules with the proper

dimensions can diffuse out and appear as observed products. For example, in the production of para dialkylbenzenes in toluene alkylation by methanol, the formation of bulkier ortho- and meta-isomers also occurs inside the pores, but their exit is restricted due to their lower diffusion coefficient compared to that of para- isomer. The selective removal of para-isomer from the pores allows the bulkier isomers to be isomerized into the less bulky para-isomers [67]. In restricted transition-state selectivity, certain reactions are prevented, as the resultant transition state requires more space than available. Such a type of reaction required more space in the catalyst pores or cavity. For example, in the transalkylation of 1-methyl-2-ethylbenzene, the formation of 1,2,5-isomer is significantly hindered because of spatial limitations on the formation of diarymethane intermediate [68]. Several researchers have also proposed various other types of shape selectivity to justify recent research results. However, the advantages of shape-selective catalysis are: (a) undesirable impurities can be continuously converted to harmless substances and/or smaller compounds that are easily removable, (b) selectivity of a particular product can be increased and (c) coke formation can be reduced.

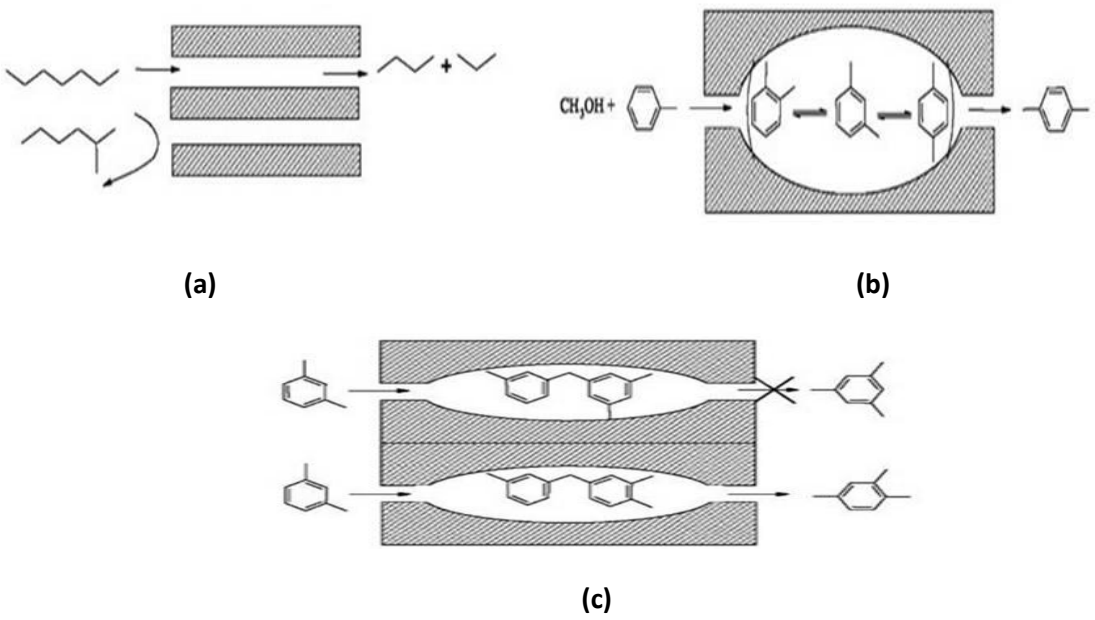

Fig. 2.4. (a) Reactant selectivity, (b) Product selectivity and (c) Restricted Transition-State selectivity [66]

2.1.3 Zeolite application

Zeolites have many potential ranges of applications including technical, environmental, industrial, commercial, agricultural, cracking and alkylation processes, and biomedical due to their porous character and their ion-exchange properties [69]. Naturally occurring zeolites are used as materials for the construction and paper industry [70]. They are also used in agriculture and other applications. Laboratory synthesized zeolites with defined pore sizes have a wide variety of applications in adsorbents, catalysts or molecular sieves and catalysts of oil refineries [69,71,72], removing radioactive contaminants [73] and wastewater treatment [71]. The structure of zeolite generally consists of a combination of numerous channels, cavities and interconnected voids, which are occupied by cations and water molecules. Synthetic zeolites are crystalline molecular sieves with pores of molecular dimensions and with well-defined structures, which have a high total surface area that makes them suitable for a wide range of applications. Industrial applications make use of synthetic zeolites of high purity, which have larger cavities than the natural zeolites. These larger cavities enable synthetic zeolites to adsorb or hold molecules which the natural zeolites struggle to do. Synthetic zeolites are used in a variety of applications as a catalyst in petrochemical cracking, ion exchange in water softening and purification, and adsorption in the removal of heavy metals [16,45,52,54]. There are numerous uses for zeolites in industry, the most important being catalysis, but others include gas separation, selective adsorption and ion exchange.

Catalysis

Zeolites are extremely useful as catalysts for several important reactions involving organic molecules [74]. The most important are cracking, isomerization and hydrocarbon synthesis. Zeolites can promote a diverse range of catalytic reactions including acid-base and metal induced reactions. Widespread applications of zeolites as catalyst materials are found in FCC and HC [52,75,76]. Apart from that, there are other applications of zeolites in oil refineries, such as alkylation, isomerization, dewaxing and reforming [52]. In petrochemical complexes, the production of cumene and ethylbenzene, as well as the isomerization of xylenes are key examples of zeolite-based catalytic technologies. More recently, methanol-to-hydrocarbons (MTH) technology has been commercialized for the production of gasoline, aromatics and olefins, including propylene [77]. Zeolites are core to MTH catalysts, while zeolite-based

catalysts have also found applications in the treatment of car exhaust gases (i.e., NO_x removal). Zeolites are also explored for their use in biomass catalysis and in the low temperature activation of methane to form oxygenates, such as methanol [78]. The reactions can take place within the pores of the zeolite which allows a greater degree of product control.

The major advantages of zeolites over usual catalysts are due to their acid strength and to their adaptability to practically all types of catalysis. Numerous potential applications of zeolites have been found in the synthesis of petrochemicals. Zeolite structures can serve as hosts for small metal particles as well as acid-base catalyst which help to apply as a support material because of their unique features such as large surface area, cage like pore structure and high thermal stability. The metal ions can bond with the zeolite crystal lattice as a very small particle with the same dimension of the zeolite cage as well as channels. Metals attached with zeolite can enhance its activity depending on the type of metal attached. The metal ions are normally introduced into zeolite by ion exchange or wet impregnation method followed by activation by calcination at high temperature.

Gas Separation

Zeolites are often applied as an adsorptive agent and widely used for gas separation [12]. The porous structure of zeolites can be used to "sieve" molecules having certain dimensions and allow them to enter the pores. The mechanism for adsorption in zeolite system depends on factors such as, pore size of the zeolite as well as the physical and chemical makeup of the zeolite. This property can be fine-tuned by variation of the structure by changing the size and number of cations around the pores [12]. Polymeric membrane technology has received extensive attention in the field of gas separation. To improve gas separation performances, researchers have focused on improving polymeric membranes selectivity and permeability by fabricating mixed matrix membranes. Here, inorganic zeolite materials have been incorporated and distributed in the organic polymer matrix to enhance the separation performance of the membranes [12]. Huang et al (2009) effectively demonstrated synthesis of aluminium zeolite beta using a silica source having high specific surface area by conventional hydrothermal route in a very short crystallization period which is used for manufacturing composite polysulfone membranes for gas separations [55]. Performance has been significantly enhanced compared to the intrinsic properties of the polymer matrix.

Ion Exchange

Most zeolites have a natural ion exchange ability which is one of the most important properties of zeolite and make them commercially attractive. Hydrated cations within the zeolite pores are bound loosely to the zeolite framework, and can readily exchange with other cations when in aqueous media. This property of zeolite is due to the isomorphous substitution of the silica ion (Si^{4+}) by an aluminium ion (Al^{3+}) in the zeolite framework resulting in a negative charge [4]. Natural or modified zeolites have been applied in water softening (salinity reduction). The mechanisms governing the salt removal process by zeolites are mainly ion exchange, adsorption, and salt storage. Factors such as zeolite's geochemical properties, pH, co-existing anions, concentration, valency, surface charge, and experimental conditions all influence the ion exchange process [71,79,80]. Clinoptilolite, a natural zeolite, was investigated as adsorbent for wastewater purification. Due to significant adsorptive properties they can be used for the removal of different pollutants such as heavy metals, oil and organic contaminants [71]. The presence of non-toxic exchangeable cations in zeolite structures such as Na^{+}, K^{+}, Mg^{2+} and Ca^{2+} makes the zeolites suitable for wastewater treatment.

2.1.4 Zeolite synthesis

The basic understanding of the chemistry of zeolite structures and their modification to get the required structure for a particular application has led to development of different routes of preparations. However, the choice of the synthesis method depends on the type of zeolite that needs to be synthesized. Each method has some advantages and disadvantages which are represented in Table 2.1. Apart from this, many attempts have also been given on the use of different sources of raw materials in order to get a suitable zeolite having versatile properties. But, the major parameter is the proper content of the alumina and silica in the raw materials. The general method for zeolite synthesis is shown in Fig.2.5. Apart from that a host of other factors such as the cost of raw material, abundant availability, presence of impurities are also important for proper selection of raw materials [43]. Following subsections describe different synthetic routes of zeolite from various raw materials.

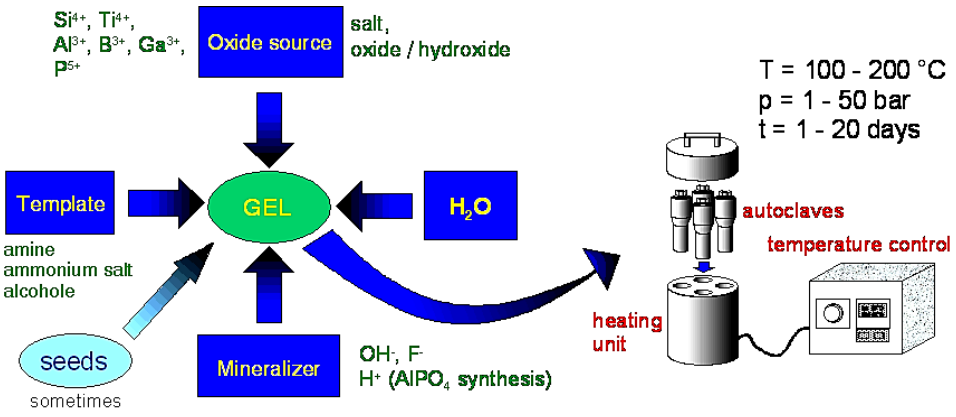

Fig. 2.5. Synthesis of Zeolite [81]

2.1.5 Method for Zeolite synthesis

Hydrothermal Method

The hydrothermal method is one of the basic methods of synthesis of zeolite which was introduced by Barrer in the year 1948. The synthesis is carried out in the presence of water as a solvent as it is an abundantly available and inexpensive source. Apart from that a base solution is used as a mineralizer at appropriate temperature and pressure. The reactants are usually put inside a Teflon-lined steel autoclave with hydrothermal synthesis pressure (up to 15 bars). The temperature varies from 90–180°C. Since the temperatures required in this method is lower, this method is comparatively effortless and cheaper than other methods [43,81]. Some of the advantages which made this method popular include low energy consumption, high reactivity, ease of maintenance, formation of metastable phases and unique condensed phases. Nucleation and crystallization of the crystals do not necessarily occur in solution but can take place at the gels present in the mixtures. This method is employed for synthesis of a wide variety of zeolites [18,29,51,81].

Synthesis of zeolite through the hydrothermal route is a multiphase reaction-crystallization process, usually encompassing at least one liquid phase and both amorphous and crystalline solid phases [18]. The major factors which affect the performance of hydrothermal method and the quality of the end product are temperature and pressure of the reaction vessel (autoclave), batch composition, silica and aluminium ratio of the precursor, reactant materials, overall alkalinity, ageing time, template condition, and seeding (Fig. 2.5). Microwave assisted hydrothermal

methods can rapidly achieve high temperature and high pressure, thereby shortening the processing time significantly and as a result found wide acceptance [82,83].

Solvothermal Methods

Solvothermal method of zeolite synthesis involves the use of any other solvent apart from water to produce the zeolite. There are however other solvents such as alcohols (e.g., methanol, ethanol, pentanol), hydrocarbons, ethylene glycol, pyridine, etc. that have been used successfully for zeolite synthesis [84]. The solvent used varies in terms of polarity and hydrophilicity. The solvothermal method is highly dependent on the temperature and pressure of the autoclave. Apart from that other factors like sources of raw material, composition of raw material, silica and alumina ratio, ageing time, alkalinity, mixing conditions, seeding time, and type of solvent used. However, the solvents may be carefully chosen based on their toxicity and safety. Environmentally benign solvents are preferable. Solvothermal methods can be combined with modern techniques like microwaves for better performance. Jamil et al (2016) demonstrated that the zeolite crystal (ZSM-22) morphology was successfully controlled using a microwave-assisted solvothermal fabrication method [85].

Ionothermal Methods

Ionothermal method of zeolite synthesis employs ionic compounds as solvent. The ionic nature of the solvents has an effect on some particular properties such as low vapor pressures. Hence, the ionic liquids simultaneously act both as solvent and potential template in the formation of solids. This is especially helpful for separation of products since both solvent and template are the same species. In addition, the ionothermal method produces a large size of crystals and the ability to create a crystalline phase. It is also easy to control the composition of growing crystals. Wang and Yan (2010) synthesized NaY zeolite by a combination of ionothermal and microwave techniques with good properties like larger surface area and mesopore volume, better thermal stability, higher cracking activity, higher gasoline selectivity, lower coke and gas selectivity [86]. Han et al (2021) prepared hierarchical porous triclinic SAPO-34 zeolites using an ionothermal method [87]. But the ionic liquids suffer from drawbacks due to high toxicity. Deep eutectic solvents which are a class of ionic liquids are used of late due to their low toxicity and environmentally friendly nature.

Sol-gel method

It is a physicochemical process that involves the formation of an inorganic colloidal suspension (sol), and the gelation of the sol in a continuous liquid phase (gel) to form a three-dimensional network structure [43]. The sol-gel process involves the transition of a solution system from a liquid “sol ”into a solid “gel ”phase. This method provides better control of the technique which ulti- mately provides higher porosity and definite particle size. The major factors which can influence the performance of this method are: (i) hydrolysis rate, (ii) temperature, (iii) heating rate and (iv) pH. For example, Pandiangan et al. (2019) prepared the porous and multiphasic zeolite A by using sol-gel technique from rice husk silica and aluminium metal [26]. Wu et al. (2009) reported a two-step sol–gel route for the synthesis of MCM-22 zeolite under static hydrothermal conditions using tetraethyl orthosilicate as a silica source [88]. Increase of temperature and pH value for the hydrolysis of tetraethyl orthosilicate favours the shortening of crystallization time and decreasing of MCM-22 particle size. Moreover, by adjusting the hydrothermal reaction parameters, such as increasing the crystallization temperature, increasing the alkalinity of the synthesis gel mixture, and decreasing the SiO_2/Al_2O_3 ratio, the crystallization is accelerated substantially [88]. Sol-gel process can be combined with other techniques like microwave heating to prepare zeolites. Sathupunya et al (2003) utilized a combination of sol-gel and microwave heating using alumatrane and silatrane as precursors to prepare Na-A (LTA) zeolite [89]. The major advantage of this method is that this method does not require specialized and expensive equipment and produces a high quality product with homogeneity due to mixing at the molecular level. However, the high cost of precursors becomes a limitation which needs to be overcome in the future.

Modern techniques

Microwave method

In the microwave heating method, microwave radiation is applied for the synthesis of zeolites and is considered a fast and energy efficient technique [90]. The microwaves are high frequency electric fields which generate the heat required for carrying out the reaction [9]. The main advantages of using microwaves includes reduction in time, and better quality of

zeolite in terms of small particle size and high purity [11]. For example, Sapawe et al. (2013) utilized microwave irradiation for synthesis of zeolite NaA and claimed that synthesis time was shortened by sixteen times compared with the conventional method [91]. Le et al. (2019) demonstrated a fast microwave heating method for the liquid phase synthesis of zeolite Y under high temperature conditions [92]. The major factors that affect zeolite synthesis by microwave method are molar ratio of SiO_2/Al_2O_3, alkalinity of medium, wavelength generated by the magnetron, zeolization time, crystallization time and temperature maintained during zeolization and crystallization [82,93]. Microwave-assisted ageing reportedly helped in shortening the crystallization time and reduced crystal size of the zeolite products without any significant impact on their catalytic activities [94]. For the synthesis of zeolites, microwave assisted is applied in combination with other methods such as hydrothermal [82,83], solvothermal [85] and ionothermal [86].

Ultrasonic method

The ultrasonic waves having frequency between 20 kHz to 2 MHz is solely responsible for the development of a new branch named sonochemistry which is widely used in synthetic chemistry for the development of new compounds or modifying the chemical reaction process [95]. Ultrasound waves have shown to significantly influence the synthesis process of various amorphous or crystalline materials and polymerization reactions. Owing to high influences on crystallization phenomenon, application of ultrasound has received immense attention in zeolite synthesis. The advantages of this method include particularly simple, rapid reaction, no requirement of complex facilities, rapid crystal growth rate, uniform particle size distribution and morphology and provide control over the nucleation process (Table 2.1) [96]. Ultrasound generates microscopic bubbles, which lead to subsequent growth and explosive collapse of the bubbles termed as cavitation process [97]. Due to this ultrasonic irradiation provides rather unusual reaction conditions (a short duration of extremely high temperatures and pressures in liquids) that cannot be realized by other traditional methods [98]. The cavitation can also raise the secondary nucleation rates and the crystal purity in the time of cooling crystallization [39]. Ultrasound energy method has also generated interest as it offers zeolite synthesis with tunable properties. For example, Pal et al. (2013) demonstrated the synthesis of NaP zeolite nanocrystals at ambient temperature within short crystallization time

using ultrasound technique [99]. Herein, sonication energy enables the formation of active radicals which lead to rapid crystallization of the zeolite phase. Huang et al (2016) reported synthesis of hierarchical structured ZSM-5 zeolites with a long life catalytic activity via the ultrasound assisted method [100].

Table 2.1: Comparison of the various methods of zeolite synthesis

Method	**Type of zeolite**	**Advantages**	**Disadvantages**	**Ref.**
Hydrothermal	A, Y, beta NaX ZSM-5	Simple equipment (autoclave), low cost, uniform size distribution of crystal	High temperature and high pressure condition	[18,19,29,55,82,101]
Solvothermal	ZSM-22	Ease of control over size, uniform shape distribution, crystalline product	Expensive autoclave requirement, requirement of organic solvent, disposal issues	[85]
Ionothermal	NaY SAPO-34	Large crystal size, ease of crystal composition control	High operating time, generation of toxic chemicals, environmentally harmful	[86,87]
Sol-gel	Na-A (LTA) NaY ZSM-5 MCM-22	Versatile method, low energy consumption, simple and inexpensive equipment	high cost of precursor, precipitation of a particular oxide during sol-formation, difficult to avoid residual porosity and hydroxyl groups	[26,88,89]
Microwave	Y Na-X ZSM-5 ZSM-22	Faster reaction rate, selective heating, higher temperature	Difficulty in heat energy control, water evaporation	[82,83,102,103]
Ultrasound energy	Y ZSM-5	simple operation, rapid and fast reaction, simple facility, high crystal growth rate, uniform particle size, uniform morphology of crystals, provide control over nucleation process	issues of scale-up, energy efficiency is questionable	[94,103–105]

Similarly, Kong et al (2014) observed that ultrasonic-assisted methods may be a favourable route to prepare nanosized hierarchical ZSM-5 with shorter induction time for nucleation, better surface area, pore size and pore volume [104]. The enhancement of nucleation and crystallization rate during the synthesis of zeolite A was observed using ultrasound method [106]. The ultrasound method is also employed in combination with conventional methods to develop zeolite materials more efficiently. Mu et al. (2017) reported pre-treatment prior to hydrothermal crystallization with a sonochemical-assisted method to manufacture SSZ-13 zeolite that helped in reduceing the overall time for zeolite synthesis [107]. Similarly, ultrasonic/microwave synergistic synthesis of zeolite Y is reported which was reported to be a good alternative for the synthesis of micro-mesoporous zeolite Y providing numerous advantages in the form of large surface area, bulky pore volume, excellent crystallinity and less hydrothermal time [103]. Apart from that, the ultrasonic monitoring technique has also elicited great interest to contribute to the understanding of the complexity of the zeolite formation process. The in situ ultrasonic monitoring technique is an indirect, non-invasive, phase insensitive method that is based on investigating the degree of interaction of ultrasonic wave transport properties with the zeolitic precursor species as it travels through the synthesis mixture [108].

Green synthesis

It is pertinent to note that though hydrothermal conditions are easier to implement, still the process suffers from certain drawbacks. The process has shortcomings as it is perceived to be not “clean” enough to be considered a “green” process [109]. The process depends on the use of organic templates that are ultimately removed by calcination at high temperature, or extraction using an organic solvent [42]. The energy and environmental costs associated with the template removal and the emission of greenhouse gases during combustion of the toxic organic templates are a cause of concern. Additionally, low concentrations of silicon and aluminium species are often required to prepare a clear aqueous solution that is suitable for the successful crystallization of zeolite. This leads to a lower yield of zeolite products and requires multiple recycling treatments for the excessive residual solution. Green synthesis of zeolites take into account the above shortcomings and counter it by adopting any of the following methodologies: (a) develop synthetic methods that do not require a template or use

a recyclable, inexpensive, or renewable template; (b) synthesis of zeolites that use sustainable silicon or aluminium sources; (c) employ methods that are solvent-free; and (d) simplistic synthesis methods aimed at improving yield and efficiency , e.g., microwave heating to shorten the crystallization time, ultrasonic irradiation for faster crystal growth with better size control, solid phase (or quasi-solid phase) synthesis to promote product yield, or continuous-flow synthesis to achieve high productive efficiency [41,42,110].

Since the principal raw materials used to manufacture zeolites are silica and alumina, different types of abundantly available clays minerals like kaolinite, bentonite, montmorillonite, etc. provide a sustainable source of the same. Kaolin and bentonite is inexpensive and contain a high percentage of silica and alumina.

Crystallization of zeolites by the conventional static hydrothermal method has a few limitations. Slow rate of mixing in conventional methods often leads to an increase in supersaturation to an unstable level that causes uncontrollable nucleation. Sometimes agitators are usually employed to overcome this issue but agitators only promote the motion of macroscopic layers. Mixing inside the layers depends on the slow diffusion of reactant molecule which remains unaddressed leading to uncontrollable nucleation and larger crystal size. Another problem in conventional methods is the long crystallization time which usually takes more than 24 hours. Sonochemical synthesis by ultrasonic irradiation offers a better alternative with faster crystal growth rate simultaneously providing better control over the nucleation process. It also improves particle size distribution and morphology. Over and above, the sonochemical synthesis is simple, fast, and does not need any complicated facilities. Hence, ultrasonic assisted hydrothermal synthesis has been widely accepted as a firm step toward green synthesis. A brief overview of the effect of ultrasonication on synthesis/modification of zeolite Y and other zeolites are presented in Table 2.2.

Table 2.2: Effect of ultrasonication on synthesis/modification of Zeolite Y and other zeolites.

Source	Treatment method	Si-Al ratio	Surface area (m^2/g)	Pore volume (cm^3/g)	Pore size (nm)	Ref.
NaY zeolite	Alkaline treatment with 0.5N NaOH followed by ultrasound treatment with 200 W for 60 min in 30°C	3.95	778.6	0.363	2.50	[105]
Chemical template	Combination of microwave and ultrasound	Not reported	752	0.4	3.89	[103]
Zeolite Y	ultrasound irradiation (30 min) and acetylacetone extraction	3.03	552	0.185		[111]
Zeolite Y from from Zeolyst International	ultrasonicated at 65°C for 5 min in an ultrasonic bath (U500H,50–60 Hz).	4.25	681	0.46		[112]
Zeolite Y from aluminosilicate gel	Ultrasonication (150 W) at 90°C (±1 °C) using circulating oil bath for 3 h followed by filtration, washing and drying overnight at 80 °C.	Not reported	80.66	0.001	14.79	[113]
ZSM-5	Ultrasonication at 80°C for 1h in an ultrasonic bath.	Not reported	478	0.41	6.36	[104]
MCM-36 from MCM-22 precursor	Ultrasonic treatment for pilloring process in an ultrasonic water bath for 3h at 50°C	Not reported	664	0.7	5	[114]
H-ZSM-5	Ultrasonication at 180°C for 1h in an ultrasonic bath (50W, 40kHz).	Not reported	416.58	0.846	14.87	[94]

2.1.6 Zeolite synthesis raw materials

Zeolites can be synthesized from different raw materials which can be either natural or synthetic. However, all raw materials are not suitable for synthesizing the zeolite from the economic and compositional point of view. Hence, raw materials should have desirable properties. They should

be cheap, abundantly available, inexpensive, and have minimum impurity. Synthetic zeolites made from natural or synthetic raw materials having a wide range of chemical properties, pore size, and better thermal stability are commercially widely used compared to natural zeolites because they are of higher purity and have a more uniform particle size. The preparation of synthetic zeolite from silica and alumina chemical sources are expensive, yet cheaper raw materials such as clay minerals, natural zeolite, municipal solid waste, coal ashes, industrial slag, incineration ashes, etc. which serve as combined sources of silica and alumina are being used as starting materials for zeolite synthesis [43,115–117]. Currently a host of ongoing research work is focused on the use of clay and other raw materials in zeolite synthesis, which has the advantage of being relatively cheaper, readily available and more abundant. Industrial byproducts such as coal fly ash, a by-product of thermal power plants, containing Si- and Al-containing compounds is reportedly one of the most abundant industrial solid wastes which is used for the zeolite synthesis [24,25]. However, presence of unwanted toxic metallic elements which are difficult to remove restrict the full application of such materials to synthesize zeolites. Rice husk ash (RHA) contains a high percentage of amorphous silica (90%–96%) and also has high calorific value besides being low cost and is considered a sustainable raw material for zeolite synthesis [26,27]. Similarly, waste perlite is a source of reactive silica, and hence can be used for the synthesis of zeolites [117]. Waste glass, which has a high proportion of SiO_2, is also proposed as a suitable precursor for the zeolite synthesis via a hydrothermal process. Blast furnace slag (BFS) which contains CaO, SiO_2, Al_2O_3 and MgO apart from metallic elements such as Fe, Ti and Mn is also a potential source of raw materials for zeolite synthesis [28].

Zeolite synthesis from clay minerals has been investigated extensively of late due to the large availability of raw clay materials, their relatively low cost and favourable chemical characteristics [43]. Many recent studies focused in particular on the use of kaolinite, because of its extensive availability and the well-known reactivity of thermally treated kaolin clays (metakaolin) with acid and alkali solutions [32,38,118–120].

2.1.7 Zeolite characterization

Zeolite characterization used to identify the crystalline product by comparing its properties to those of known standards (Fig. 2.6). X-Ray diffraction, Scanning electron microscopy, thermogravimetric analysis, compositional analysis (X-Ray fluorescence) and the crystal size of the synthesized zeolite are methods used to describe a particular type of zeolite.

Atomic absorption spectrometry (AAS)

Atomic absorption spectrometry (AAS) is applied for the measurement of the concentration of an element. This analytical technique involves the absorption of light by free atoms or ions of an element at a wavelength specific to that element. In AAS, emission, absorption and fluorescence energy is applied into the atom population by thermal, electrical, electromagnetic and chemical forms of energy which is converted to light energy by various atomic and electronic processes before measurement. It is applied for the detection as well as for the quantitative determination of many elements present in samples. The technique is very specific and individual elements in each sample can be reliably identified. AAS technique is also very sensitive, making it possible to detect minute amounts of an element (upto parts per billion) in a sample.

X-Ray diffraction (XRD)

X-ray diffraction (XRD) is an essential tool in the identification and characterization of zeolites at various stages in their syntheses, modifications, and application as catalysts. XRD is commonly used to identify the presence and quantitatively determine the amount of crystalline zeolite present. It provides the unit cell parameters of the product. X-ray diffractometer is primarily based on the elastic scattering theory. During this activity, the sample is subjected to an X-ray beam. The intensity of the emergent rays is recorded as a function of the deflection angle 2Ɵ. The diffraction patterns differ depending on the types of zeolites and hence the diffraction patterns are unique for each zeolite. The purpose of XRD patterns is to determine the unit cell parameters and thus its unit cell volume. Powder XRD measurements use Cu-Kα radiation to study the crystal structure of zeolite, crystal size of zeolites, approximate extent of heteroatom substitution, and presence of defect in zeolites. Phase identification can also be performed by XRD.

Fourier transform infrared spectrometry (FTIR)

The FTIR measures vibrations caused by internal stretching of the framework tetrahedra and vibrations related to the external linkages between the tetrahedra. The spectrometer has two mirrors, a fixed mirror and a moving mirror, a detector and a beam splitter. A radiation from the IR source is directed to the beam splitter, which splits the beam into two parts, one to the

fixed mirror and the other to the moving. FTIR is operated based on the principle of diffuse reflectance. An incident beam emits a spectra of both absorbance and reflectance features. A detector records radiations that pass through the sample. Calibrations on the detector enable radiation to be read in the form of energy signals. In case of zeolites, FTIR is used to confirm the fundamental vibrations of silica-alumina in the zeolite structure. FTIR spectroscopy is used to specify the functional units of zeolites and to predict the reaction mechanism in the zeolite framework. The FTIR spectrum is also used to indicate the secondary building units which are present in the zeolite structure.

Scanning Electron Microscopy (SEM)

SEM is a versatile advanced instrument, which is largely employed to observe the surface phenomena of the materials. It is used to study the surface of solids and give information about their morphology and topology. It has played a major role in the understanding of zeolitic materials. The size of zeolites studied with this apparatus is between 20nm and 20μm. Information gathered from the SEM picture makes us understand the material morphology (shape and size) and topography which indicates the surface features i.e. “how it looks”, texture, roughness. In case of zeolite, the SEM analysis of its crystal form helps to determine the type of zeolite, crystal form and size, external surface such as relative roughness, presence of other zeolite types or any other impurity.

SEM consists primarily of an electron gun, electron lenses, scan coils and detectors. The electron gun generates a beam of electrons from a cathode or filament usually made of tungsten. The electrons escape at high voltage from the filament. The final size of the beam is controlled by the electron lenses. Scan coils make the beam scan over the sample or target. When the electrons hit the target, they collide with electrons in the inner atomic shells. Backscattered and secondary electrons that escape from the sample are detected. If there is no detection, the image will be black [36]. In some cases, the sputter coating sample preparation technique is applied to improve image quality and resolution. Due to their high conductivity, coating materials can increase the signal-to-noise ratio during SEM imageing and thus producing better quality images. The most common sputter coating material is gold.

Thermogravimetric Analysis (TGA/DTA)

TGA is one of the fundamental methods in thermal analysis which is simply the determination of the mass of a sample as a function of temperature. Here, the sample is subjected to a controlled temperature program by a suitable technique. The sample is placed into a ceramic crucible on a sensitive microbalance. The crucible is surrounded by a computer controlled oven. A flowing stream of gas allows the background atmosphere to be controlled. To avoid oxidation of the sample, inert gas like nitrogen is applied. The mass of the sample decreases by the evolution of a gas or the volatilization of a liquid decomposition product which is measured as a function of temperature or time. A typical thermogram is a series of plateaus at decreasing mass, as each successive step of decomposition occurs. This measurement provides information about physical phenomena, such as phase transitions, absorption and desorption; as well as chemical phenomena including chemisorption, thermal decomposition, and solid-gas reactions (e.g., oxidation or reduction). In most cases the differential weight loss over time (-dm/dt) known as Difference Thermogravimetry (DTG) is also measured simultaneously.

Differential Thermal Analysis (DTA) is a technique where the temperature difference between a substance and a thermally inert reference material is measured as a function of the temperature. Both the substance and reference material are subjected to a controlled temperature program. The sample material and an inert reference are made to undergo identical thermal cycles, (i.e., same cooling or heating program) and in the process the temperature difference between sample and reference is recorded. This differential temperature is then plotted against time, or against temperature (DTA curve, or thermogram). The changes in the sample, either exothermic or endothermic, is possible to be detected relative to the inert reference. Thus, a DTA curve provides data on the transformations that have occurred, such as glass transitions, crystallization, melting and sublimation. The area under a DTA peak is the enthalpy change and is not affected by the heat capacity of the sample. DTA is one of the oldest and fundamental thermoanalytical methods. The technique is similar to differential scanning calorimetry (DSC).

Gas adsorption/desorption analysis (BET)

In this technique an inert gas, mostly nitrogen, is adsorbed on the surface of a solid material. The physical adsorption mostly occurs on the outer surface but in case of porous materials, also on the internal surface induced by pores. The most widely known is the determination of the BET surface area by gas adsorption, popular as BET analysis. Adsorption of nitrogen at a temperature of liquid nitrogen, i.e. 77 K, leads to a so-called adsorption isotherm, or BET isotherm, which can be measured over porous as well as non-porous materials. The type of material can be classified based on standard isotherm types. Non-porous materials will display a type II isotherm on which the BET surface area can be determined. Porous materials will typically provide a type I or type IV isotherm, depending on the type of pores present. Sometimes the use of argon adsorption or carbon dioxide adsorption is preferred in case of presence of small micropores. Samples having low surface area are characterized preferably by krypton gas adsorption. The principle of monolayer formation of gas molecules on the solid surface is used to determine the specific surface area. The BET model employing a linearized BET equation is then used to transform the experimental adsorption isotherm into a BET plot to determine the monolayer volume. The cross section area of the gas molecule together with the monolayer volume is then used to calculate the total specific surface area expressed in m^2/g. The gas adsorption technique is also applied to assess the presence of pores, not only in terms of pore volume but also as a pore size distribution. The principle of capillary condensation in pores is applied to determine the pore size distribution since the capillary condensation in pores is pore size dependent. A higher pressure is needed to induce condensation in larger pores. Likewise, smaller pores are filled at lower partial pressure of the adsorbing gas. It is necessary to pre-treat the sample at elevated temperature in vacuum or flowing gas in order to remove any contaminants before the actual measurement. It is crucial to tune the pre-treatment conditions to the materials properties as a too low or too high temperature can seriously affect the BET surface area derived from the subsequent BET analysis. Figure 2.6 provides a glimpse of the classification of the characterization techniques applied for the structural and compositional analysis of zeolites.

2.2 Zeolite Y structure and properties

Zeolite Y has faujasite (FAU) framework structure, having an internally connected complex network of micropores. The pores, which are formed by 12 Si or Al atoms, are linked through O atoms forming a tetrahedral structure. The pores have a moderately large diameter of 7.4 Å forming a porous structure. 10 sodalite cages surround the inner cavity with a diameter of 12

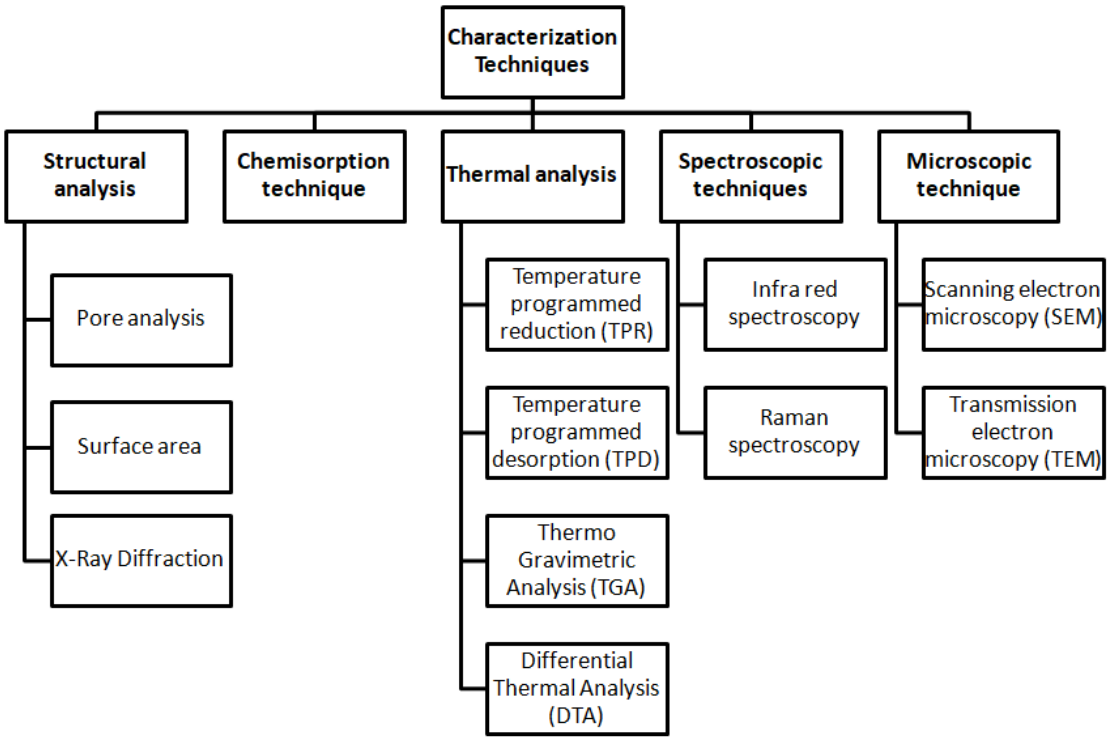

Fig. 2.6. Characterization techniques applied for the structural and compositional analysis of zeolites

Å. The unit cell of the zeolite has a cubic structure having high thermal stability and good Bronsted acidity [44,45]. Zeolite Y has a similar three-dimensional structure to faujasite, where the unit cell is cubic with a very large dimension (a = 24.7 Å), and it contains 192 total SiO_4 and AlO_4 tetrahedra [56]. The structure consists of 24-truncated cub-octahedral units "sodalite cages" created by SiO_4 and AlO_4 tetrahedra, joined by six membered rings "known as hexagonal prisms". The structure can be considered as a diamond structure, with the sodalite playing the role of a carbon atom, and the double 6-rings the role of C-C bonds. The unit cell contains eight "super-cages" cavities, with free diameters of about 11.8-13 Å, and

apertures of 12-membered oxygen rings with free diameters of about 7.4 Å, which interconnect these cavities. This is the largest void space of any known stable zeolite and amounts to over 50% volume of the crystal. The pore volume equals 0.35 cm^3/g and the rigid framework structure of type Y zeolites amounts to around 1.30 g/cm^3, giving a topology density of 0.48 solid volume/unit cell volume. It is highly acidic with the Si/Al molar ratio of 2.43, which makes it an ideal cracking catalyst [69]. These attractive characteristics play a vital role in widespread application of zeolites.

(a)

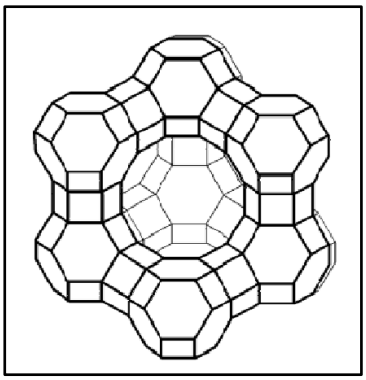

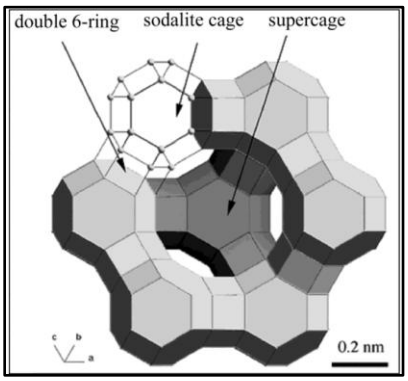

(b)

Fig. 2.7. (a) The structure of Zeolite Y [121], (b) The double ring, sodalite and super cage of zeolite Y [122]

2.2.1 Zeolite Y synthesis

Zeolite Y can be synthesized by using various sources of silica (SiO_2) and alumina (Al_2O_3). As the chemical sources are costly and hence increase the cost of final product, hence cheaper raw materials sources such as clay minerals, waste material like rice husk, coal ashes, industrial slag, incineration ashes, etc. which contain good amount of silica and alumina are being used as raw materials for zeolite synthesis. Currently a host of ongoing research work is focused on the use of clay in zeolite synthesis, which has the advantage of being relatively cheaper, readily available and more abundant. Industrial byproducts such as coal fly ash, a by-product of thermal power plants, containing silica and alumina containing compounds is reportedly one of the most abundant industrial solid wastes which is used for the zeolite Y synthesis. However, presence of unwanted toxic metallic elements which are difficult to remove restrict the full application of such materials to synthesize zeolites. Rice husk is an agricultural waste and is mainly used for energy generation but has been reportedly used as

raw materials to develop technological products such as high purity silica ash, silicon carbide and zeolites [27]. Rice husk contains about 20-30 weight percent silica. RHA, attained by burning of rice husk is also an agricultural excess. RHA is generally used as soil ameliorants to help break up clay soils and improve soil structure but is also used as a silica source as an insulator in the steel industry and as a pozzolan in the cement industry. Silica derived from RHA has been used to synthesize zeolite Y [27]. Fly ash from thermal power plants is known to cause environmental and health problems but also has been an important silica source and has been used to synthesize zeolite Y. As fly ash contains mainly amorphous aluminosilicate (glassy phase) and some crystalline minerals (quartz, mullite, hematite, etc.), it can be effectively used as a raw material for the synthesis of zeolite Y [24]. Natural silica-rich materials including acidic volcanic glasses, such as natural and expanded perlite and pumice has been used as a suitable precursor to synthesize zeolite Y [117].

Zeolite synthesis from clay minerals has been investigated extensively of late due to the large availability of raw clay materials, their relatively low cost and favourable chemical characteristics. Previous studies focused in particular on the use of kaolinite, because of its extensive availability and the excellent reactivity of thermally treated kaolin clays (metakaolin) with acid and alkali solutions[38,123,124] .

Table 2.3: Analysis of kaolin clay obtained from various regions.

Composition	**Kankara, Nigeria** [118]	**Iraq** [125]	**Yunnan, China** [126]	**Bongawan, Malaysia** [19]	**Poland** [127]	**Iran** [128]	**Bangka, Indonesia** [129]
SiO_2	47.3	58.1	56.9	63.5	52.5	57.6	49.8
Al_2O_3	36.8	15.9	31.6	27.9	34.5	30.7	30.5
Fe_2O_3	0.71	3.19	0.47	2.61	0.8	0.15	0.69
TiO_2	0.16	-	-	0.8	-	0.08	0.29
Na_2O	0.05	0.15	0.46	-	0.0	0.04	0.45
MgO	0.16	1.22	0.18	1.39	0.1	0.001	1.07
CaO	0.08	4.11	0.11	-	0.1	0.08	1.49
K_2O	1.01	0.07	1.95	3.45	0.6	0.01	0.59

Table 2.4: A brief overview of acid treatment of kaolin clay

Kaolin Treatment	**Region**	**Remarks**	**Ref.**
Different concentration of H_2SO_4	WB, India.	Al_2O_3, MgO, CaO, K_2O, TiO_2 and ZnO contents in the acid treated material decreased progressively simultaneously increasing the SiO_2 content.	[130]
6M HCl Treatment	Inner Mangolia, China	Converted to metakaolin by calcining kaolinite at 800 ºC for 2h. Then leached in 6M HCl solution (solid/liquid ratio 1:5, g mL^{-1}) with stirring.	[131]
3M HCl Treatment	Saudi Arabia	Calcination conditions were optimized at 600 ºC and 1 h result in 62.94% extraction of alumina.	[132]
Different concentration of H_2SO_4	Nileshwar, Kerala	Refluxing the sample with various conc. of H_2SO_4 in the S/L ratio 1:4 for 45 minutes at 600ºC. Enhances its surface acidity. The maximum acidity was shown by 3N H_2SO_4 treated sample.	[32]
Purification and H_2SO_4 treatment	Arobieye village, Ogun state	Clay was purified by clay split method. The purified clay was calcined and converted to metakaolin at 850 ºC for 6 h. The metakaolin was dealuminated by using conc. H_2SO_4. Due to this all impurities like quartz and oxides of metals were removed.	[133]
H_2SO_4 treatment catalyst for esterification	Amazon kaolins Flint Kaolin	Catalysts for the esterification of oleic acid with methanol was done. MC9S4 was the sample with the lowest Al content and greatest number of acid sites gives highest conversion values.	[134]
HCl treated catalytic pyrolysis using clay	CES, NUST , Pakistan	Polymer waste material was subjected to catalytic pyrolysis using acid treated kaolin clay. Higher acidity as in the case of kaolin clay treated with 5M increased the gas yield.	[135]

2.2.2 Zeolite Y synthesis from Kaolin

Since, kaolin clay originates from various sources; their composition varies with geographical location (Table 2.3). The chemical composition and crystalline phases also vary with the

geological layer of the soil from where they are extracted. Hence, the protocol for synthesis of zeolite Y from kaolin clay is not standardized.

The main steps of zeolite Y synthesis from kaolin clay include: initial physico-chemical treatment for impurity removal (metal oxides along with some amount of dealumination) which is done by acid or alkaline treatment followed by calcination at high temperature; addition of external silica and/or dealumination depending on the silica-alumina ratio; activation of kaolin at high temperature for 4-6 hours to get metakaolin; ageing of reaction mixtures at ambient temperature (gel formation) followed by crystallization. Acid activation results in leaching of the clays with inorganic acids, causing disaggregation of clay particles, elimination of mineral impurities, and dissolution of the external layers, thus altering the chemical composition and the structure of the clays[130]. The solubility of the clay minerals in acids differs. The solubility of kaolinite in acids varies with the nature and concentration of the acid, the acid-to-kaolinite ratio, the temperature, and the duration of treatment [130]. For acid activation, HCl and H_2SO_4 are desirable as it requires moderate process conditions and produces better results with respect to structural properties [33,136]. As kaolin clay is more soluble in H_2SO_4, leaching with H_2SO_4 results in better structural meltdown thus altering the clay structure and transforming the chemical composition by removing metal impurities [30,130,137]. The reaction between kaolinite and H_2SO_4 is described by the chemical equation [138] $Al_2O_3 \cdot 2SiO_2 \cdot 2H_2O + 3H_2SO_4 \rightarrow Al_2(SO_4)_3 + 2SiO_2 + 5H_2O$. Acid treatment of kaolinite by H_2SO_4 has been reported in literature [119,139]. A brief overview of kaolin clay treated with various acids is presented in Table 2.4. The time required for activation, ageing, crystallization and temperature required for activation, crystallization varies with respect to the clay composition. Consequently the SiO_2/Al_2O_3 ratio and the surface properties like pore volume, pore size and surface area of the synthesized zeolite can be tuned considerably.

2.2.3 Zeolite Y synthesis from Bentonite

Bentonite clay is available in abundance in the Kachchh region in Gujarat, India with an estimated reserve of 144 million tons [140]. The reserves are rich in both sodium and calcium based bentonite. Bentonite clay is industrially valued due to its favourable physico-chemical properties such as high plasticity, lubricity, dry bonding strength, shear and compressive strength and low permeability and compressibility which makes it extremely suitable for

variety of applications such as drilling fluid for mining activities, foundry sand binding, iron ore pelletization, waterproofing and sealing agent, etc. However, additional positive textural properties like high specific surface area and pore volume, highly organized layered structure, excellent cation exchange capacity coupled with chemical and mechanical stability makes bentonite clay appropriate for application as catalyst as well as adsorbents in a wide range of chemical process industries [141–145]. Being a green, nontoxic and low-cost raw material, additional treatment of raw bentonite clay can modify the structure of clay and augment the required textural properties making it a valuable material for catalytic and adsorbent applications.

The structural transformation and properties modification can be done by different treatment methods like chemical activation, mechano-chemical activation, intercalation, thermo-chemical activation etc [146]. Other advanced methods like ultrasonic irradiation [147,148] and microwave irradiation [149–151] for structural enhancement are also reported in literature. Acid treatment of clay creates more acidic sites along with greater surface areas compared to the pristine clay which is promising for application as catalyst [152]. Greater emphasis on green catalysis makes acid activated bentonite clay a potential candidate for environmental friendly applications. Acid activated and ion exchanged bentonite clay based designer catalysts are suitable for organic synthesis. Moreover, impregnation of the acidified bentonite clay with additives like Lewis or Brønsted acid compounds, pure metals and/or metal oxides, inorganic reagents can further improve their properties and applicability. Conversely, basicity can also be implied on bentonite clay by compounds like KOH which is used for producing biodiesel from fatty oils. Activated clay-supported heteropolyacids are used for esterification of acetic acid too [37]. Activation using acid is a proven and reliable technique that causes a controlled, peripheral dissolution of the clay generating active sites. The layered structure of bentonite has an alumina octahedral sheet in between two silica tetrahedral sheets providing an uniform crystalline structure. The space in between the layers is occupied with cations like Al^{3+}, Na^{+}, Ca^{2+}, K^{+} etc which are exchangeable. Usage of mineral acids for activation not only provides H^{+} ions which replaces the cations but also causes dissolution of impurities present in the structure [153]. Activation of Bentonite clay using hydrochloric acid (HCl) [153,154], sulfuric acid (H_2SO_4) [155,156] and other acids [157,158] has been reported. Out of all acids, H_2SO_4 is preferred mostly as the activation can

be performed at mild process conditions and the quality of the end product is better with high specific surface area and porosity. The impact of acid treatment on structural properties depends on the leaching condition and the nature of parent bentonite. Bentonite clay obtained from different geographical regions and the result of their treatment with H_2SO_4 is presented in Table 2.5. It can be observed that compared to parent bentonite, the acid treated bentonite shows better textural properties considering large surface area and pore volume with high fraction of mesopores.

Table 2.5: Overview of the physico-chemical changes of raw Bentonite clay before and after H_2SO_4 treatment.

Source	**Treatment conditions**	**Si-Al ratio**		**Specific surface area (m^2/g)**		**Specific pore volume (cm^3/g)**		**Ref.**
		before	after	before	after	before	after	
Hancili, Turkey	Reflux: 3M H_2SO_4, 100^{o}C, 4h.	4.00	5.88	52.77	130	0.11	0.27	[156]
Unye, Turkey	Reflux: 0.4(w/w) H_2SO_4, 90^{o}C, 3h.	2.58	8.09	61	304	0.1	0.4	[159]
Cankiri, Turkey	Reflux: 2M H_2SO_4, 98^{o}C, 5h.	3.73	-	75	241	not reported		[155]
Khorasan, Iran	Reflux: 6N H_2SO_4, 80^{o}C, 2h;Calcination: 600^{o}C, 4h.	4.04	6.09	23	171	not reported		[160]
North China	Reflux: 10 (Wt%) H_2SO_4, 80^{o}C, 4h.;Calcination: 600^{o}C, 4h.	4.67	5.23	10	46.9	not reported		[161]

This structurally enhanced bentonite clay is suitable to be applied as catalysts in esterification reaction [145], oxidation reactions [162], photo Fenton reactions [163], pyrolysis [158], petroleum refining [164]; as catalyst supports for immobilization of nanoparticles [165], TEPA for CO_2 capture, Ag/ZnO for water purification [151] and as adsorbent for removal of pollutants from wastewater [14,154]. Further treatment of this material can be carried out to

develop commercial adsorbents or solid catalysts. Different kinds of solid materials like KOH, NaOH, Zr-SBA-15 can be impregnated on the acid treated bentonite clay to form heterogeneous catalysts for biodiesel production [141,143,144]. It can be further processed to synthesize various type of zeolite like zeolite A [166] and zeolite Y [167,168].

2.2.4 Application of Zeolite Y as catalyst

Zeolite Y is widely used in catalytic cracking due to its specialized properties such as structure stability, hydrophobicity, tunable acidities, confinement effects and catalytic activity [48]. Zeolite Y possessing three-dimensional pore channels with supercages of 1.2 nm in diameter is a leading catalyst in FCC, hydrocracking, and alkylation processes [48]. Catalytic cracking of large molecules such as heavy oil and biomass is one of the most interesting catalytic processes because of its perspective to provide a sustainable route for industrial applications [47]. The ultrastable Y zeolite in fluid cracking catalysts is commonly stabilized by ion-exchange with rare earth (RE) cations and the RE-exchange provides hydrothermal stability to the zeolite by improving surface area retention and inhibiting dealumination, resulting in greater preservation of acid sites [75]. Zeolite Y has been the primary active component of FCC catalysts since its first commercial introduction about 50 years ago. This is mainly because of the unique combination of a few important properties of zeolite Y: (1) high surface area and relatively large pores (~7.4 Å in diameter); (2) strong Brønsted acidity; (3) excellent thermal and hydrothermal stability; and (4) low cost. When other zeolites are used as active components in FCC catalysts, their catalytic performance (activity and product selectivity) cannot compare with that of zeolite Y due to its specialized properties.

2.3 Esterification reaction

Esters are essential natural compounds found in living organisms. They are industrially important compounds with a wide range of applications. Esterification is the process of combining an organic acid (RCOOH) with an alcohol (ROH) to form an ester (RCOOR) and water; or a chemical reaction resulting in the formation of at least one ester product in the presence of an acid catalyst. Many homogeneous acid and base catalysts were used efficiently in esterification reactions earlier. But major shortcomings in the form of separation, reusability, corrosion, product purity and environment hazards have been observed. Esterification reaction using catalysts in homogeneous conditions is more common but suffers

Table 2.6: Esterification reactions using zeolite Y as catalyst

Type of Zeolite	Reaction system	Con.# (%)	Reaction condition*	Remarks	Ref.
H-Y	Acetic acid with C_3 and C_4 alcohols	92	0.5;1:1;130;1	The esterification reaction was found to follow the Eley-Rideal pathway.	[169]
H-Y	Maleic anhydride with methanol	60	4.7;1:3;90;4	The activation energy was found to be 44.65 kJ/mol.	[170]
TPA -H-Y	Oleic acids and free fatty acids with methanol	92.7	14;1:20;120; 6	The catalyst is proved to be reusable. The activation energy of the esterification reaction is 66.3 kJ/mol.	[171]
Co-Ni-Pt-H-FAU	Oleic acid with ethanol	93	6.35;1:6;70;2	Esterification followed pseudo first-order kinetics.	[172]
Y(Iraqi Kaolin)	Oleic acid with ethanol	85	14;1:6;70;1	85% conversion after 60 min reaction time using a 6/1 molar ratio of ethanol/oleic acid at 70 °C.	[125]
HY (Si/Al=15)	Phenylacetic acid with Ethanol	69	1;110;17	Effective for the direct esterification of phenols with carboxylic acids.	[173]
H-Y (Si/Al=80)	oleic acid with Methanol	92	28;1:3;100 ;5	Solid catalyst with Si/Al (H-Y-80) ratio showed 92% conversion	[174]
FAU30	Acetic acid with methanol	-	0.1;1:5;100;3	Introduction of mesoporosity further enhances esterification activity.	[175]
Y(Bangka Kaoline)	Acetic acid with benzyl alcohol	94	1.5;1:4;200;8	Conc. of sulfuric acid during activation of metakaolin affects the synthesis of zeolite Y	[176]
Y (Decationized)	Acetic acid with ethanol in vapor phase	79	14;1:2;150;	reaction kinetics validated using Rideal model and bimolecular surface reaction model.	[177]
Y(shale rock)	Oleic acid with ethanol	78	14;1:5;70;1.5	Esterification reaction showed 78% conversion after 90 mins	[178]
H-Y	Salicylic acid with phenol	78	1;1:1.5;160;6	Exhibit excellent selectivity towards the formation of phenylsalycilate	[179]
Ce/ HUSY	Soybean oil and ethanol	99	1:30;200;24	biofuel produced showed high ester content	[180]
Na Y from kaolin	Oleic acid with ethanol	81	14;1:6;70;2.5	reused NaY zeolite is loses 31% of its activity.	[8]
USY	Oleic acid with oleic alcohol	91	2.4;1:1;150;1 .5	crystallite size and surface composition control both activity and selectivity.	[181]
PA/NaY	Oleic acid with ethanol	79	1.7;1:7105;7	Activation energy 43.4 and 59.7 kJ/mol for forward & backward reaction	[182]

*Reaction conditions = amount of catalyst (g): mole ratio of acid to alcohol: reaction temperature °C: reaction time (h). ; # Con = Conversion

major shortcomings with respect to separation of catalysts, reusability of catalyst, corrosion, purity of product and other environmental issues related to disposal. In contrast, the heterogeneous catalytic systems provide several advantages in terms of product separation and better reusability of catalysts. They also seem to provide more active sites. This makes clay based acid catalysts a potential alternative to the homogeneous catalyst in ester forming processes opening scope of ample research activity [183]. Table 2.6 provides an overview of esterification reactions especially catalyzed using zeolite Y.

2.3.1 Esterification of succinic acid with ethanol

Succinic acid is a dicarboxylic acid with the chemical formula $(CH_2)_2(COOH)_2$. It can be manufactured both by chemical route and biochemical route. It is a type of organic acid, and is applied in many food, chemical, and pharmaceutical industries as a precursor to generate many end use chemical products like solvents, dyes, lacquers, perfumes, plasticizer, photographic chemicals etc. Succinic acid is also used as an antibiotic and curative agent. Esterification of succinic acid results in formation of esters which are commonly used as intermediate for producing plasticizer, medicine and a host of fine chemicals. Specifically, succinic acid can be esterified using ethanol through a consecutive reaction to yield diethyl succinate (DES). Esterification of succinic acid results in formation of esters which are commonly used as intermediate for producing plasticizer, medicine and a host of fine chemicals. The scheme of reaction when bioplatform molecule succinic acid (SA) (limiting reactant) reacts with ethanol (excess reactant) resulting in production of monoethyl and diethyl succinate is presented below:

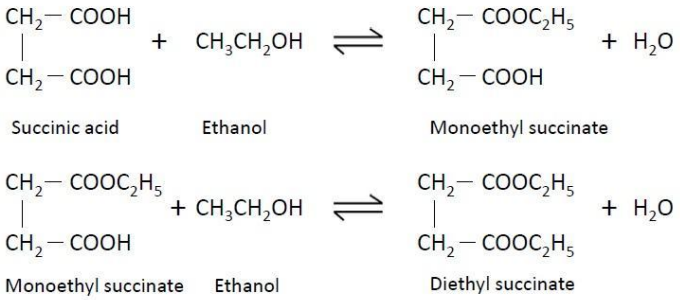

Many homogeneous acid and base catalysts were used efficiently in esterification reactions earlier. But major shortcomings in the form of separation, reusability, corrosion, product purity and environment hazards and disposal have been observed. In contrast, the heterogeneous catalytic systems provide several advantages in terms of product separation and better reusability of catalysts. They also seem to provide more active sites. This makes clay based acid catalysts a potential alternative to the homogeneous catalyst in ester forming processes opening scope of ample research activity [183]. A variety of heterogeneous catalysts has been developed and applied for esterification of succinic acid e.g., Amberlyst-15 ion-exchange resin, Nafron NR, starbon-400, ion exchange resin, carbonaceous materials , Al-MCM-41 and ZSM-5 and numerous others [137].

2.4 Research gap and challenges

Natural kaolin clay from Kachchh, Gujarat region is used as a sustainable novel raw material for zeolite Y synthesis. Since, kaolin clay originates from various sources; their composition varies with geographical location and the chemical composition and crystalline phases vary with the geological layer of the soil. The protocol for synthesis of zeolite Y from kaolin clay is not standardized. The main steps of zeolite Y synthesis from Kachchh kaolin clay include: initial physico-chemical treatment for impurity removal (metal oxides along with some amount of dealumination) which is done by acid or alkaline treatment followed by calcination at high temperature; addition of external silica and/or dealumination depending on the silica-alumina ratio; activation of kaolin at high temperature to get metakaolin; ageing of reaction mixtures at ambient temperature (gel formation) followed by crystallization. The process variables like acid concentration, time required for activation, ageing, crystallization and temperature required for activation, crystallization needs to be determined and adjusted with respect to the clay composition to get the required structural properties. The green method of synthesis of zeolite Y is carried out by applying ultrasonication ageing followed by conventional heating. This green synthesis procedure along with strategic combination of synthesis parameters and the use of sonication help achieve uniform nanosized crystals. The acoustic cavitation and high-energy shockwaves affect the crystallization time, as well as the size and morphology of crystals, leading to a shorter ageing stage and faster crystallization rate. This results in homogeneous phase and crystalline products with uniform morphologies.

Consequently the SiO_2/Al_2O_3 ratio and the surface properties like pore size, pore volume and surface area of the synthesized zeolites need considerable tuning to provide the required properties suitable for catalytic and other applications.

CHAPTER - 3

Material and Methods

Kaolin and Bentonite clay of Kachchh region of Gujarat, India were acid treated and synthesis of zeolite Y was attempted. The synthesis of zeolite Y was also carried out by a unique method of sonication. The synthesized zeolites Y were compared with a standard reference zeolite Y prepared by standard procedure and a commercial zeolite Y obtained from Zeolyst international. The application of synthesized zeolite Y was checked as a catalyst in the esterification reaction. Fig. 3.1 shows the experimental approach.

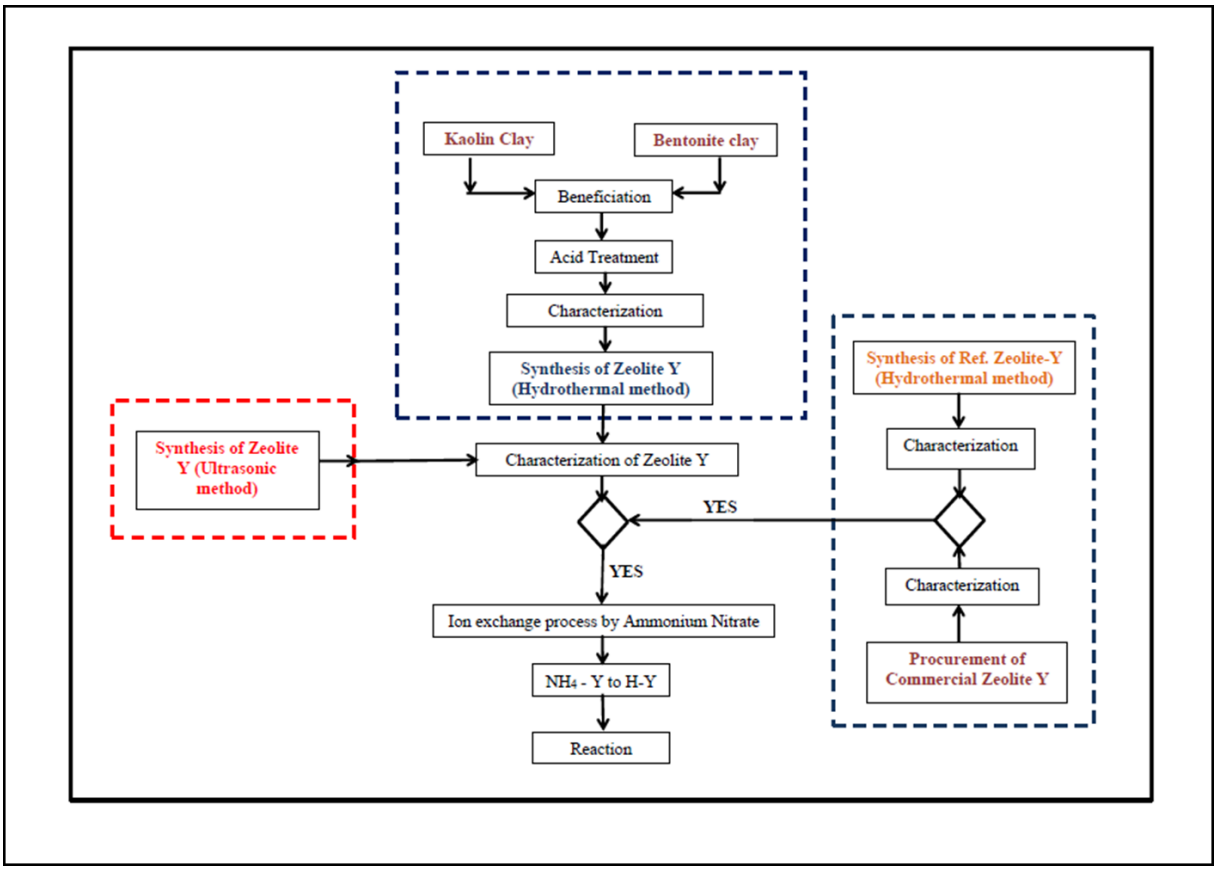

Fig.3.1. Experimental approach

3.1 Materials used

3.1.1 Equipment and instruments

The following equipments and instruments were used in the present investigation and characterization:

Digital balance (Scale Tec Instruments), Magnetic stirrer, hot air oven, Muffle furnace, heating mantle, constant temperature hot plate, mechanical stirrer, Vaccum pump, High intensity ultrasonic processor (20KHz 500 Watts) (Life Care equipments Pvt. Ltd., India), Fourier transform infrared spectroscope (ATR-FTIR, VERTEX 80, Bruker Corp., Germany), GC-MS (Perkin Elmer Turbo mass), Scanning electron microscope (ZEISS Gemini Sigma 300), Dispersive XRF spectrometer EDX-7000 (SHIMADZU Corporation, Japan), TA/DTA thermal analyser (Perkin Elmer STA-8000), Surface area analyzer TriStar II 3020 (Micromeritics Instruments Corporation,US), XRD (Rigaku Miniflex).

3.1.2 Glasswares/plastic wares

Volumetric flask (20 ml to 1 L), measuring cylinder (10 ml to 100 ml), Beaker (50 ml to 1 L), conical flask (50 ml to 250 ml), PP bottle, three neck round bottom flask (500 ml to 1 L), Crucible, Dean stark equipment , condenser with standard joints, funnels, thermometer, desiccator, burette, pipette, glass rod, reagent bottles, sampling bottles.

3.1.3 Chemicals

The kaolin clay and bentonite clay were procured from M/s Gunjan Minerals Pvt. Ltd., Bhuj, Kachchh. Sodium silicate water glass having the following composition SiO_2 21.44%, Na_2O 6.76% (by weight) and sodium aluminate having Al_2O_3 20.25% and Na_2O 19.28% (by weight) were used in zeolite synthesis. The commercial sample of Zeolite Y is procured from Zeolyst International, Pennsylvania, USA. The DI water was procured from Merck Ltd of

conductivity 5-10 μS cm^{-1}. All other chemicals used were of AR grade purchased from M/s S. D. Fine Chemicals. The chemicals used were H_2SO_4, Succinic Acid, Ethanol, NaOH, HCl,

3.2 Experimental

3.2.1 Synthesis of Reference Zeolite Y (RZeoY) by conventional method

The RZeoY was synthesized from feedstock gel which is the main silica alumina source following standard procedure as described in literature [184] (Fig. 3.2). Seed gel having composition of 10.67 Na_2O: 1 Al_2O_3: 10 SiO_2: 180 H_2O was prepared. The Na_2SiO_3 solution was added in the solution of $NaAlO_2$, NaOH and H_2O drop wise. The mixture was stirred till a homogeneous phase was attained and transferred into a capped polypropylene bottle for ageing (24h) at room temperature. The feedstock gel having molar ratio 4.30 Na_2O : $1Al_2O_3$: $10SiO_2$: $180H_2O$ was prepared following the similar method of seed gel described above. Feed gel was used immediately without ageing. The seed gel was slowly added to feed gel with continuous stirring at 1600 rpm using a 2.5 inch diameter, paddle type radial mixer. The resulting gel having the following composition 4.7 Na_2O : $1Al_2O_3$: $10SiO_2$: $180H_2O$ was aged at room temperature for 24h and shifted to Teflon coated autoclave, capped tightly and crystallized for 5h at 100°C. The sample was cooled down to room temperature after crystallization. The final solid product was recuperated after filtration, meticulously washed using warm distilled water and dried at 110°C.

Preparation of Seed gel:

Seed Gel Composition: 1 Al_2O_3 : 10 SiO_2 : 10.67 Na_2O : 180 H_2O

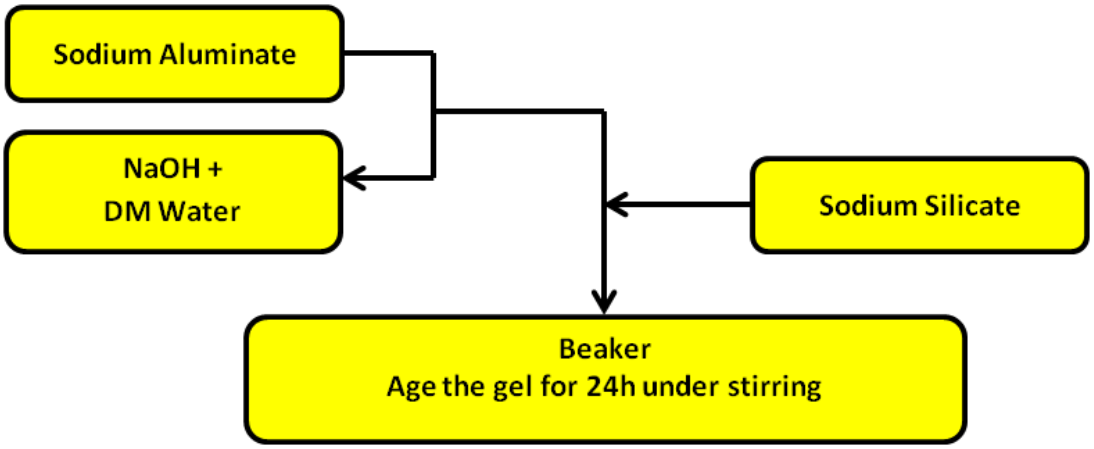

Preparation of Feedstock Gel:

Overall Gel Composition: l Al_2O_3 : 10SiO_2 : 4.7 Na_2O : 180 H_2O

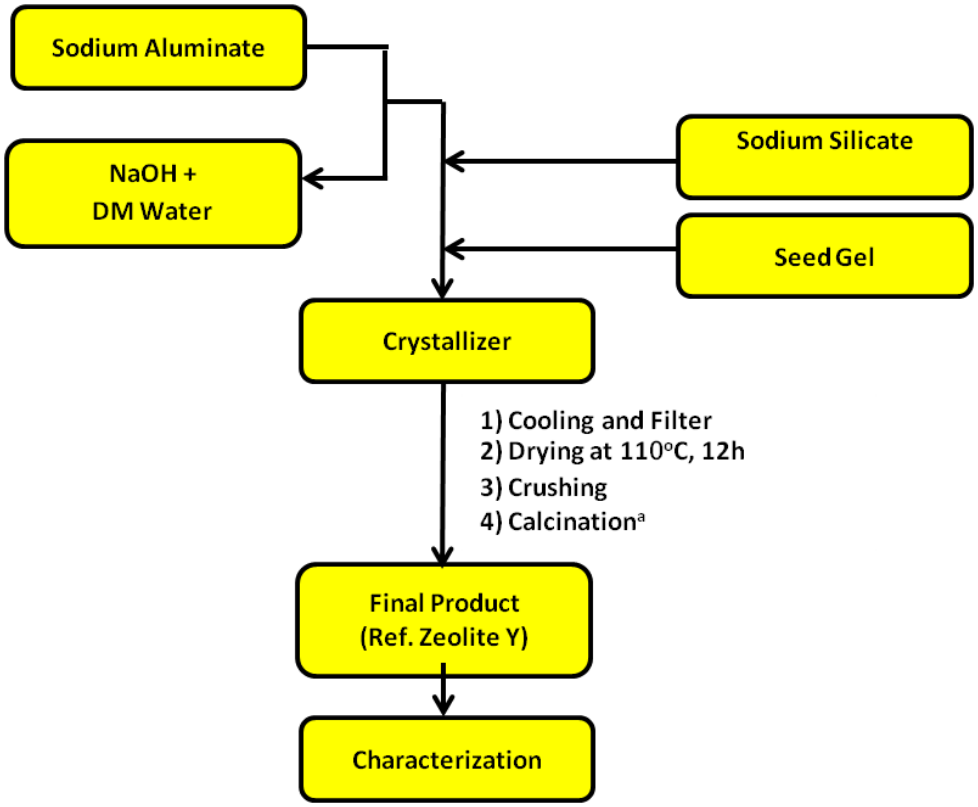

Fig. 3.2. Schematic diagram of Synthesis of Reference Zeolite Y

3.2.2 Synthesis of Zeolite Y by using Kachchh clay

Kaolin and Bentonite clay of Kachchh region of Gujarat, India (Fig. 3.3) were acid treated and synthesis of zeolite Y was attempted.

Fig. 3.3. Sample of (a) kaolin Clay (b) Bentonite Clay

3.2.2.1 Clay treatment of kaolin clay

The Kaolin Clay was provided by M/s Gunjan Minerals Pvt. Ltd., Bhuj, Kachchh, originally mined in Padhar, Bhuj (Latitude: 23.2449984, Longitude: 69.8253968). It is off white in colour and comes in hard, lumpy form. Kaolin clay from mines underwent a beneficiation process for impurity removal followed by acid treatment as shown in Fig. 3.4.

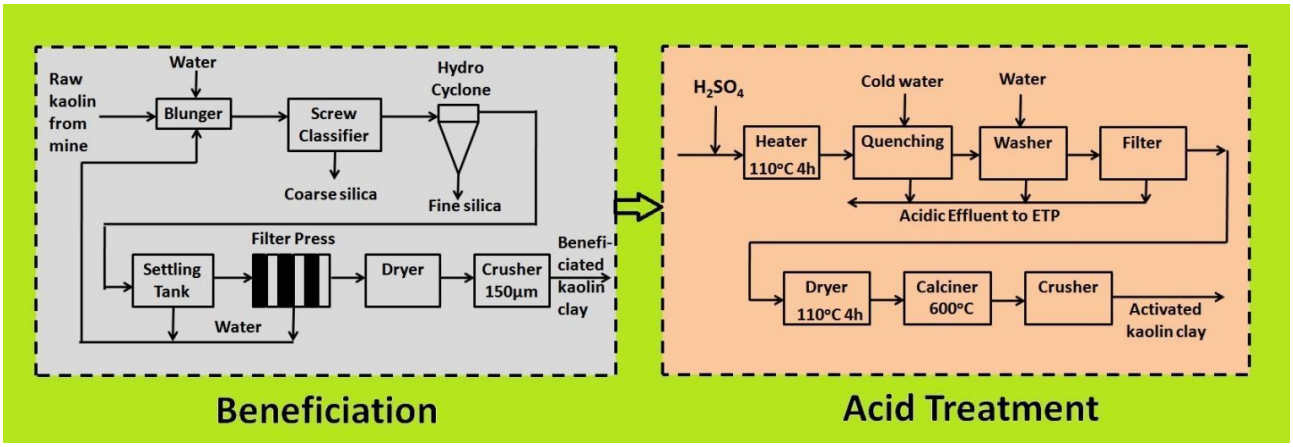

Fig. 3.4. Flow diagram representing clay treatment.

[1] Beneficiation process

The beneficiation process involves physical operations to get required particle size, size distribution and other physico-chemical operations to get required properties. Kaolin clay contains impurities in the form of coarse silica sand (affects particle size), Fe_2O_3 (0.2 – 1.2%), TiO_2 (1 –2.2%) (Imparts colour), mica and carbon (affects the physical and firing properties of clay). The raw clay undergoes levigation in blungers having slurry concentration 30-35%. The clay slurry outflow from the blunger contains different particles of silica sand and pure clay of different sizes (2µm to 2mm). The coarse silica sand is separated by a screw classifier where around 80% of impurities get separated. The remaining impurities in the form of fine silica sand between -60 mesh to +300 mesh are separated by gravitational method using simple channelling followed by hydro cyclones. The purified slurry is allowed to settle (12-24h) in huge settling tanks. The thick concentrated slurry is sent to the filter press. The wet cake is naturally dried and crushed to powder form.

[2] Acid treatment

Fig. 3.5. Acid treatment of kaolin clay.

In this work, Kaolin clay from the Kachchh region of Gujarat is treated with acid. Among all acids, HCl and H_2SO_4 are favored for acid activation [33,34,136]. H_2SO_4 is preferred in case of Kaolin clay as it is more soluble in H_2SO_4 [30,130,185]. Leaching of Kaolin clay with H_2SO_4 causes disaggregation of clay particles, elimination of mineral impurities and dissolution of the external layer which alters the chemical composition as well as the clay structure [130]. 100g of Kaolin clay (150μm) was taken in a round bottom flask with a reflux condenser and 400ml of (7M/10M) concentrated H_2SO_4 was added. The mixture was slowly heated up to 110°C and maintained at that temperature for 4h. The mixture was rapidly quenched with ice cold water. The acid treated powder was washed with distilled water multiple times to remove unspent acid. The powder was separated from the solution by filtration using Whatman filter paper. The wet cake was dried in a hot air oven at 110°C, followed by calcination at 600°C in a muffle furnace under open air condition for 4h. The dry sample was ground to powder form (Fig. 3.5).

3.2.2.2 Clay treatment of Bentonite clay

Greater emphasis on green catalysis makes acid activated bentonite clay a potential candidate for environmental friendly applications. Acid activated and ion exchanged bentonite clay based designer catalysts are suitable for organic synthesis. Activation of Bentonite clay using hydrochloric acid (HCl) [153,154], sulfuric acid (H_2SO_4) [155,156] and other acids [157,158] has been reported. Out of all acids, H_2SO_4 is preferred mostly as the activation can be performed by mild process conditions and the quality of the end product is better with high specific surface area and porosity. The Bentonite clay was acquired from mines located at Kachchh district of Gujarat state. The mines are located at Vandh, Mandvi (Latitude: 23.09325, Longitude: 69.48685). The raw clay underwent a beneficiation process for impurity removal. The sample was received in powder form (200μm) which was light brown in colour. A round bottom flask fitted with a reflux condenser was used. Bentonite clay (100g) was taken and 400 mL of concentrated H_2SO_4 (5M/10M) was added slowly under atmospheric conditions. The temperature was slowly increased by controlled heating up to 110°C. The mixture was then maintained at 110°C for 4h with continuous stirring at 400 rpm. The bentonite suspension was quickly cooled using cold water. Next the final suspension was filtered using a Whatman filter paper. The solid cake layer over the filter paper was washed

several times by distilled water for removal of any unspent acid till the filtrate was neutral. Drying of the wet cake was carried out at 110°C using a hot air oven. Subsequently calcination was carried out at 600°C for 4h in a muffle furnace. The lumpy dried sample was collected and grounded to fine powder using mortar and pestle (Fig. 3.6).

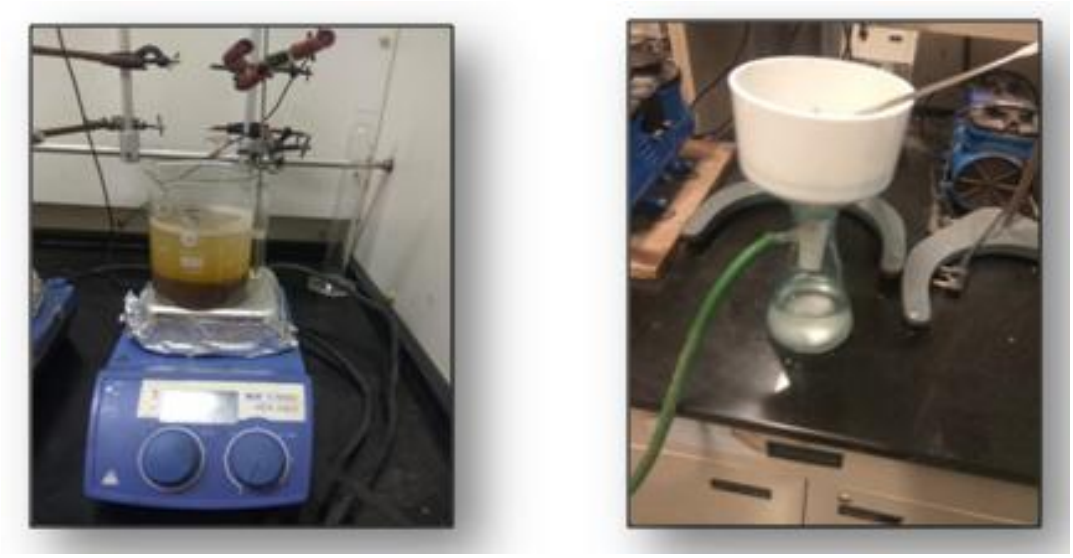

Fig. 3.6. Acid treatment of Bentonite clay.

3.2.2.3 Synthesis of Zeolite Y from clay

[1] Synthesis of Zeolite Y (KZeoY) from kaolin clay

The schematic representation of the synthesis process of zeolite Y from kaolin clay is shown in Fig. 3.7. Seed gel having composition of 10.67 Na_2O: 1 Al_2O_3: 10 SiO_2: 180 H_2O was prepared conventionally. The Na_2SiO_3 solution was added in the solution of $NaAlO_2$, NaOH and H_2O drop wise. The mixture was stirred till a homogeneous phase was attained and transferred into a capped polypropylene bottle for ageing (24h) at room temperature. Activated kaolin was mixed with aqueous NaOH solution and fused in a muffle furnace at 800^oC for 8h. Solid mixture was cooled down to room temperature and crushed in the form of fine powder. Demineralized water was added to fused clay powder and prepared mixture. Sodium silicate solution was dispersed drop wise to the mixture, stirred continuously by a

turbine mixer till smooth gel formation. Finally seed gel was added slowly with continuous stirring until complete dispersion of seed gel was achieved. Final composition was kept at 180 H_2O :1 Al_2O_3 : 10 SiO_2 : 4.62 Na_2O . The prepared gel was transferred to a polypropylene bottle and sealed for 24 h at 50°C for ageing. The crystallization time is varying from 24h to 48h at 100°C in an oven. On cooling, the solid (containing the NaY Zeolite) settled at the bottom with a hazy supernatant. The ageing and crystallization time are varying and try to get the best result. The final solid product was recuperated by filtration, washed with warm demineralized water till pH reached to 9 and then dried at 110°C for 16h (Fig. 3.8).

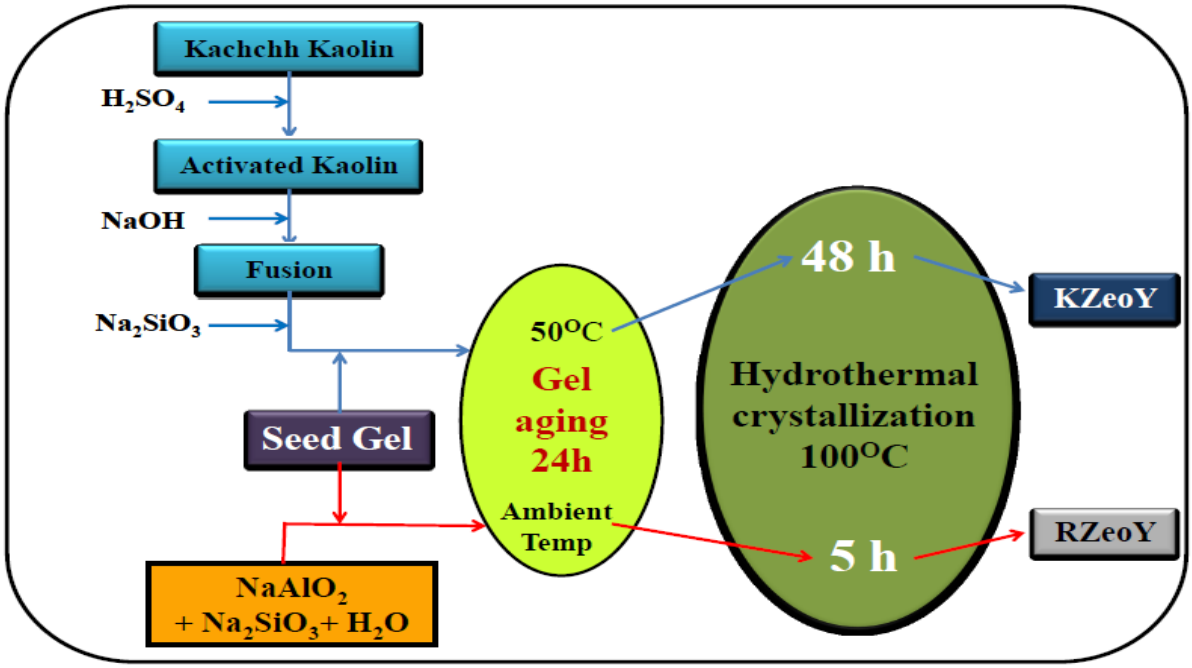

Fig. 3.7. Synthesis of Zeolite Y from Kaolin clay (KZeoY)

[2] Synthesis of Zeolite Y from bentonite clay

The synthesis of zeolite Y from treated bentonite clay was tried by varying parameters. The synthesis steps are shown in Fig. 3.9. Seed gel having composition of 10.67 Na_2O: 1 Al_2O_3: 10 SiO_2: 180 H_2O was prepared conventionally. The Na_2SiO_3 solution was added in the solution of $NaAlO_2$, NaOH and H_2O drop wise. The mixture was stirred till a homogeneous

Fig. 3.8. Experimental steps of synthesis of Zeolite Y from Kaolin clay (KZeoY).

phase was attained and transferred into a capped polypropylene bottle for ageing (24h) at room temperature. Activated bentonite clay was mixed with aqueous NaOH solution and fused in a muffle furnace at 800^{o}C for 6h. Solid mixture was cooled down to room temperature and crushed in the form of fine powder. Demineralized water was added to fused clay powder and prepared mixture. Sodium silicate solution was dispersed drop wise to the mixture, stirred continuously by a turbine mixer till smooth gel formation. The amount of NaOH for fusion and Sodium silicate solution are decided based on composition of treated bentonite clay. Finally 10% seed gel was added slowly with continuous stirring until complete dispersion of seed gel was achieved. Final composition was kept at 180 H_2O :1 Al_2O_3 : 10 SiO_2 : 4.62 Na_2O . The prepared gel was transferred to a polypropylene bottle and sealed for 24h at 50°C for ageing followed by crystallization for 48h at 100°C in an oven. The crystallization time is varying and batches were taken. On cooling, the solid settled at the bottom with a hazy supernatant. The final solid product was recuperated by filtration, washed with warm demineralized water till pH reached to 9 and then dried at 110°C for 16h. The ageing time and crystallization time varying and batches were taken (Fig. 3.10).

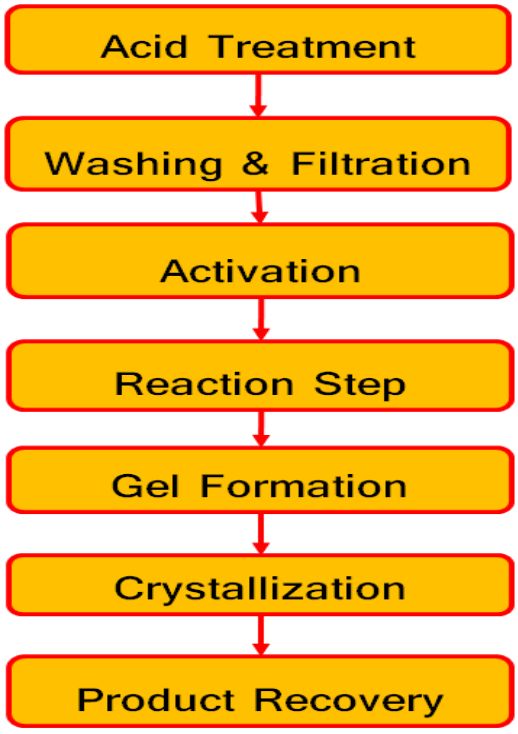

Fig. 3.9. Synthesis of Zeolite Y from Bentonite clay

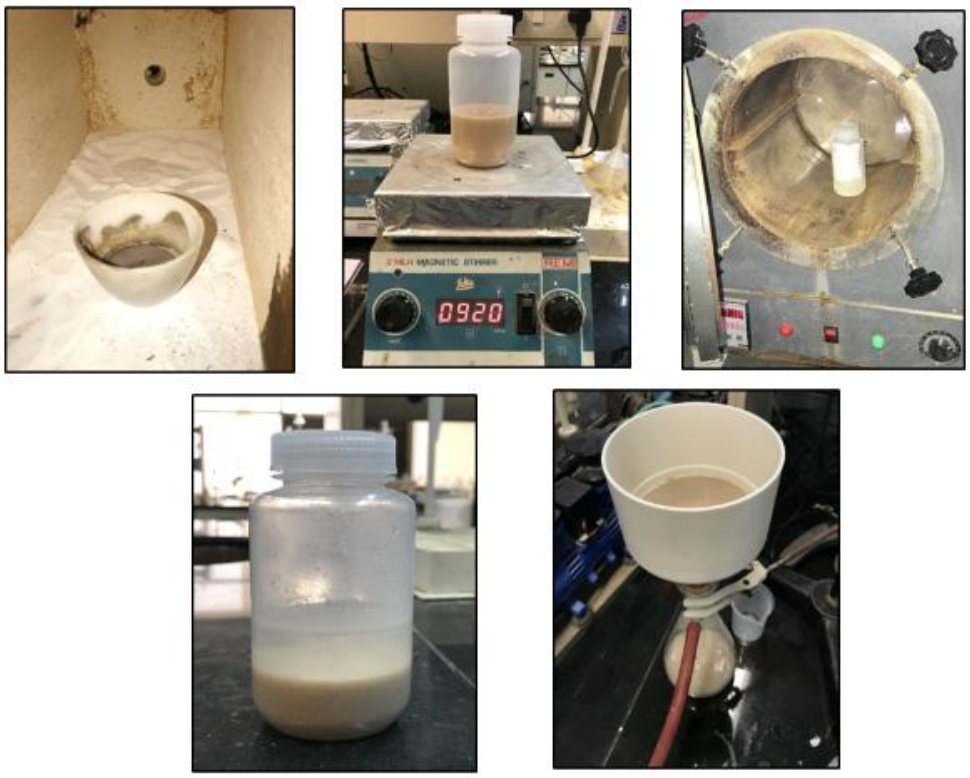

Fig. 3.10. Experimental steps of synthesis of Zeolite Y from Bentonite clay

3.2.3 Synthesis of Zeolite Y by using ultrasonication

Zeolite Y is synthesized by Ultra sonication (UZeoY) as shown in Fig. 3.11. The chemicals used for the UZeoY synthesis were Sodium silicate water glass having the following composition SiO_2 21.44%, Na_2O 6.76% (by weight) and sodium aluminate having Al_2O_3 20.25% and Na_2O 19.28% (by weight). All chemicals used were of AR grade. Seed gel having composition of 10.67 Na_2O: $1Al_2O_3$: 10 SiO_2: 180 H_2O was prepared. The feedstock gel having molar ratio 4.30 Na_2O: $1Al_2O_3$: 10 SiO_2: 180 H_2O was prepared following the similar method as of seed gel. Feed gel was used immediately without ageing. The seed gel was slowly added to feed gel with continuous stirring for 20 min at 1600 rpm using a 2.5 inch diameter, paddle type radial mixer. The resulting gel had the following composition 4.7 Na_2O : 1 Al_2O_3 : 10 SiO_2 : 180 H_2O. This precursor gel was sonicated with an ultrasonic processor (20 kHz, 500 Watts) for 90min. Finally the sample was treated hydrothermally without

stirring at 100°C for 90 min. The final solid product was recuperated by filtration, washed with warm demineralized water till pH reached to 9 and then dried at 110°C for 16h. The synthesized zeolite-Y (UZeoY) was characterized and compared with a RZeoY prepared by conventional method.

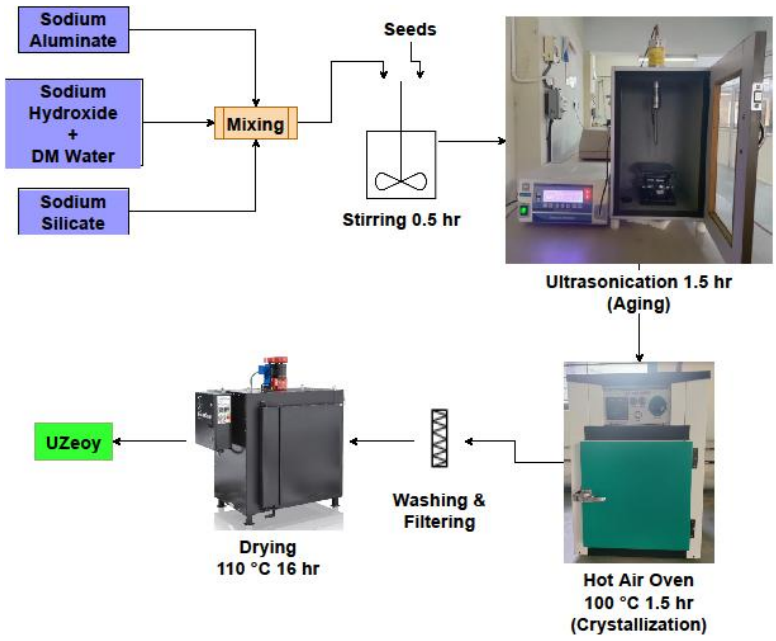

Fig. 3.11. Synthesis of Zeolite Y by using ultrasonication

3.2.4 Ion exchange by NH_4NO_3 - Catalyst activation

Before applying as catalyst, UZeoY, RZeoY and KZeoY were altered into H form of zeolite Y by using ion-exchange method as represented in Fig. 3.12. First the zeolite Y was dissolved in 1M solution of NH_4NO_3 at a ratio of 1:10 (w/v) and continuously stirred for 8h at 80°C. After first ion-exchange, zeolite Y was recovered by filtration using Whatman filter paper and the ion-exchange process was repeated second time. The recovered product was subsequently washed with hot water and dried for 8h at 100°C. The calcination of resulted powder was carried out at 500°C for 5h and allowed to cool naturally. This H form of zeolite Y was used as a catalyst further.

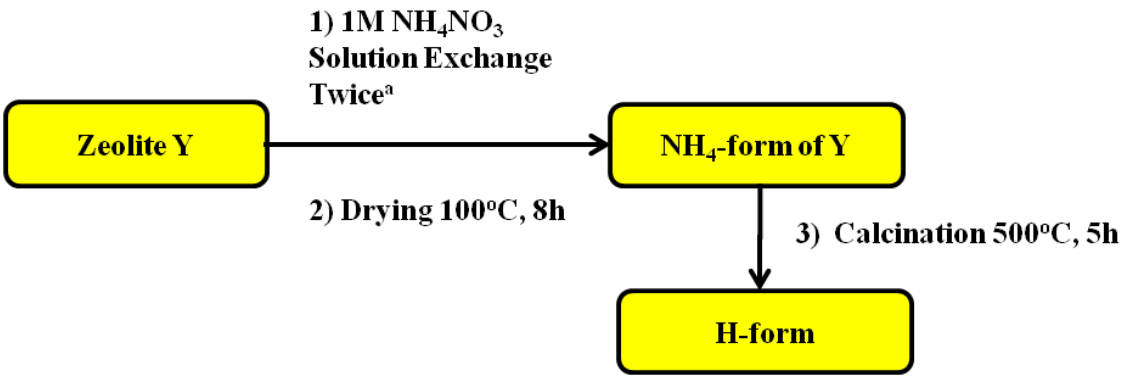

a: zeolite:liq =1:10 by vol, 80°C, 8h stirring, Repeated twice

Fig. 3.12. Schematic diagram of ammonium nitrate ion exchange of all synthesized Zeolite Y

3.2.5 Esterification reaction

Esterification of succinic acid (SA) results in formation of esters which are commonly used as intermediate for producing plasticizer, medicine and a host of fine chemicals. Esterification reaction using catalysts in homogeneous conditions is more common but suffers major shortcomings with respect to separation of catalysts, reusability of catalyst, corrosion, purity of product and other environmental issues related to disposal. In contrast, the heterogeneous catalytic systems provide several advantages in terms of product separation and better reusability of catalysts. They also seem to provide more active sites. The molar ratio, temperature and amount of catalyst for KZeoY are varying and in this work, final reaction condition was succinic acid and ethanol (1:3 molar ratio) were reacted in a stirred batch reactor equipped with a condenser with additional Dean–Stark apparatus and guard tube (Fig. 3.13). The Dean–Stark apparatus was attached to the round bottom flask to separate out the water generated during the reaction. The esterification reaction was carried out at 72°C for 12h using 1g catalyst. After reaction, the catalyst was recovered by filtration and reused after washing two times with deionized water at 70°C and dried for 6h at 110°C. The same procedure was repeated for recovery and reuse in each cycle. The esterification using recycled catalyst was carried out under the same reaction conditions. A figure of the experimental set up is shown below (Fig. 3.14).

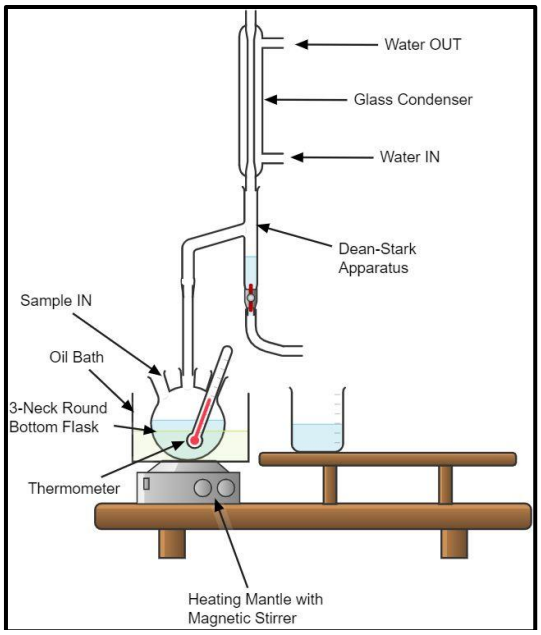

Fig.3.13. Schematic diagram of esterification reaction

Fig.3.14. Esterification reaction experimental set up

3.3 Analytical methodologies

The physicochemical properties of all samples of clays and zeolites are studied by various characterization techniques such as XRF, DTA, XRD, FTIR, N_2 adsorption-desorption and SEM etc.

3.3.1 X-Ray Diffraction

Preliminary source to identify zeolites is XRD analysis. It mentions diffraction patterns with crystalline, amorphous or both phases which further identify by comparison with those in the IZA (http://www.iza-structure.org/databases/). This thesis provides XRD patterns of both as-made and calcined zeolites. In some XRD pattern comparison of as-made and modified zeolite is discussed.

XRD is one of the most widely used techniques for characterization of materials. It is an important tool for determining the structure of materials that are distinguished by long-range order. X-rays are extremely intrusive electromagnetic radiation which is electrically neutral. Their wavelength is in the range of 0.04 to 1000 Å. X-rays with only shorter wavelengths (from few Å to 0.1 Å) are used for diffraction applications because these are comparable to the size of the atoms. Hence, the X-rays are ideally suited for deducing the structural arrangement of atoms in a variety of materials.

The diffraction method involves interaction of the incident monochromatic X-rays (like Cu Kα) with the atoms of a periodic lattice. The X-rays are scattered by atoms constructively as per Bragg's law. This law relates the wavelength (λ) of electromagnetic radiation to the lattice spacing and the diffraction angle in a crystalline material.

$n\lambda = 2\ d \sin\theta$; n = 1, 2, 3…

Where, n is an integer called order of the reflection, λ is wavelength of the X-rays, d is the distance between two lattice planes and θ is the angle between the incoming X-rays and the normal to the reflecting lattice plane. The lattice spacing (d) can be obtained from Bragg's equation, which is characteristic of a particular material. Width of the diffraction peaks indicates the dimension of the reflecting planes.

The XRD patterns of all the zeolites reported in this thesis were recorded using a Rigaku Miniflex (Cu-Kα nod material) (Fig. 3.15) with continuous scanning rate of 2^{o}/min, generator settings of 10 mA and 40 kV at the Bragg's angle 2θ range 3–40^{o}.

Fig. 3.15. Rigaku Miniflex instrument for XRD pattern

3.3.2 Infrared Spectroscopy

Fourier transform infrared (FTIR) spectroscopy is widely used in the characterization of material due to its capacity to provide information without destroying the matrix. On the other hand, the use of special cells allows tracking the changes occurring in the IR bands of basic probes, adsorbed on the catalyst acid sites, due to changes in the nature and distribution of these sites. FT-IR spectroscopy is also used to probe the structure of clays [186]**.** In this work FTIR spectra were recorded on a Bruker (Alpha) infrared spectrophotometer (Fig. 3.16) with resolution of 4 cm^{-1}, in the range of 400 – 4000 cm^{-1}.

3.3.3 Thermal Analysis

Thermal stability of zeolites is one of the important features that makes clay applicable as selective sorbents and potential catalysts. All kinds of organic, inorganic, petroleum,

Fig. 3.16. Fourier transform infrared spectroscope (ATR-FTIR, VERTEX 80, Bruker Corp., Germany)

pharmaceutical and polymer materials have been analyzed by Thermogravimetric (TGA) analysis Thermogravimetric analysis uses heat to force reactions and physical changes in materials. TGA provides quantitative measurement of mass change in materials associated with transition and thermal degradation. TGA records change in mass from dehydration, decomposition, and oxidation of a sample with time and temperature. Characteristic thermogravimetric curves are given for specific materials and chemical compounds due to unique sequences from physicochemical reactions occurring over specific temperature ranges and heating rates.

In the instrumental set-up, N_2 inert gas and O_2 oxidative gas was used. Their flow rates provide the suitable environment for either thermal decomposition, or oxidative decomposition, or a thermal-oxidative combination. A sample of 10 mg weight was heated in a silica crucible at a constant heating rate of 10°C/min operating in a stream of N2 atmosphere by using a platinum crucible with a pierced lid at a flow rate of 20 mL/min from 35°C to 700°C. This analysis provides the presence of endotherms and exotherms during heating, cooling. A simultaneous Thermo gravimetric Analyzer/ Differential Thermal Analyzer (Perkin Elmer STA-8000 instrument) was used in this work.

3.3.4 X-ray fluorescence (XRF)

XRF analyses of the samples were done on SHIMADZU Corporation, Japan make Energy Dispersive X-ray Fluorescence Spectrometer-EDX-7000 (Fig. 3.17). The sample is irradiated with X-rays from an X-ray tube; the atoms in the sample generate unique X-rays that are emitted from the sample. This "fluorescent X-ray" has a unique wavelength and energy that is characteristic of each element that generates them. Consequently, qualitative analysis was performed by investigating the wavelengths of the X-rays.

Fig. 3.17. Dispersive XRF spectrometer EDX-7000 (SHIMADZU Corporation, Japan)

3.3.5 N_2-adsorption-desorption

High surface area and ordered pore structure of zeolites result in their unique adsorption properties. Zeolites are characterized by large surface area because of its highly porous nature. As a result of high surface area zeolites can adsorb large quantities of adsorbate depending on adsorbate size, aperture size, temperature and surface acidity of zeolites.

The most accepted technique for measuring surface area of materials is the one that is based on the theory developed by Brunauer, Emmett and Teller in 1938 by taking into account the multilayer adsorption of adsorbate molecules on the adsorbent surface. Its assumptions are; (i) there is no intermolecular interaction, (ii) adsorption energy remains constant from zero coverage to full coverage for the primary layer of the adsorbate and each successive layers

above, (iii) a new layer can be initiated before the completion of the one under formation and (iv) enthalpy of adsorption is same for any other layer except the first one. Porosity and Surface area measurements were done by N_2 adsorption/desorption isotherms at −196°C using the Micromeritics Instruments Corporation (TriStar II 3020) (Fig. 3.18). The samples were first outgassed at 200°C for 3h, at 5×10^{-3} mmHg and then at room temperature for 2h, at 0.75×10^{-6} mmHg before measurement. The isotherms were analyzed in a conventional manner in the relative pressure range P/P0 = 0.0005 to 1.0. The total pore volume of the samples was calculated at P/P0 = 0.9. The BJH method was used to determine the pore size distribution from the adsorption/desorption branches of the isotherms.

Fig. 3.18. Surface area analyzer TriStar II 3020 (Micromeritics Instruments Corporation, US)

3.3.6 Electron Microscopy

The electron microscopy has many variants. In this section, we deal only with scanning electron microscopy. The former is very useful for the examination of physical features of the sample, like size and shape of crystals in the samples of clays and zeolites.

Scanning Electron Microscopy (SEM)

SEM is a type of electron microscopy technique that generates images of a sample by scanning it with a focused high-energy beam of electrons in a raster scan pattern. It is a simple technique to investigate the morphological characteristics of the samples [187]. A probe of electrons (5-50 eV) scans over a sample surface and the yield of either secondary or back-scattered electrons is detected as a function of the position of the primary beam. The interaction between the incident electrons with the atoms in the sample produces different types of signals, which carry detailed information about the sample surface topography and the composition of the sample. A major advantage of SEM is that bulk samples can also be directly studied by this technique. In this work the morphology and elemental composition of samples were evaluated using field emission scanning electron microscopy using ZEISS Gemini Sigma 300 microscope (Fig. 3.19). The vacuum dried samples were sputter coated with Gold using Argon gas at 10mA for 80s before loading in the microscope.

Fig. 3.19. Scanning electron microscope (ZEISS Gemini Sigma)

CHAPTER - 4

Result and Discussion

4. Result and discussion

4.1 Characterization of reference Zeolite Y (RZeoY)

The reference zeolite Y is synthesized in the laboratory by hydrothermal method using standard chemicals. The reference zeolite Y (RZeoY) is examined by multiple characterization techniques and compared with a commercial sample of zeolite Y of Zeolyst international (CZeoY). XRD exhibited well-resolved peaks in the high 2θ region of 3-40^{o}; the peak positions are nearly identical with CZeoY demonstrating that RZeoY achieved good crystallinity. Lattice parameters and Miller indices were matched with standards. Well-dispersed morphology & comparable crystallinity was confirmed by scanning electron microscopy. BET surface area of 571 m^2g^{-1} and 0.31 cm^3g^{-1} pore volume were comparable with CZeoY. Pore size and BJH pore volume was more than CZeoY. The N_2 adsorption-desorption isotherms show representative hysteresis loops of type I, which is attributed to a characteristic of introduction of some mesopores structure in the sample.

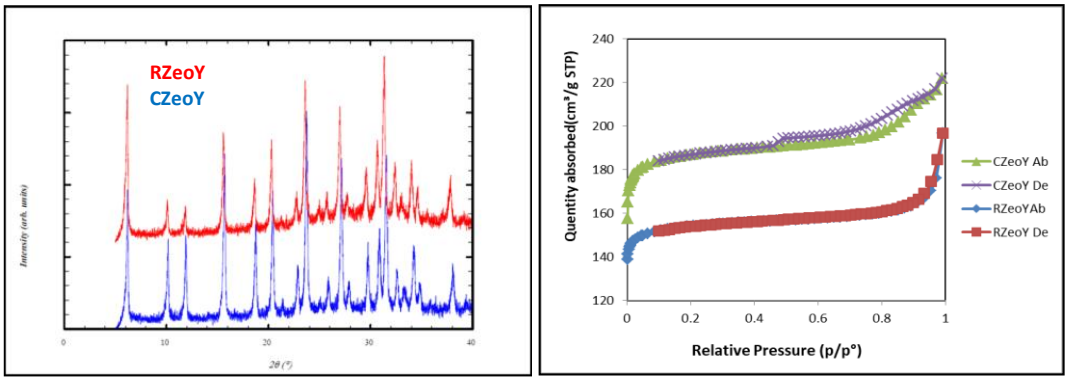

Fig. 4.1 XRD and N_2 adsorption-desorption isotherms of RZeoY and CZeoY

Table 4.1 : Textural properties of RZeoY and CZeoY

Material	Surface Area ($m^2 g^{-1}$)				Pore volume ($cm^3 g^{-1}$)		Pore size (nm)	
	S_{BET}	S_{BJH}	S_{EXT}	S_{Micro}	V_{BJH}	V_{Micro}	d_{BJH}	d_{Avg}
CZeoY	693.47	58.00	54.37	639.10	0.081	0.265	5.6	1.98
RZeoY	571.15	42.32	40.29	530.85	0.087	0.220	8.1	2.11

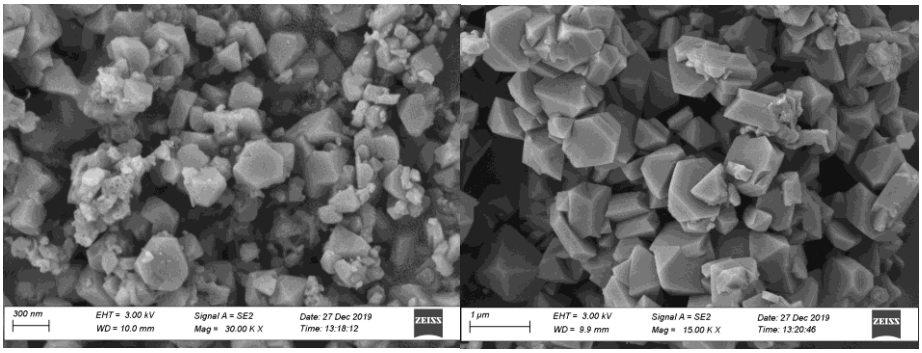

Fig. 4.2 SEM images of (a) RZeoY and (b) CZeoY.

4.2 Clay Treatment

4.2.1 Kaolin clay

The kaolin clay has alternate layers of silicon- oxygen tetrahedral layer joined to alumina octahedral layer constituting a two-layer crystal structure. These Si-O and Al-O structures are inactive and it is difficult to synthesize zeolites directly, and therefore kaolin must be pre-activated to change this inert structure [20]. The kaolin clay leached with H_2SO_4 to achieve the required silica-alumina ratio for zeolite and to remove impurities. The physico-chemical characteristics of acid leached kaolin clay were studied by XRF, XRD, FTIR, TG- DTA, SEM and N_2 adsorption techniques.

I. XRF analysis:

XRF analysis was undertaken to determine the chemical composition of the kaolin clay and the ensuing chemical changes that occurred due to acid treatment. The results are presented in Table 2. The kaolin clay contained alumina (Al_2O_3) and silica (SiO_2) in major proportions (together ~95%) whereas other oxides namely magnesium oxide (MgO), calcium oxide (CaO), potassium oxide (K_2O), zinc oxide (ZnO) and titanium oxide (TiO_2) were present in trace amounts. The reaction between kaolin and H_2SO_4 as described by Makó et al is as follows [138]:

$$Al_2O_3 \cdot 2SiO_2 \cdot 2H_2O + 3H_2SO_4 \rightarrow Al_2(SO_4)_3 + 2SiO_2 + 5H_2O \quad \text{- - - - - -} \quad (1)$$

During the acid treatment considerable change in the composition of the kaolin clay was observed. With increase in acid strength the Al_2O_3, MgO, CaO and K_2O contents in the clay decreased resulting in an increase in SiO_2 content from 54% to 68%. Simultaneously, the silica-alumina ratio also increased from 1.3 to 2.4.This is nearly the same with the requirement for zeolite synthesis. It is clearly observed that treatment with 10M H_2SO_4 resulted in more reduction in metal impurities compared to 7M H_2SO_4. The decrease in the alumina content in the acid treated clay can be attributed to the leaching of the Al^{3+} ions from the octahedral layer due to hydrolysis under acidic conditions [130]. The dissolution of Al_2O_3 is primarily controlled by the diffusion of H_2SO_4 from the surface to the interior of the solid particles [30].

Table 4.2: XRF analysis of raw and H_2SO_4 (7M and 10M) treated kaolin clay

Material	**Chemical component (wt%)**									**Silica-Alumina ratio**
	SiO_2	**Al_2O_3**	**MgO**	**CaO**	**K_2O**	**TiO_2**	**Fe_2O_3**	**Na_2O**	**MnO**	
Raw kaolin	53.786	41.194	0.094	0.367	0.274	3.032	0.690	0.138	0.016	1.3
7M kaolin	58.136	38.858	0.022	0.012	0.194	2.058	0.308	0.035	0.007	1.5
10M kaolin	67.985	28.613	0.011	0.017	0.197	2.408	0.292	0.044	0.007	2.4

II. FTIR analysis

The FTIR spectrum of the raw and acid treated kaolin clay is shown in Fig. 4.3. The FTIR spectrum of raw kaolin clay clearly matched with kaolin from other regions within India [119,188]. The adsorption bands at 3687 and 3683 cm^{-1} are attributed to the stretching vibrations of -OH groups coordinated to the Al^{3+} ions reflecting the crystalline order of kaolin. The intensity decreased gradually with increasing concentration of acid treatment. For kaolin treated with 10M H_2SO_4, the structural hydroxyl vibration band was found to be particularly weak indicating loss of structural hydroxyl groups resulting in dehydroxylation and successive leaching of Al^{3+} ions from the octahedral layer. The weak twin peaks at 2900 cm^{-1} region is due to C-H stretching mode which revealed the presence of organic matter [189]. The weak peaks around 1600 cm^{-1} is due to the bending vibration mode of physisorbed water on the surface of free silica caused by leaching [190]. The amount of physisorbed water increased with acid concentration due to formation of water (reaction 1). The band at 1115 cm^{-1} showed a characteristic band of kaolin indicating apical Si-O [190], which is almost absent in 10M H_2SO_4 treated kaolin. The high intense band around 1033 and 1007 cm^{-1} are typical of kaolin and can be attributed to Si-O stretching vibrations which decreased gradually with increasing acid concentration. The weak band at 937 cm^{-1} is caused due to the vibration of inner -OH groups (Al-OH vibrations) [188]. The high intense peak at 914 cm^{-1} was due to vibrations of inner hydroxyl groups [130]. The peak clearly reduced with increase in acid strength. At 10M H_2SO_4, the peak reduced to quite an extent indicating rapid dealumination. The IR peaks at 789 and 752 cm^{-1} can be assigned to Si-O-Si vibrations of the clay sheet, the intensity of which also decreased with acid strength. The spectral region between 800 and 750 cm^{-1} is very sensitive against crystallinity and the purity of kaolin material. The two peaks at 789 and 752 cm^{-1} are characteristics of pure kaolin and indicate presence of free silica and/or quartz admixtures which are always present in natural clay [136]. The peaks at 688 cm^{-1} is assigned to Si-O stretching and bending vibrations [188], the intensity of which decreased when treated with 10M H_2SO_4. It also specifies the presence of quartz particles of small size which are responsible for providing mechanical strength required for ceramic applications [189]. The FTIR result conformed to the XRF study which indicated considerable degradation of the kaolin clay sheet as a result of H_2SO_4 treatment.

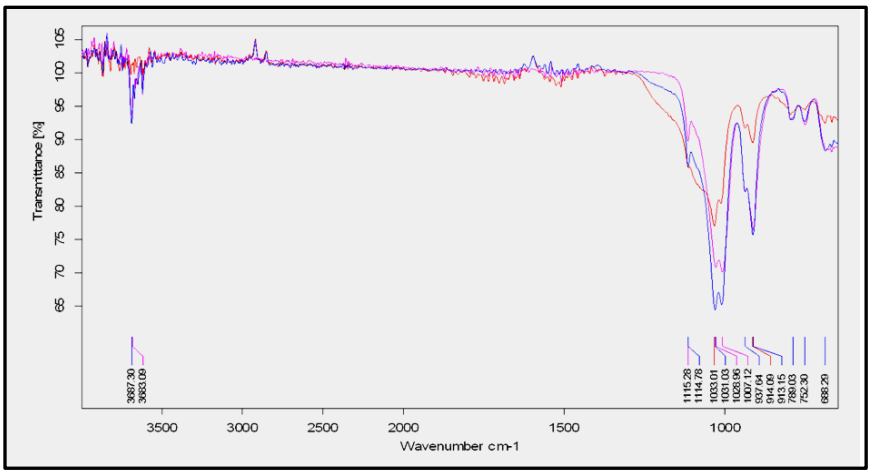

Fig. 4.3 FTIR analysis of (a) raw kaolin clay (blue) (b) 7M H_2SO_4 treated kaolin clay (pink) (c) 10M H_2SO_4 treated kaolin clay (red).

III. SEM study

SEM images of kaolin before and after acid treatment showed the transformed morphological features (Fig. 4.4). The SEM micrograph of kaolin clay revealed the presence of large particles that appeared to have been formed by agglomeration of flaky particles. Acid treatment led to complete disaggregation and reduction in size of clay structure. The SEM images of kaolin after treatment with 7M H_2SO_4 (Fig. 4.4b) showed disaggregated small sized particles and also indicated initiation of cluster formation. Micrographs of kaolin after treatment with 10M H_2SO_4 (Fig. 4.4c) clearly revealed formation of clusters consisting of well-bonded agglomerated particles.

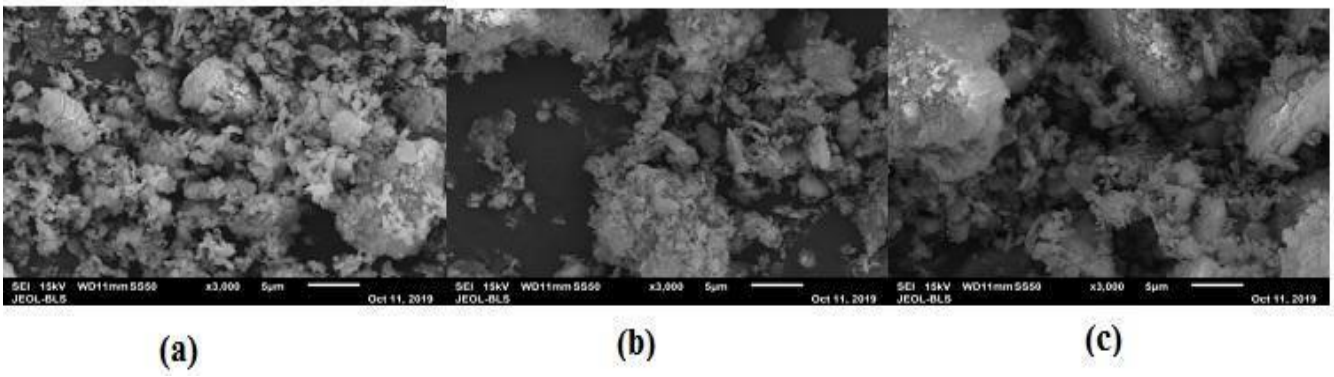

Fig. 4.4 SEM images of (a) raw kaolin clay (b) 7M H_2SO_4 treated kaolin clay (c) 10M H_2SO_4 treated kaolin clay.

IV. TG-DTA study

The thermo gravimetric analysis of raw kaolin clay and post treatment with 7M and 10M H_2SO_4 is shown in Fig. 4.5a. The initial minor weight loss below 100^oC was due to loss of physisorbed water present in small quantities, which are loosely bound water molecules and can be easily removed. Treatment with H_2SO_4 increased the amount of physisorbed water which increased with acid concentration. This might be due to increase in the amount of amorphous silica because of acid treatment which led to increased surface area resulting in higher water adsorption. Also the formation of water molecules during the reaction between kaolin and H_2SO_4, might have resulted in increased physisorbed water. The major weight loss (16%) occurred between 400-600^oC due to loss of structural hydroxyl groups that are strongly bonded. Treatment with H_2SO_4 led to removal of the octahedral Al^{3+} ions along with simultaneous removal of structural hydroxyl groups [130]. It was also observed that the removal of structural hydroxyl groups increased with acid concentration. High removal of structural water was achieved using 10M H_2SO_4, indicated by the flatter TGA profile.

The differential thermal analysis profiles of clay before and after acid treatment were also checked for confirmation (Fig. 4.5b). The DTA curve of raw kaolin clay showed two endothermic peaks. The endothermic peak at 46^oC was due to physisorbed water and the large peak at 520^oC was caused by liberation of water owing to dehydroxylation of coordinated and structural water molecules [130]. The increase in the amount of physisorbed water was due to acid treatment. The quantity of physisorbed water increased with acid concentration as indicated by the peaks at 46^oC. However, the acid treatment decreased the structural water content which decreased with increased acid concentration. Almost complete removal of structural water could be achieved using 10M H_2SO_4. Absence of any major endothermic peak at 520^oC for 10M H_2SO_4 also confirmed the same.

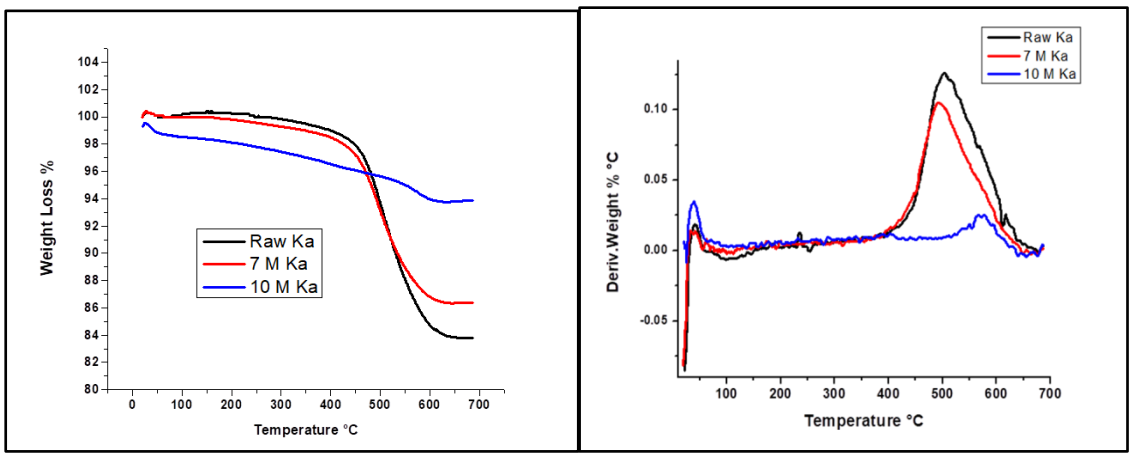

(a) **(b)**

Fig. 4.5 (a) TGA of raw kaolin and H_2SO_4 treated kaolin clay (b) DTA of raw kaolin and H_2SO_4 treated kaolin clay.

V. XRD study

The structural changes that occurred in the clay material due to acid treatment were studied using X-ray diffraction technique. Fig. 4.6 shows the XRD profiles of the raw and acid treated kaolin clay. The raw kaolin clay showed well-defined reflections at 2Θ value of 12° and 25° (corresponding to the d values of 7.1 Å, these peaks correspond to the reflections from [001]), which are typical characteristic peaks of kaolin. Raw kaolin clay pattern was matched with JCPDS card 00-014-0164 of standard kaolin and confirmed. However, the peaks corresponding to the 2Θ value 34–36°, 38–42°, 45–50°, and 54–63° may vary to some extent for kaolin of different origin [130]. The high intense peaks confirmed the crystalline behavior of the raw kaolin clay. Upon acid treatment the peak intensity was found to decrease progressively. This was due to the structural disorder owing to the acid treatment, which affected the crystalline character of the clay. At low acid strength (7M), the reflections of the original kaolin phase became narrower, which may be related to the increase in crystallite size and/or the decrease in the mean lattice strain. The kaolin clay treated with 10M H_2SO_4 did not show small peaks in diffractograms. This indicated removal of most of the metals creating a large degree of structural disorderliness in these samples. Since leaching is quite severe at this acidic strength, the layered structure of clay material disintegrated and reduced the crystallinity leading towards amorphous structure.

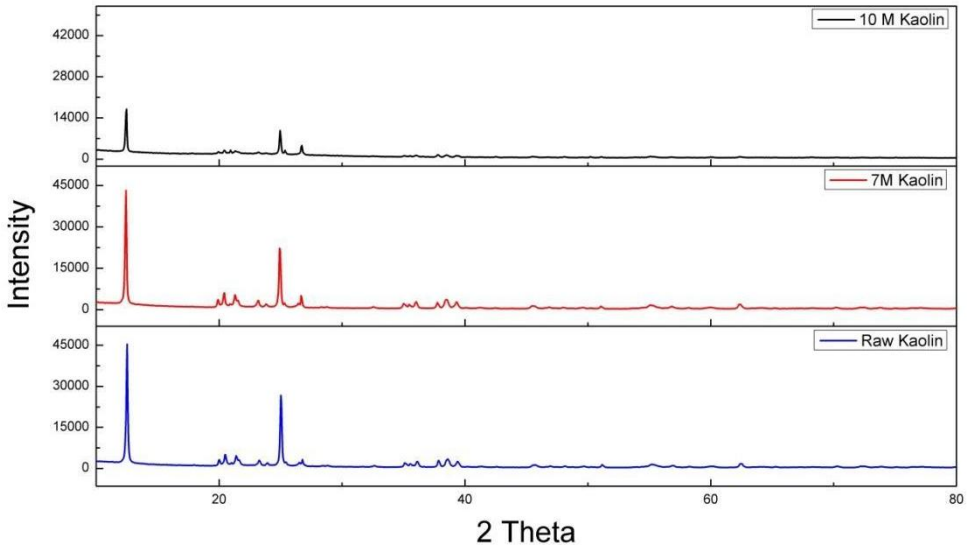

Fig. 4.6 XRD analysis of (a) raw kaolin clay (blue) (b) 7M H_2SO_4 treated kaolin clay (red) (c) 10M H_2SO_4 treated kaolin clay (black).

VI. Nitrogen adsorption-desorption study

The N_2 adsorption–desorption isotherms of the raw kaolin clay and post H_2SO_4 treatment are presented in Fig. 4.7. The IUPAC classification of adsorption isotherms imply six types of isotherm: microporous (type I), nonporous or macroporous (types II, III, and VI), and mesoporous (types IV and V) [2]. The isotherms of samples in the present work can be classified as type IV signifying typical mesoporous structures. There is also a correlation between the shape of the hysteresis loop and the texture of a mesoporous material. The isotherms also indicate that though the majority of pores are mesoporous in nature, some micro pores and macro pores are also present.

Raw kaolin clay with 80 - 95 wt% of kaolinite generally have specific surface area (SSA) between 9 and 45 m^2g^{-1} [191], depending on its nature. In general, porous materials (SSA> 100 m^2/g) can be considered as catalyst support [192]. The pore volume and SSA of the raw and acid treated kaolin clay is summarized in Table 3. The raw kaolin clay was majorly a mesoporous material having low SSA of 10.322 $m^2\ g^{-1}$ and average pore size of 10.286 nm. Table 3 shows that both the pore volume and SSA increased with increasing acid strength. Treatment with 10M H_2SO_4 caused 5.25 times increase in SSA and 3.7 times increase in pore volume compared to raw kaolin clay. XRF analysis pointed out that the weight percentage of

Al_2O_3 decreased from 41.2 to 28.6 after acid treatment. The acid treatment might have caused partial leaching out of Al^{3+} ions from the octahedral sheet as well as dissolution of other metal oxides/removal of impurities, which resulted in the formation of additional mesopores in acid activated kaolin clay and is the most probable reason for the observed increase in the SSA and specific pore volume. No major change was observed in the average pore diameter which indicated that the leaching process was smooth. The altered mesopores and new mesopores were more or less of the same size.

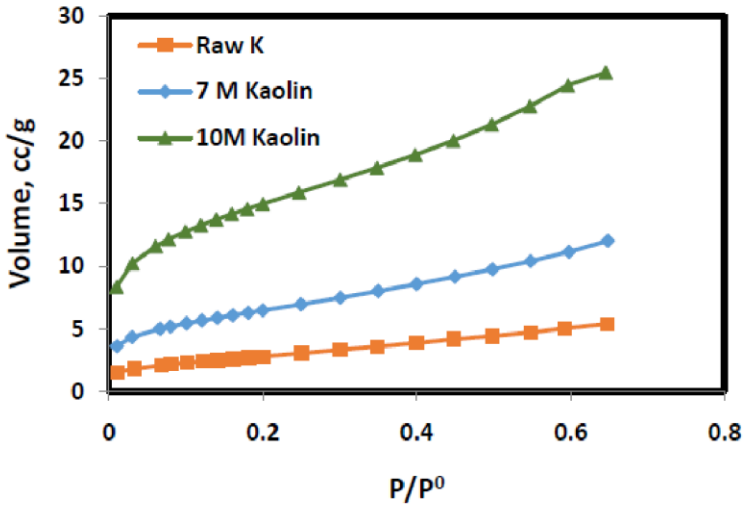

Fig. 4.7 N_2 adsorption isotherm of (a) raw kaolin clay (orange) (b) 7M H_2SO_4 treated kaolin clay (blue) (c) 10M H_2SO_4 treated kaolin clay (green).

Table 4.3: Textural properties of raw and acid treated kaolin clay

Material	**Surface Area ($m^2 g^{-1}$)**				**Pore volume ($cm^3 g^{-1}$)**		**Pore size (nm)**	
	S_{BET}	**S_{BJH}**	**S_{EXT}**	**S_{Micro}**	**V_{BJH}**	**V_{Micro}**	**d_{BJH}**	**d_{Avg}**
Raw kaolin	10.322	11.27	6.91	3.41	0.0413	0.00012	14.8	10.286
7M kaolin	23.567	24.14	16.49	7.09	0.086	0.00039	15.1	11.13
10M kaolin	54.19	49.74	39.72	14.47	0.153	0.00056	13.2	9.4

Finally, the 10M H_2SO_4 acid activated kaolin clay, which is used further for zeolite Y synthesis showed reduction in Al_2O_3 content from 41% to 21% (XRF analysis). As a result, the silica–alumina ratio increased from 1.3 to 2.4 which was favorable for the synthesis of zeolite. The dissolution of Al_2O_3 is primarily controlled by the diffusion of H_2SO_4 from the surface to the interior of the solid particles [30]. The BET surface area of acid treated kaolin increased from 10.322 to 54.193 m^2g^{-1} and pore volume from 0.041 to 0.152 cm^3g^{-1} compared to raw kaolin. The acid treatment caused partial leaching out of Al^{3+} ions from the octahedral sheet due to hydrolysis as well as dissolution of other metal oxides/removal of impurities, which resulted in the formation of additional mesopores and is the most probable reason for the observed increase in the specific surface area and specific pore volume [152]**.** The calcination of acid treated clay at 600ºC led to dehydroxylation which was responsible for partially disorderliness of structure with a smaller shrinkage of the dimensions of the sample and the rise in porosity which was further confirmed by the Nitrogen adsorption–desorption study [193]**.** The commercial cost of the acquired kaolin clay after the mining and beneficiation process is $75/t. The acid treatment involves usage of 4L of 10M H_2SO_4 solution per kg of beneficiated clay. The cost of H_2SO_4 required for treatment is $360/t. The processing cost including heating (steam), washing (DM water), drying (hot air), calcination (electrical furnace) is calculated at $170/t. Thus the overall cost of activated clay can be approximated at $600/t which is low. This inexpensive base material can be further processed to produce high grade, low-cost catalysts which can be very useful for large-scale applications in petroleum and other industries. Also being natural and eco-friendly, it can be highly compatible with naturally engineered technologies.

4.2.2 Bentonite clay

The bentonite clay possesses the Si–O or Al–O octahedral and tetrahedral sheets, which creates a charge imbalance in the 2:1 layer and might be a potential raw material to synthesize zeolites [168]. The Si–O and Al–O structures in bentonite are inactive. This means that it is difficult to directly synthesize zeolites and the bentonite must be pre-activated to change this inert structure [168]. The bentonite clay leached with H_2SO_4 to achieve the required silica-alumina ratio for zeolite and to remove impurities. The physico-chemical characteristics of

acid leached bentonite clay were studied by XRF, XRD, FTIR, TG- DTA, SEM and N_2 adsorption techniques.

I. XRF analysis

XRF analysis was carried out to confirm the changes in the chemical composition of the bentonite clay due to acid treatment as described in Section 2.3. The results are presented in Table 4. The raw bentonite sample predominantly contained silica (SiO_2), alumina (Al_2O_3) and iron oxide (Fe_2O_3). In addition, some impurities in the form of magnesium oxide (MgO), calcium oxide (CaO), potassium oxide (K_2O), manganese oxide (MnO), sodium oxide (Na_2O) and titanium oxide (TiO_2) were present in low proportions. The overall composition matched with bentonite from other regions [194]. Significant changes in the composition of the raw clay were observed after the acid treatment. The acid treatment initially leached metal ions from the internal clay mineral network due to which the Al_2O_3, MgO, CaO, K_2O, Fe_2O_3, MnO and Na_2O contents in the clay decreased significantly. The reaction between bentonite and H_2SO_4 can be described by the following reaction: $Al_2O_3{\bullet}2SiO_2{\bullet}2H_2O + 3H_2SO_4 \rightarrow Al_2(SO_4)_3 + 2SiO_2 + 5H_2O$ [146]. With increase in acid concentration, Al_2O_3 along with other metal oxides except TiO_2 seemed to dissolve from the octahedral layer consequently increasing the SiO_2 content from 51% to 92%. Hence, a large increase in the silica-alumina ratio from 2.256 to 24.11 was noted. Greater reduction in metal impurities could be observed by treatment with 10M H_2SO_4 compared to 5M H_2SO_4. The Na_2O and CaO contents decreased sharply when treated with 5M H_2SO_4 whereas the leaching of Al_2O_3, Fe_2O_3, MgO was more in case of 10M H_2SO_4. Similar phenomenon was also observed in case of treatment with other acids like HCl [153]. The acid treatment led to a steady increase in SiO_2 composition because of the removal of the octahedral cations and tetrahedral Al^{3+} from the internal clay mineral network. The opening of the edges of the crystal structure resulted in dissolution of most of the exchangeable cations with maximum effect on the Fe^{2+} and Mg^{2+} ions and detachment from the octahedral sheet [159,195].

Table 4.4: XRF analysis of raw Bentonite (RB) clay and after acid treatment using 5M and 10M H_2SO_4

Material	**Chemical component (wt %)**									**Silica-Alumina ratio**
	SiO_2	**Al_2O_3**	**MgO**	**CaO**	**K_2O**	**TiO_2**	**Fe_2O_3**	**Na_2O**	**MnO**	
Raw Bentonite	51.379	22.771	2.302	2.106	0.173	1.581	17.464	1.577	0.182	2.256
5M Bentonite	70.624	17.328	0.938	0.458	0.143	2.204	6.906	0.092	0.014	4.075
10M Bentonite	91.868	3.810	0.205	0.170	0.089	2.307	1.203	0.085	0.012	24.11

II. FTIR analysis

The FTIR spectra of both raw bentonite and acid activated bentonite were compared as shown in Fig. 4.8. The structural modification of bentonite caused by acid treatment was clearly revealed by the FTIR spectra. The 3000-3700 cm^{-1} region represented the OH and water vibrations. The adsorption bands at 3690 cm^{-1} and 3618 cm^{-1} are attributed to the stretching vibrations of OH groups coordinated to Si-OH and Al-OH groups of the tetrahedral and octahedral sheets. This indicated the crystalline order of bentonite which became more diffuse with increase in acid strength [155,194]**.** For bentonite clay treated with 10M H_2SO_4, loss of structural hydroxyl groups or in other words dehydroxylation was observed due to weakening of the structural hydroxyl vibration band followed by extensive leaching of Al^{+} ions from the tetrahedral and octahedral layer. It also indicated the development of free OH sites on the acid activated bentonite. The peaks near 1631 cm^{-1} were associated with bending vibration mode of physisorbed water. Due to the acid activation, the octahedral cations (mostly Al^{3+} and Mg^{2+}) percolated from the bentonite structure causing further damage to the octahedral layer which was demonstrated by the reduction in the intensity of bending bands at around 1635 cm^{-1} which is a typical feature of Al-Al-OH present in octahedral sheet. The bands of the spectrum with high intensity were mostly observed in the low-frequency zone. The high intense band around 1003 cm^{-1} and small peak at 1115 cm^{-1} are typical of bentonite which can be linked to Si-O stretching vibrations providing a confirmation of silicate structure. The most noteworthy change was the significant decrease in the intensity of this band which might

be because of development of three-dimensional structural configuration of amorphous silica, resulting in exposure of additional adsorption sites [154]**.** The peaks around 912 cm^{-1} were associated with the bending vibration of Al-Al-OH for all the samples. At 10M H_2SO_4, this peak reduced significantly indicating rapid dealumination. The decrease in intensity of the band related to OH-bending vibrations signified the dissolution of the octahedral sheets owing to acid treatment of the bentonite clay [153]**.** The IR peaks at 782 cm^{-1} may be attributed to the Si-O-Si vibrations of the layered clay structure. The intensity of these peaks increased with the strength of acid used for clay treatment indicating increased presence of silica. The spectrum between 800 and 750 cm^{-1} showed high sensitiveness towards crystallinity and purity of the bentonite clay sample. The twin peaks nearby 782 cm^{-1} are typical features of pure bentonite that indicated the existence of free silica and sometimes quartz particles, a common occurrence in natural bentonite and other types of clay samples. The peak at 689 cm^{-1} can be attributed to Si-O stretching as well as bending vibrations. The intensity of this peak decreased with increase in acid concentration. It further confirmed the presence of fine quartz particles. The FTIR result was in agreement to the XRF and XRD results which suggested substantial structural damage of the bentonite clay sheet due to acid treatment.

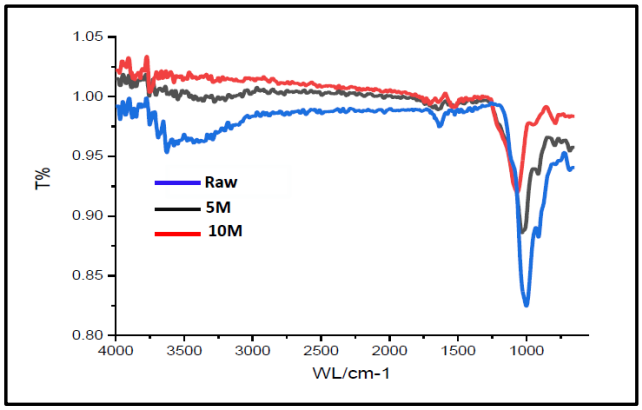

Fig. 4.8 FTIR analysis of (a) raw Bentonite clay (blue) (b) bentonite clay treated by 5M H_2SO_4 (black) (c) bentonite clay treated by 10M H_2SO_4 (red).

III. DTA study

The DTA curves of the raw bentonite and after acid treatment are shown in Fig. 4.9. The DTA curve of the raw sample is distinctive of bentonite with profound similarity with

bentonite of other regions. The two main losses at around 100^{o}C and 520^{o}C are endothermic. This is certainly a result of decrease in physisorbed water as well as chemisorbed water [196]. The endothermic reactions represent desorption of internal and external water (dehydration), loss of structural water from the crystal network (dehydroxylation) and ultimately destruction of the smectite structure. Treatment of the bentonite clay with acid resulted in elimination of the octahedral ions (mostly Al^{3+} and Mg^{2+}) besides the structural hydroxyl groups. It is to be noted that organics on decomposition also contributed to exothermic weight loss. The area covered by the endothermic and exothermic peaks reduced gradually with an increase in the acid concentration from 5M to 10M [197]**.** In 5M H_2SO_4 treated bentonite clay, the dehydroxylation peak was observed near 500^{o}C. Usage of 10M H_2SO_4 resulted in almost entire elimination of the structural water which was confirmed by the very small endothermic peak at 480^{o}C. The dehydroxylation temperature was observed to be inversely related to acid concentration. The decrease might be due to the elimination of the hydroxyl units from the fractured edges due to the structural destruction of bentonite [159]. The acid treatment resulted in important structural changes with decrease in interlayer distance owing to the loss of both -OH groups as well as water present between layers [198]**.**

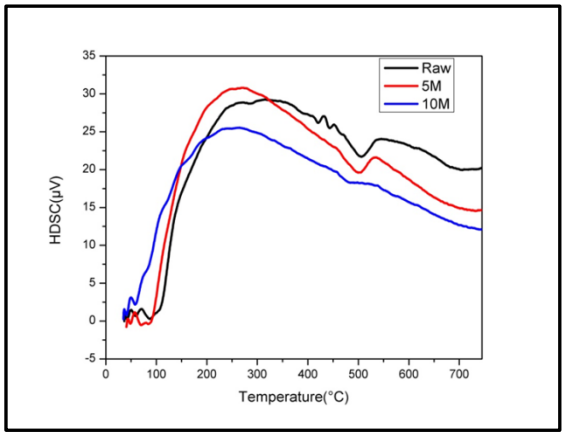

Fig. 4.9 DTA of (a) raw Bentonite clay (black) (b) bentonite clay treated by 5M H_2SO_4 (red) (c) bentonite clay treated by 10M H_2SO_4 (blue).

IV. XRD study

The intention behind the X-ray diffraction technique study was to further confirm the structural changes in bentonite clay owing to H_2SO_4 treatment. The XRD profiles of the raw

bentonite and after acid treatment are shown in Fig. 4.10. The highly intense peaks in the XRD profile confirm the crystalline behavior of the raw clay sample. The presence of many diffraction peaks corresponding to 00-013-0135, the principal crystalline phase matched with Smectite, more precisely with Ca-montmorillonite and some matched with 00-029-1498 (Na-montmorillonite). The patterns showed the planes (001), confirming the presence of mainly bentonite in the sample. Some of the peaks did not match which showed the presence of impurities like kaolinite, quartz and gypsum [198].

The XRD patterns of raw bentonite clay samples revealed basal reflections at angles 12.25˚, 19.95˚, 29.3˚, 34.99˚ and 61.73˚ which are associated to the presence of the smectite whereas, other peaks were of impurities such as quartz, gypsum and kaolinite [194]. H_2SO_4 activated samples exhibited more alterations up to 40Å of 2Θ due to structure breakdown and presence of amorphous silica. A reduction in peak intensity was observed after acid activation of bentonite by 5M H_2SO_4. The decrease in peak intensity along with increase in broadness of peak at 12.25Å and 19.95Å in XRD pattern of 5M H_2SO_4 clearly indicated that the acid activation affected the crystal structure of the bentonite which ultimately led to decomposition, which again confirmed the appearance of an amorphous phase [197]. Treatment with 10M H_2SO_4 caused severe leaching owing to the high concentration which led to disintegration of layered structure. Meanwhile, the d_{060} peak at 1.50 Å, which is characteristic of dioctahedral smectites, reached a maximum in 5M H_2SO_4 but reduced in case of 10M H_2SO_4. The intensities of the $d_{020\text{-}110}$ and $d_{130\text{-}200}$ reflections of bentonite at 4.45 and 2.56Å decreased continuously with increasing strength of acid. The peak at 25.27(2θ), having distance of 3.51Å, became noticeably visible in the spectrum of 5M H_2SO_4 which attained maximum intensity in the XRD pattern of 10M H_2SO_4 following dissolution of the octahedral cations. The peak at 12.25Å almost disappeared from the 10M XRD pattern and other peaks reduced and further broadened significantly. This indicated further structural destruction of bentonite as acid treatment caused leaching of metal from octahedral sheet and then from tetrahedral sheet and attributed to more X-Ray amorphous matter, which could be further confirmed by FTIR and XRF study [159]. The downfall of the smectite structure can be attributed to dehydroxylation along with development of fresh Si–OH and Al–OH bonds which are weak in nature. Also, new peaks could be observed and the intensities of reflections

corresponding to the impurities increased alongside demonstrating significant loss of smectite structure [199].

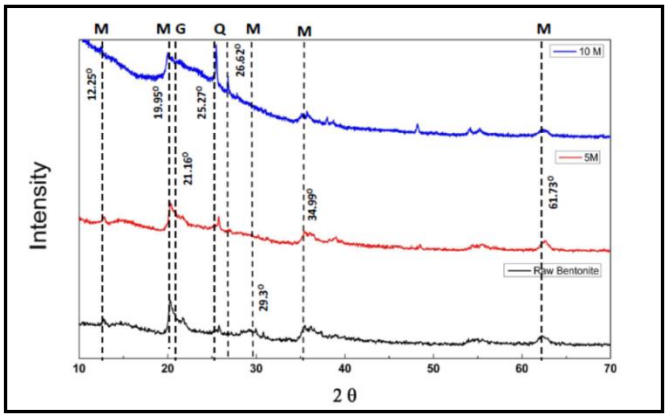

Fig. 4.10 XRD analysis of raw bentonite clay, treated by 5M and 10M H_2SO_4, M-Montmorillonite-bentonite, Q-Quartz, G-Gypsum

V. SEM study

The morphological features of bentonite clay before and after H_2SO_4 treatment are presented in the form of SEM micrographs at 500× magnification (Fig. 4.11). Raw bentonite samples displayed the existence of large particles and presence of lumps which might have formed by agglomeration of flaky particles. It further indicated that the well aggregated large flocs are moderately dispersive to dispersive which are apparently separate and dispersed from one another as shown in Fig. 4.11a. Bentonite treated with 5M H_2SO_4 displayed partial disaggregation and reduction in particle size (Fig. 4.11b). After acid treatment bigger clay particles were reduced to smaller irregular particles with rough surfaces displaying damaged crystalline structure which was also reported elsewhere [200]. Treatment with 10M H_2SO_4 (Fig 4.11c) led to complete disaggregation of the clay particles with total absence of lumps and drastic reduction in particle size. The 5M H_2SO_4 treatment resulted in formation of a highly porous structure which was clearly visible in Fig. 4.12. The visible increase in pores may be attributed to the acid leaching of octahedral metal ions resulting in opening of the smaller pores. Additionally there may be creation of some relatively larger new pores during acid treatment. This led to an overall increase in the pore volume and surface area which was further confirmed by N_2 adsorption-desorption study.

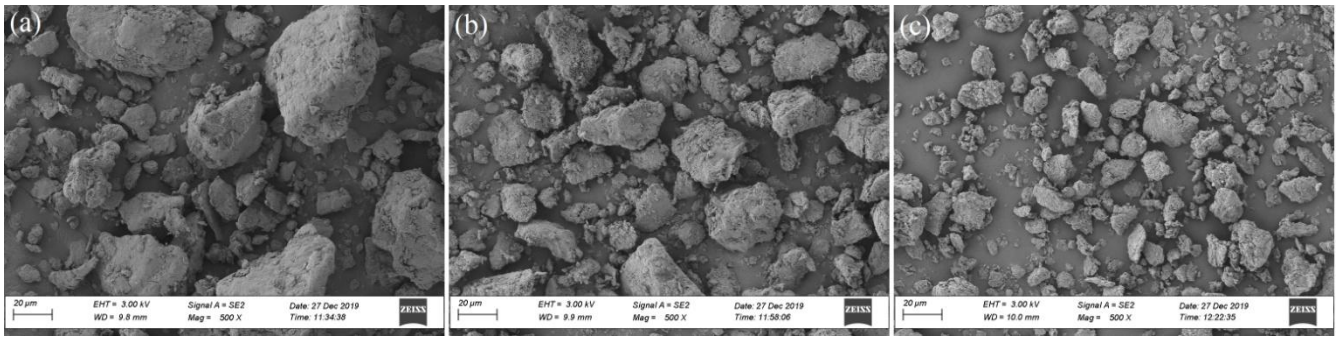

Fig. 4.11 SEM micrographs (500×) of (a) raw bentonite clay (b) bentonite clay treated by 5M H_2SO_4 (c) bentonite clay treated by 10M H_2SO_4.

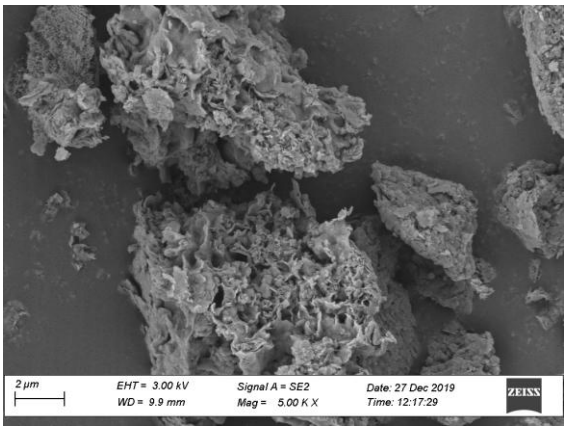

Fig. 4.12 SEM micrographs (5000×) of acid treated bentonite clay revealing highly porous structure caused due to acid treatment using 5M H_2SO_4 followed by calcination.

VI. Nitrogen adsorption-desorption study

The physical properties like surface area, pore volume and pore size of the acid activated clay play an important role when applied as catalyst and adsorbent. The specific surface area and pore volume of the raw and acid treated bentonite (5M and 10M) were obtained using N_2 adsorption-desorption isotherms (Table 5). The S_{BET} of raw untreated bentonite was found to be 86.63 m^2g^{-1} which was in line with bentonite clay of Indian origin (50 - 100 m^2/g) [15]. Acid treatment with 5M H_2SO_4 increased the S_{BET} to 305.56 m^2g^{-1} which was a 253% increase. A similar trend was observed in S_{BJH}, but the micropore area, $S_{\mu P}$ decreased 44%. This increase in S_{BET} was due to removal of impurities; substitution of cations like K^+, Na^+, and Ca^+ with H^+ ions; leaching of metal ions like $A1^{3+}$, Fe^{3+} and Mg^{2+} from the octahedral

and tetrahedral sheets; as a result of which the edges of the plates were opened and exposed [201]. It also reflected the presence of empty octahedral and tetrahedral sites remaining from the metal ions which were leached by acid treatment [195]. As a result the surface area increased which correspondingly confirmed the generation of porosity during the activation which was also revealed by the SEM images. In addition, the 5M H_2SO_4 treated bentonite showed 380% increase in V_{BJH} from 0.0235 to 0.1135 cm^3g^{-1} but at the same time 46% decrease in $V_{\mu P}$ was observed. Treatment of bentonite with 5M H_2SO_4 caused a large increase in pore volume in the range of macropores and mesopores and consequently increased the average pore diameter. This also suggested that considerable structural change and decomposition occurred in this clay sample. This decreased the micropore volume, due to leaching of octahedral metal ions on the surface of small sized pores. A combination of all these factors was probably responsible for the increase in pore volume. However, treatment with 10M H_2SO_4 led to decreased S_{BET} and S_{BJH} compared to 5M H_2SO_4 treated bentonite, which can be attributed to the collapse of pores due to high acid strength. The empty spaces caused due to leaching grew larger resulting in few micropores being converted into mesopores. High acid strength resulted in local decomposition of the crystal structure leading to disappearance of some of the mesopores which might have caused the reduction in specific surface area and pore volume. Partial destruction of smectite structure due to high acid strength might have led to generation of non-bonding free silica which dispersed at the surface resulting in closed pores [197]. V_{BJH} of 10M H_2SO_4 treated bentonite clay was also less than 5M H_2SO_4 treated bentonite whereas $V_{\mu P}$ was found to be high. However, formation of new micropores did not contribute to the total pore volume much. Similar phenomenon was also observed in case of Bentonite clay treated with other acids like HCl from other regions [146,155,194].

Finally, Bentonite clay obtained from Kachchh, Gujarat, India was structurally modified by treating with H2SO4 of different concentration followed by calcination. Detailed characterization of the raw and acid treated bentonite clay was carried out. XRF analysis showed that acid treatment caused substantial removal of metal and other oxides. The metal oxide content of clay decreased with acid strength. Treatment with 5M H_2SO_4 resulted in an increase in SiO_2 content from 51% to 71% subsequently increasing the Si/Al ratio from 2.25 to 4.04, which was favorable for the synthesis of zeolite. FTIR and DTA analyses showed that

Table 4.5: Textural properties of raw Bentonite clay and after acid treatment using 5M and 10M H_2SO_4.

Material	Specific Surface Area ($m^2 g^{-1}$)			Specific Pore volume ($cm^3 g^{-1}$)	
	S_{BET}	S_{BJH}	$S_{\mu P}$	V_{BJH}	$V_{\mu P}$
Raw Bentonite	86.63	42.61	38.20	0.024	0.013
5M Bentonite	305.56	207.61	21.26	0.113	0.007
10M Bentonite	286.41	186.94	30.05	0.102	0.012

increase in acid strength enhanced dehydroxylation by removal of large amounts of structural water accompanied by substantial leaching of Al^{3+} ions from the octahedral and tetrahedral layer leading to disintegration of the clay sheet. XRD results confirmed considerable structural disorderliness with increase in acid concentration resulting in amorphous nature. The N_2 adsorption-desorption study shown, the 5M H_2SO_4 treated bentonite clay having surface area (305 m^2/g) and pore volume (0.113 cm^3g^{-1}) and SEM micrographs revealed a highly porous structure caused by acid treatment leading to escalation in pore volume and surface area with high fraction of macropores and mesopores. This result clearly demonstrated that acid treatment is an economical and effective way of preparing low cost (~ $400/t) porous activated bentonite clay which can be a potential source of alumina silica in synthesis of zeolite and solid acid/proton source for numerous organic reactions. The 5M H_2SO_4 treated bentonite clay was considered further for zeolite Y synthesis.

4.2.3 Environment impact assessment

The only waste generated during treatment of clay is the diluted H_2SO_4 containing metal oxides, especially alumina. The acidic effluent should be neutralized and adequately treated before disposal into water bodies. An alternative way can be the recovery of precious metal/metal oxides like alumina/TiO_2 from the acid before disposal which can recover some cost of treatment [132,202]. The acid can be re-concentrated and recycled back using a suitable process [203]. Nevertheless, further study is required to determine the effect of

gradual accumulation of metal oxides in the recycled acid and its suitability for clay treatment and other uses.

4.3 Synthesis of Zeolite Y from clay

4.3.1 Kaolin clay to Zeolite Y (KZeoY)

I. XRF analysis:

Chemical composition of raw kaolin, KZeoY and RZeoY are shown in Table 6. For raw kaolin Silica (SiO_2) and alumina (Al_2O_3) contributed main proportion (~95%) of the oxides along with traces of other oxides namely MgO, CaO, K_2O, ZnO and TiO_2. The SiO_2/Al_2O_3 ratio was 1.3 which is generally observed between 1–1.5 for kaolin clay of Indian origin [204].

The KZeoY is rich in silica (66.53%) and alumina (21.52%) which is considered as main elements along with MgO, CaO, K_2O, Fe_2O_3 and MnO which are present in trace form. The content of Al_2O_3 is >90% higher in raw kaolin compared to KZeoY which shows significant leaching of Al_2O_3 during acid treatment thus increasing the SiO_2/Al_2O_3 ratio in KZeoY. The content of other oxides decreased (MgO, CaO, K_2O, MnO, Fe_2O_3) slightly. TiO_2, a valuable metal oxide remains almost the same. Presence of Na_2O in KZeoY was high at 10.21% compared to raw kaolin (0.138%) due to the introduction of NaOH into the activated kaolin for maintaining high alkaline conditions essential for zeolite Y synthesis. The percentage of Na_2O was around 12.64% in RZeoY. The SiO_2/Al_2O_3 ratio of KZeoY and RZeoY was determined at 3.09 and 3.03 respectively which was greater than 3, usually required for zeolite Y [125,133].

Table 4.6: Composition of raw kaolin clay and synthesized zeolite Y (KZeoY) with respect to reference zeolite Y (RZeoY)

Material	**Chemical component (wt %)**									**Silica-Alumina ratio**
	SiO_2	**Al_2O_3**	**MgO**	**CaO**	**K_2O**	**TiO_2**	**Fe_2O_3**	**Na_2O**	**MnO**	
Raw kaolin	53.786	41.194	0.094	0.367	0.274	3.032	0.690	0.138	0.016	1.3
KZeoY	64.99	21.021	0.009	0.020	0.213	2.777	0.451	10.21	0.009	3.09
RZeoY	65.387	21.556	0.037	0.076	0.074	0.019	0.136	12.64	0.006	3.03

II. XRD study

X-ray diffraction technique was applied to compare the structure of raw kaolin clay with zeolite Y (Fig. 4.13). The raw kaolin clay XRD pattern (Fig. 4.13a) showed well-defined reflections at around Bragg's angle (2Θ) of 12° and 25° which are distinctive characteristic peaks of kaolin. The sample pattern of raw kaolin was confirmed with standard kaolin (JCPDS card 00-014-0164). The minor peaks at 34–36° and 38–42° (2Θ) may vary depending on the origin of kaolin. The sharp and intense peaks confirmed the crystalline behavior of the raw kaolin clay sample.

In case of KZeoY, the characteristic peak intensities were observed at 2Θ value of 6.2°(1032), 10.1°(340), 11.9°(389), 15.6°(1345), 18.6°(622), 20.3°(988), 23.6°(1965), 26.9°(1526), 31.3°(2855) and 34.6°(486) (Fig. 4.13b). Similarly, the characteristic peak intensities for the RZeoY were observed at 2Θ value of 6.2°(1760), 10.1°(394), 11.9°(311), 15.6°(1219), 18.6°(585), 20.3°(1037), 23.6°(1794), 26.9°(1343), 31.3°(2025) and 34.6°(390). According to the International Zeolite Association, (AIZ, 2017), a zeolite Y is expressed by the presence of the crystalline phases at 2Θ 6.18°, 10.08°, 15.58° and 18.58°. All these peaks were observed in KZeoY at 2Θ 6.2°, 10.1°, 11.9°, 15.6°, 18.6°, 20.3°, 23.6°, 26.9° , 31.3° and 34.6° which matched well with standard zeolite Y. The small differences observed are attributed to the presence of impurities such as Fe^{2+}, Ti^{2+} and Ca^{2+} in the parent clay. The first XRD peak in the diffraction pattern was due to diffraction from planes with the lowest Miller indices. In

KZeoY first peak of 6.18 showed Miller indices of 111 which confirmed the face centered cubic (FCC) structure of zeolite Y.

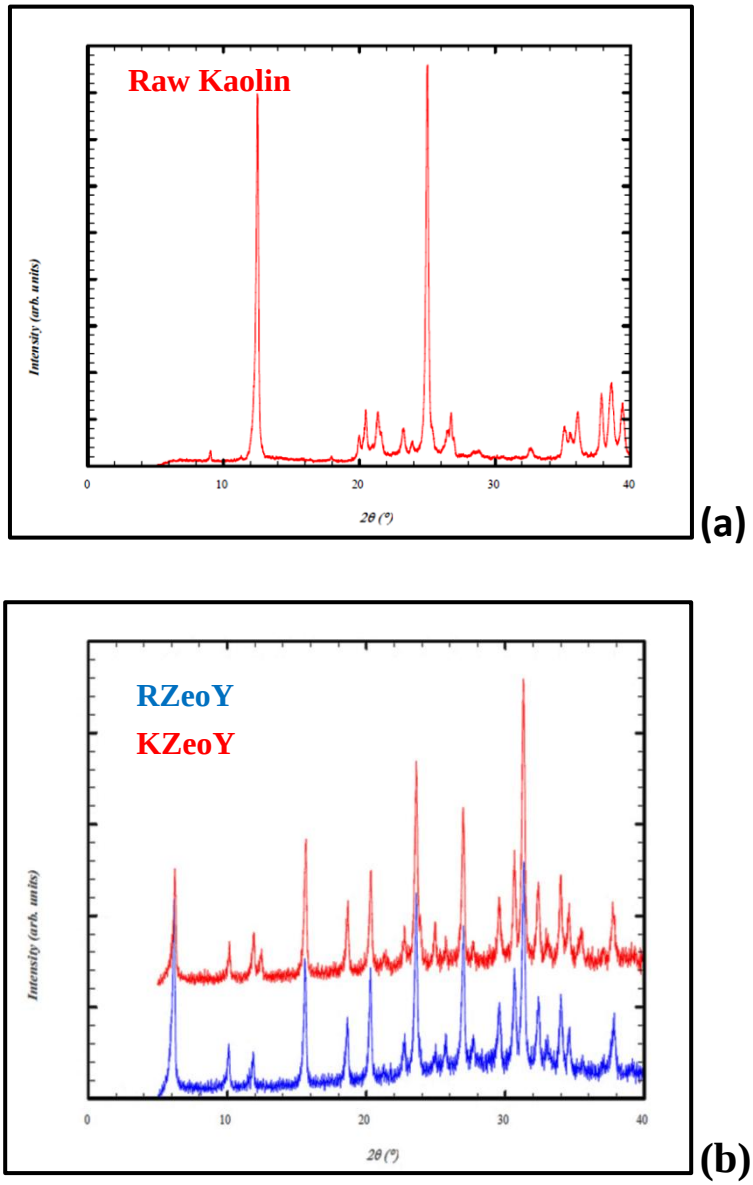

Fig. 4.13 Comparison of the XRD patterns of (a) raw kaolin clay (b) synthesized zeolite Y (KZeoY) from kaolin clay and reference zeolite Y (RZeoY).

Table 4.7: Crystallinity calculation of synthesized zeolite Y (KZeoY)

Common peak	CZeoY	RZeoY	KZeoY
6.18	1535	1760	1032
10.14	914	394	540
11.88	993	311	389
15.62	2075	1219	1375
18.6	1117	585	622
20.3	1548	1037	988
22.8	573	280	278
23.7	2610	1794	1965
25.8	382	257	360
30.8	907	859	898
31.3	1888	2025	2855
Total	14542	11521	10102
	100.00	**78.34**	**76.34**

Table 4.8: Lattice parameter calculation

Type of Zeolite	a (Å)
CZeoY	24.68
RZeoY	24.77
KZeoY	24.65

For further confirmation hkl values for peaks of XRD were calculated that were 111, 220, 311, 222, 331, 511, 440 and 531. Same lowest Miller index was also observed for RZeoY. The other hkl values of RZeoY were also matched with standards [205]. The lattice constant was calculated from XRD data in both the cases and were 24.65Å and 24.77Å for KZeoY and RZeoY respectively conforming to the reported values [121]. Furthermore, the characteristic peak intensity of a mineral not only show the extent of crystallinity but also indicates the concentration of the crystalline content [206]. For the KZeoY and RZeoY samples, the crystallinity (estimated using ratio of the sum of the characteristic XRD peaks intensity) was

76.34% and 72.35% respectively indicating both were at par, when compared with respect to commercial zeolite Y sample obtained from Zeolyst international.

III. SEM analysis

The SEM images of the raw kaolin, KZeoY and RZeoY are presented in Fig. 4.14. The SEM micrograph of raw kaolin clay (Fig. 4.14a) indicated the existence of particles of large size which might have formed by accumulation of flaky particles. The images demonstrated that the agglomerated flaky particles of kaolin were transformed into well-defined crystal structure. The SEM image of KZeoY (Fig. 4.14b) showed well-developed crystals of varied structure and size along with some kaolin debris. The crystallinity of KZeoY was due to an increased percentage of Na_2O caused by addition of NaOH to activated kaolin during fusion [118]. The growth of the crystal increases with crystallization time and 48h is optimal for the synthesis of zeolite Y from kaolin clay [207]. The fully grown crystals of zeolite Y having an average particle size of 272 nm were visible which were dispersed uniformly on activated kaolin substrate. The kaoline substrate could be identified by its unique hexagonal prism structure, typical of kaolinite. The crystal sizes of zeolite Y depend on activated kaolin particles, as the nucleation starts on the surfaces of kaolin and crystals grow from nutrients provided by activated kaolin [51]. However, the crystals of KZeoY were smaller and in some cases not as well-developed as those of RZeoY. This might be due to defects that were caused by impurities present in activated kaolin [208]. The irregular crystals of various sizes formed were typical of the hydrothermal route. In case of RZeoY (Fig. 4.14c), equally dispersed agglomerated zeolite crystals were observed amid more uniformity in crystal structure (average particle size 289 nm). Boundaries of individual crystals were clearly visible. Overall the SEM study was in agreement with the mineralogical composition of the synthesized zeolite, which was further supported by BET and XRD investigation of the zeolite products.

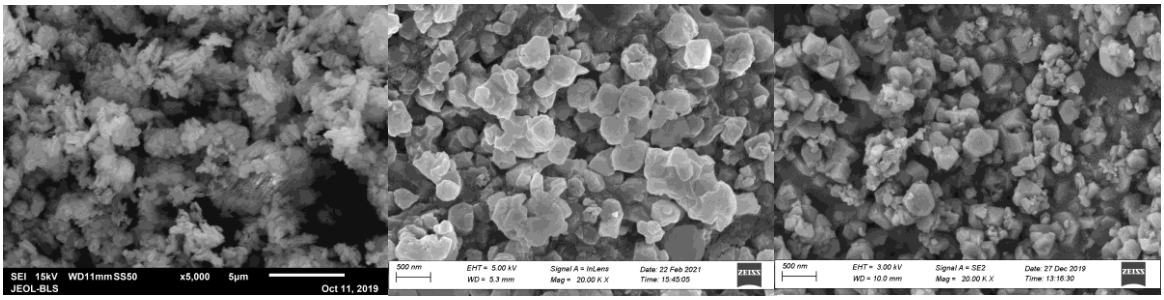

Fig. 4.14 SEM images of (a) raw kaolin clay (b) KZeoY (c) RZeoY.

IV. N_2 adsorption-desorption study

Pore size distribution is an important characteristic for porous materials. The surface area and particle size indicates the effectiveness of the synthesized zeolite in application point of view as larger surface area leads to higher cracking efficiency in the petroleum industry. Raw kaolin with 80 - 95 weight percent of kaolinite generally has Brunauer–Emmett–Teller (BET) surface area between 9 and 45 m^2g^{-1} [191]. It also depends on the nature of clay, element compositions (SiO_2/Al_2O_3 ratio) and presence of other metal oxides. Table 9 compares the textural properties of raw kaolin and zeolite Y obtained from the two routes based on N_2 adsorption-desorption study. Analysis of the raw kaolin clay revealed a low S_{BET} of 10.32 m^2g^{-1} and d_{Avg} of 10.29 nm. The t-plot analysis showed very less V_{Micro} and S_{Micro} confirming that the raw kaolin was primarily a mesoporous material. The S_{BET} of KZeoY increased manifold compared to raw kaolin. However the Barret–Joyner–Halenda (BJH) surface area increased only about three times compared to S_{Micro} which increased manifold. Similarly the V_{BJH} doubled whereas t-plot analysis revealed manifold increase in V_{Micro}. All these analyses pointed towards generation of a lot of micropores resulting in formation of crystalline Zeolite Y having predominantly micropores and less mesopores. This was further confirmed by reduction in both d_{BJH} and d_{Avg}. The N_2 adsorption-desorption study of RZeoY confirmed the formation of highly microporous crystalline Zeolite Y. The S_{BET} of KZeoY (320 m^2/g) was found to be lower than RZeoY (571 m^2/g) suggesting that the former has lower adsorption capacity and lower specific surface area than the latter. The S_{Micro} constituted more than 87% and 93% of the S_{BET} available for KZeoY and RZeoY respectively, indicating presence of a larger percentage of mesopores in KZeoY. The V_{BJH} was slightly higher in RZeoY, but

RZeoY displayed 62% more V_{Micro} compared to KZeoY which also corroborated with the fact that RZeoY had more micropores. The presence of more micropores in RZeoY was also confirmed by the fact that the average pore diameter of RZeoY was lower than KZeoY. Fig. 4.15a showed the N_2 adsorption-desorption isotherms of KZeoY and RZeoY at 77 K. Both the isotherms belonged to type-I based on IUPAC classification. The sharp surge at low relative pressures ($P/P^0 < 0.01$) was a result of the filling of the micropores in zeolite [209] which is less in KZeoY compared to RZeoY. KZeoY exhibited uptake at high relative pressure ($0.85 < P/P^0 < 1.0$), which showed presence of more mesopores compared to RZeoY. Fig. 4.15b displayed that the pore diameter up to 50 nm had high density of cumulative volume for KZeoY whereas in case of RZeoY maximum density was visible up to 7nm indicating more mesoporosity in KZeoY.

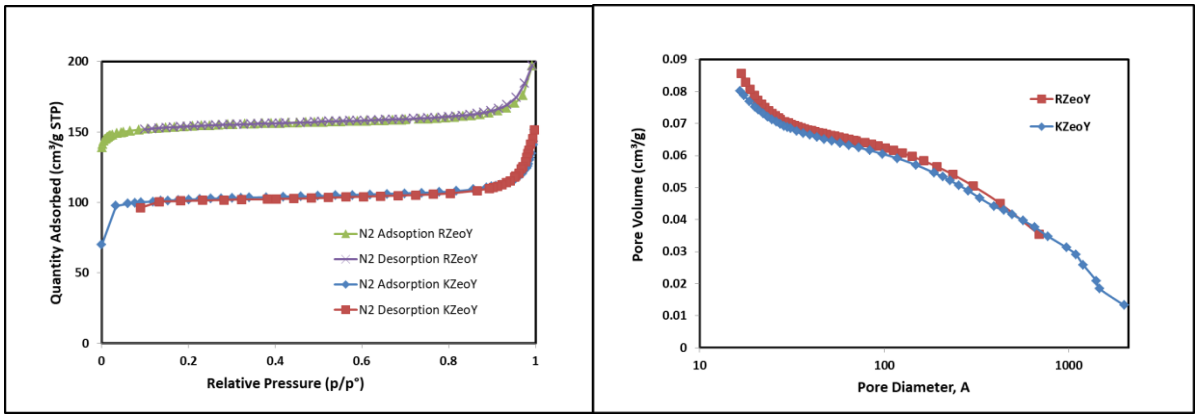

Fig. 4.15 (a) N_2 adsorption-desorption isotherms (b) Pore volume distribution of KZeoY and RZeoY

Table 4.9: Textural properties of raw kaolin clay and synthesized zeolite Y

Material	**Surface Area ($m^2 g^{-1}$)**				**Pore volume ($cm^3 g^{-1}$)**		**Pore size (nm)**	
	S_{BET}	**S_{BJH}**	**S_{EXT}**	**S_{Micro}**	**V_{BJH}**	**V_{Micro}**	**d_{BJH}**	**d_{Avg}**
Raw kaolin	10.32	11.27	6.91	3.41	0.0413	0.00012	14.8	10.29
KZeoY	320	33.52	39.05	281.05	0.0801	0.13618	9.56	2.89
RZeoY	571	42.32	40.29	530.85	0.0869	0.22038	8.1	2.11

4.3.2 Bentonite clay to Zeolite Y (BZeoY)

The synthesis of zeolite Y from 5M treated bentonite clay was tried by varying parameters. The chemical composition of the overall gel was kept as 180 H_2O :1 Al_2O_3 : 10 SiO_2 : 4.62 Na_2O for all batches. The XRD pattern of the initial experiments showed total amorphousity and Y formation was not initiated even after 48 hrs. The XRD images of 72, 84 and 96 h are shown in Fig. 4.16. The first peak was not even initiated in any samples. Other peaks are not coordinated. This may be due to the high percentage of Fe_2O_3 in the treated sample. The XRF analysis of 10M treated bentonite clay showed that the percentage of Fe_2O_3 reduced to 1% but at the same time high removal of Al^{3+} was also observed and Si/Al ratio was increased up to 24. In this case the need of both chemicals is increased to match the final composition and the purpose of green sustainable resources is not served. It seemed that because of the presence of a high percentage of Fe_2O_3 and almost complete removal of Al^{3+} ion due to acid leaching, the Si/Al ratio could not be adjusted as required. Hence, it did not lead to formation of the required structure of zeolite Y. In future, further experimentation can be carried out and this work can be taken up employing some new idea and synthesis of zeolite Y can be attempted.

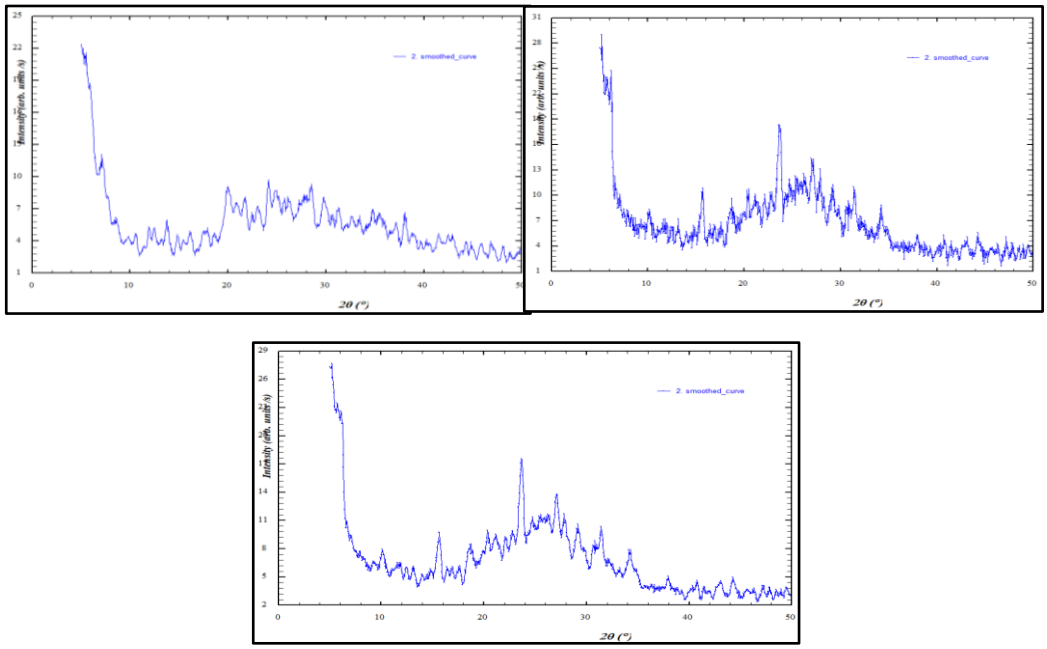

Fig. 4.16 XRD of samples of bentonite base synthesized Y for different crystallization time (a) 72 h (b) 84 h and (c) 96 h

4.4 Zeolite Y synthesized by ultrasonic method (UZeoY)

I. XRD study and Compositional analysis

The XRD pattern exhibited well-resolved peaks in the high 2θ region of 3-40^{o} (Fig. 4.17). The peak positions of RZeoY and CZeoY are nearly identical and correspond to pure well crystallized zeolite Y structure. UZeoY displayed high crystallinity compared to the conventional heating method in a shorter time. Ultrasonic assisted ageing methods promoted the formation of zeolite Y by enhancing the rate of nucleation and shortening the crystallization time during the crystallization process. The lattice constant was calculated from XRD data in both the cases (Table 11) and were 24.67Å and 24.68Å for UZeoY and CZeoY respectively conforming to the reported values. For the UZeoY sample, the crystallinity was 98.63% indicating that the sample is at par, when compared with CZeoY. The UZeoY was rich in silica (62.80%) and alumina (21.71%) along with trace amounts of MgO, CaO, K_2O, Fe_2O_3 and MnO. Presence of Na_2O in UZeoY was high at 15.21% compared to other samples. The SiO_2/Al_2O_3 ratio of UZeoY and RZeoY was determined at 2.9 and 3.09 respectively and are between 2.5 and 3.0 which correspond to zeolite Y.

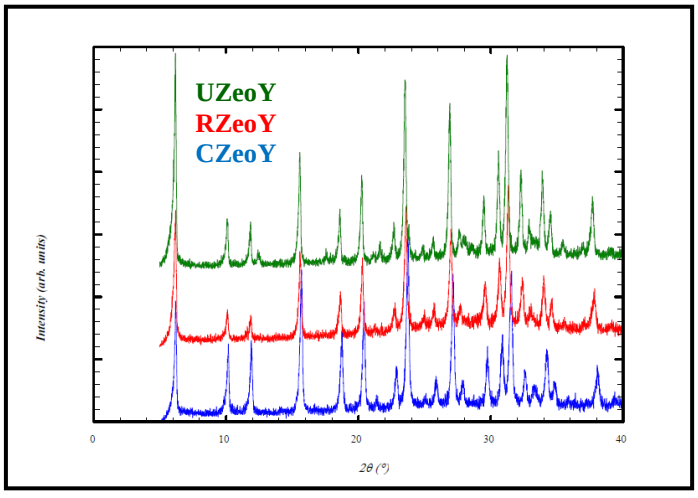

Fig. 4.17 XRD of synthesized UZeoY, RZeoY and CZeoY

Table 4.10: Lattice parameter of UZeoY

Type of zeolite	a (Å)
CZeoY	24.68
RZeoY	24.77
UZeoY	24.67

Table 4.11 : Crystallinity calculation of UZeoY

Common peak	CZeoY	UZeoY
6.11	1535	3137
10.14	914	708
11.88	993	513
15.62	2075	1677
18.6	1117	750
20.3	1548	1297
22.8	573	392
23.7	2610	2817
25.8	382	296
Total	11747	11587
	100.00	**98.63**

II. SEM study

The SEM images of Fig.4.18b show the crystals of zeolite obtained during the ultrasound treatment and compared with CZeoY (Fig.4.18a). The UZeoY particles exhibited close nanocrystal aggregates having uniform particle size distribution with slight reduction in size compared to CZeoY. The physical phenomenon involved in sonication is acoustic cavitation that generates high energy shock waves, resulting in high nucleation rates. Also, the fast bubble collapse produced a rapid rate of temperature decrease which prevented the organization and agglomeration of the particles, resulting in crystal formation of small size [210]. This well-dispersed morphology along with the highest crystallinity minimized the diffusion length of reactant molecules into the pores and correspondingly the products out of zeolites.

(a)

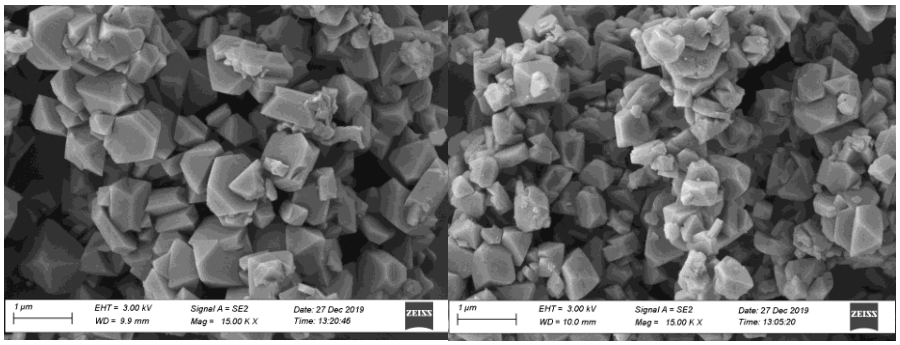

(b)

Fig. 4.18 SEM images of (a) CZeoY and (b) UZeoY.

III. N_2 adsorption-desorption study

The UZeoY textural properties were measured from nitrogen isotherms (at 77 K) and are listed in Table 12. The zeolites obtained in this work presented the highest BET surface area among all the synthesized zeolite Y. The BET surface area and pore volume were both at par with CZeoY and more than RZeoY. In case of UZeoY, d_{avg} was 1.75 nm which was minimum pore size and V_{Micro} was 0.298 cm^3g^{-1} was maximum pore volume among all samples. These results are in correspondence with higher crystallinity and smaller crystal size. The N_2 adsorption – desorption isotherms of UZeoY obtained in this study (Fig. 4.19a) present a hysteresis loops of Type I profile. The isotherms of UZeoY showed an initial adsorption step at very low relative pressure (P/P°=0.02), indicating the complete filling of the micropores. The UZeoY sample synthesized using sonication showed higher N_2 adsorption capacity than the RZeoY obtained by conventional hydrothermal method because of its higher crystallinity. Moreover, the very small hysteresis loops in the isotherm curve for the porous monocrystalline UZeoY at relatively high pressure suggest presence of some mesoporosity compared to RZeoY. This result is visible in Fig. 4.19b of pore distribution by BJH model. The material mesoporosity resulted from the filling of inter-crystalline voids shaped in the nanocrystals packing due to their morphology [40]. The hysteresis loop at relative pressure between 0.45 and 0.85 is associated with slit shaped pores, while the hysteresis loop at high relative pressure (P/ P°=0.85–1.00) corresponds to more spherical voids.

Table 4.12: Textural properties of synthesized UZeoY, CZeoY and RZeoY

Material	Surface Area ($m^2 g^{-1}$)				Pore volume ($cm^3 g^{-1}$)		Pore size (nm)	
	S_{BET}	S_{BJH}	S_{EXT}	S_{Micro}	V_{BJH}	V_{Micro}	d_{BJH}	d_{Avg}
CZeoY	693.47	58.00	54.37	639.10	0.081	0.265	5.6	1.98
RZeoY	571	42.32	40.29	530.85	0.087	0.220	8.1	2.11
UZeoY	751	34.88	34.55	716.95	0.032	0.297	3.7	1.75

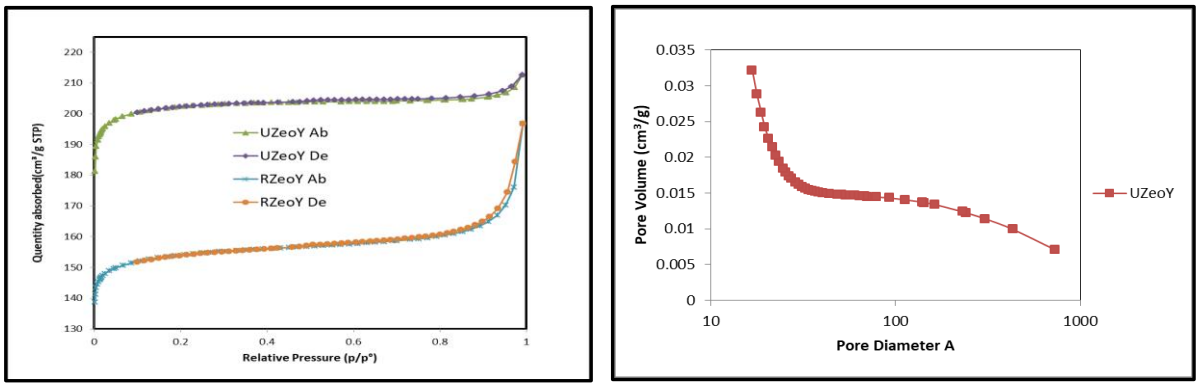

(a) **(b)**

Fig. 4.19 (a) N_2 adsorption-desorption isotherms and (b) Pore volume distribution of UZeoY and comparison with references

4.5 Application in esterification reaction

4.5.1 Ion exchange by NH_4NO_3 - catalyst activation

XRF characterization after ion-exchange process and calcination (Table 4.13) indicated that Na-cations from both zeolites (RZeoY, KZeoY and UZeoY) were detached and replaced with NH_4^+ which subsequently became H^+ after calcination [211]. This also indicated formation of active acid sights required for reaction. The results indicated that Na-cations from framework at zeolites were removed and exchanged with NH_4^+ and then become H^+ after calcination [212]. To prevent disintegration of the structure by acid attack, sodium is first ion-exchanged with the NH_4^+. Then the acidic form is generated by thermal decomposition of NH_4^+ to H^+ and NH_3 [213]. Ammonium ions are decomposed by heating to H^+ and outgoing NH_3 gases consequently forming HY modification [214]. The catalytic property of zeolites is a result of the combination of the intrinsic properties found in zeolite liable for its overall behavior. The

creation of active sites as discussed and shown in Fig. 2.3 [62] which result from the exchange of cations with ammonium hydroxide followed by calcination which is regarded as one of the most important step in zeolite catalyst production. These sites are referred to as the bridging hydroxyl which is formed at each oxygen bridge site near the clustering of the Si-O-Al where the cation that neutralizes the negative charge is represented by protons. The presence of acid sites is the main reason behind zeolites being used as catalyst in industries. This is as a result of the formation the hydroxyl group inside the pore structure of the zeolite that has high electrostatic field attracting organic reactant molecules resulting in a rearrangement of bonds. Some of the reactions that take place in the formation of acid sites are represented using equations 1 and 2 respectively. These reactions are mostly associated with zeolite having low silica like zeolite X and zeolite Y [4].

$$NaZ_{(s)} + NH^{+}_{4(aq)} \longrightarrow NH_4Z_{(s)} + Na^{+} \quad \ldots\ldots\ldots \quad (2)$$

$$NH_4Z_{(s)} \longrightarrow NH_3 + HZ \quad \ldots\ldots\ldots\ldots \quad (3)$$

Table 4.13: Na_2O content of zeolites before and after activation by ion exchange.

Material	**Na_2O content (% weight)**	
	Synthesized	**Activated by ion exchange**
KZeoY	10.21	3.425
RZeoY	12.64	3.868
UZeoY	15.087	3.001

4.5.2 Esterification reaction

The performance of zeolites and clay as a catalyst was explored for esterification of succinic acid (SA) with ethanol. The mechanism of esterification is the protonation of SA, followed by nucleophilic attack of alcoholic groups to yield respective monoesters [5,137]. Owing to the carboxylic group present in monoesters, it gets further esterified by the same mechanism leading to formation of diesters, both occurring consecutively. It is a reversible reaction and hence thermodynamically limited [215]. In order to overcome the equilibrium limitation and to increase the yield, ethanol was supplied in excess amount. During the entire reaction

process, the ethanol being excess reactant, its concentration was more throughout. Therefore ethanol occupied more active sites in the catalyst compared to SA at any time. The carboxylic group present in the monoester gets further esterified following the same mechanism that resulted in the formation of diester, which occurred consecutively as shown below.

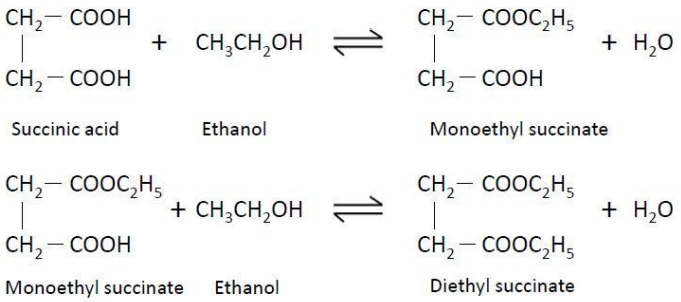

------ (4)

4.5.2.1 Kaolin clay

The conversion of SA and yield of ester is reported in Table 4.14. In case of raw kaolin clay, conversion of SA was 27% and led to formation of mainly monoester (monoethyl succinate) remaining being diester (diethyl succinate). This showed that most of the available active sites were used for the formation of monoesters initially. The 7M H_2SO_4 treated kaolin which has more active sites due to formation of additional mesopores (because of acid leaching) showed a marginal increase (32%) in conversion of SA. The ethanol quantity being more at any time during reaction, occupied the excess available active sites due to competitive adsorption which consequently converted the monoester to diester. Usage of 10M H_2SO_4 treated kaolin further increased the conversion of SA to 56%. More Al^{3+} ion exholved from the structure of kaolin by 7M and 10M acid activation boosted the Bronsted acidity for esterification of dicarboxylic acid to diester [5,34]. The decrease in the yield of monoester and increase in the yield of diester was observed simultaneously. This clearly demonstrated that with increase in active surface area of kaolin clay the product yield shifted from monoester to diester. The reusability study of the 10M H_2SO_4 treated kaolin catalyst in the esterification reaction was performed for three consecutive cycles under the same reaction conditions. The conversion of SA after each cycle was 55.29%, 54.12% and 52.69% respectively. The results showed a stable performance with minor decrease in the catalytic activity compared to the fresh

catalyst, which established that the 10M H_2SO_4 treated kaolin catalyst can be regenerated and reused easily without losing its catalytic activity displaying good stability. Similar observation has also been reported in literature for catalysts prepared from kaolin clay of other regions [216–218]. This structurally modified clay can be used for synthesis of zeolite which can further increase the conversion of SA consequently enhancing the yield [137].

.

4.5.2.2 Bentonite clay

The conversion of SA and yield of both the esters in percentage is shown in Table 4. When raw bentonite was used as a base case, the conversion of SA was 25%. As reported, the esterification reaction proceeds first by protonation of SA and then by nucleophilic attack of ethanol to produce monoester [5,137]. Consecutive reaction occurs, which results in an increase in ethanol conversion. Owing to the carboxylic group present in MES, it gets further esterified by the same mechanism leading to formation of DES, both occurring consecutively. DES formation is a consecutive reaction and can be confirmed from the fact that there is a simultaneous decrease in percentage yield of MES along with increase in percentage yield of DES. H_2SO_4 activation of bentonite affected catalytic activity by a combination of various factors like substitution of interlayer cations with H^+ ions; selective leaching of metal ions like $A1^{3+}$, Fe^{3+} and Mg^{2+} from the broken octahedral and tetrahedral sheets resulting in more acid sites; and a reduction in the size of clay platelets [161,219]. When 5M H_2SO_4 treated bentonite was used as a catalyst the conversion of SA increased to 62%. More Al^{3+}, Fe^{3+} ions were exholved from the structure of bentonite by 5M H_2SO_4 which boosted the required Bronsted acidity [5,137]. It has been established that esterification of dicarboxylic acid to diester requires strong Bronsted acidity [5]. In the case of 10M H_2SO_4 treated bentonite, 55% SA was converted into esters. Conversion of SA is reduced due to lower surface area compared to 5M H_2SO_4 treated bentonite. Also Al^{3+} and Fe^{3+} content decreased with increase in concentration of H_2SO_4. The catalytic activity increased when the clay was treated up to a certain optimum strength of acid, while higher acid strength resulted in decreased activity. This conformed to literature findings that when the bentonite clay samples are treated with acids of low strength then higher Bronsted acidity and corresponding catalytic activity are obtained [155,159,220]. Thus treatment with higher acid strength may not be beneficial.

4.5.2.3 Zeolite Y from kaolin (KZeoY)

The catalytic applicability of the H form of RZeoY and KZeoY were also explored for esterification reactions. The conversion of SA for raw kaolin clay was 28% (Table 4.14) which led to formation of largely monoester (monoethyl succinate) with a small amount of diester (diethyl succinate). Bulk of the accessible active sites seemed to be initially utilized for

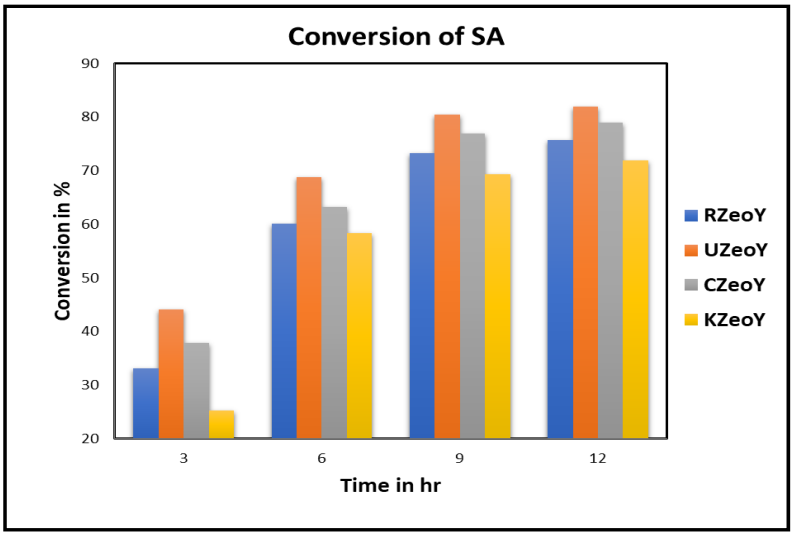

Fig. 4.20 Conversion of Succinic acid with time for all Zeolites

the production of monoesters. The conversion of succinic acid (SA) was 72% and 76% with KZeoY and RZeoY respectively. No significant difference was observed in conversion of SA between both zeolites even though the difference in S_{BET} existed. BET study showed that both KZeoY and RZeoY had comparable S_{BJH} and V_{BJH} even though S_{BET} was less for KZeoY. KZeoY is showing more mesoporosity with high value of d_{BJH} and d_{Avg} than RZeoY, which increased molecular diffusion rates; overall pore accessibility, enhanced transport characteristics and reduced transportation lag of molecules. Wide-pore zeolites increased the catalyst effectiveness by attaining higher intra crystalline diffusivity but each individual molecule acts differently as per their role. The reactants enter while products leave the same pore resulting in slow transport and restricted accessibility. Apart from that the reactant and product molecule size also play a key role [221]. This result confirmed that the initial active sites were used in conversion of SA and consequently the reaction progressed (Fig. 4.21). More hydrophobic esters were produced due to presence of hydrophobic environment in

active catalyst pore which encouraged partition of succinic acid molecules [222]. The ethanol being an excess reactant occupied the majority of the surplus active sites owing to competitive adsorption. This resulted in the conversion of the monoester to a more valuable diester. The final yield of diester increased to 60% with usage of KZeoY. Fig. 4.21 showed the consecutive decrease in the concentration of monoester with increase in diester concentration with time. The yield of the diester is furthermore compared with other catalysts as reported in literature (Table 4.15). It is observed that significantly higher yield of diester is obtained for high acid to alcohol ratio [222]. Similarly more reaction time and higher amount of catalyst also resulted in higher diester yield [215,223]**.** The performance of present synthesized KZeoY catalyst is also at par by obtaining reasonably good yield of diester at moderate reaction conditions. Furthermore, the catalyst could be easily recovered from the aqueous reaction mixture by filtration and subsequently regenerated and reused. In case of RZeoY more active sites were available and hence mono ester could react with excess ethanol resulting in more quantitative conversion of diester.

Table 4.14: Esterification of succinic acid with ethanol using H form of synthesized zeolites from kaolin clay as catalyst.

Catalyst (H form of Zeolites)	**% Conversion of Succinic acid**	**Yield of Esters**	
		Monoester	**Diester**
Raw Kaolin	27	76	24
KZeoY	72	40	60
RZeoY	76	20	80

Reaction Condition: mole ratio of succinic acid to ethanol: 1:3, amount of catalyst: 1g, reaction time: 12h, reaction temperature: 72^{o}C

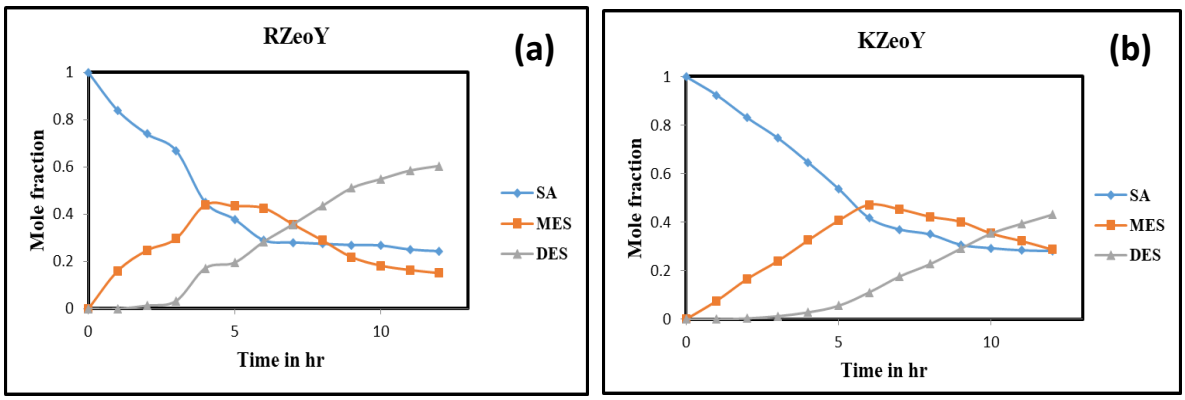

SA: Succinic acid; MES: Monoester; DES: Diester

Fig. 4.21 Catalytic activity of Y zeolites [(a) RZeoY and (b) KZeoY] with time on stream

Table 4.15: Comparison of the performance of reported catalysts in the esterification of succinic acid with ethanol.

Catalyst	Reaction conditions**	% yield of diester	References
Amberlyst XN-1010	1:4; 80; 20; 192	89	[215]
TPA-MCM-41	1:3; 80; 0.1; 8	68*	[5]
Amberlyst-15	1:10; 90; 2; 12	70	[223]
DARCO®-HSO_3	1:30; 80; 0.1; 24	90	[222]
Starbon®-400-HSO_3	1:30; 80; 0.1; 8	95	[222]
Mn+-montmorillonite	1:3; 50; 0.5; 8	64	[224]
Al-MCM-41	1:3; 120; 0.1; 12	43	[225]

* Esterification of Succinic acid with Butanol

** Reaction conditions: mole ratio (acid to alcohol); reaction temperature (°C); amount of catalyst (g) : reaction time (h)

4.5.2.4 Ultrasonic Zeolite Y (UZeoY)

The highest conversion of 82% of succinic acid was achieved with UZeoY (Table 4.16). This was even more than CZeoY. The UZeoY presented high BET surface, attributed to

nanocrystals with a uniform morphology which are dispersive among each other; thus, leading to more cell crystals and more exposed pore mouths, resulting in an external and BET surface area increase.The increase in the external surface area is consistent with a reduction in particle size due to the number of crystals per crystallite present in the material. The SEM image showed well-dispersed morphology & with the highest crystallinity with smaller crystal size. This minimizes the diffusion length of reactant molecules into the pores and correspondingly the products out of zeolites. It leads to increased molecular diffusion rates; overall pore accessibility, enhanced transport characteristics and reduced transportation lag of molecules. Apart from that the reactant and product molecule size also play a key role [221]. This result confirmed that the initial active sites were used in conversion of SA and consequently the reaction progressed (Fig.4.22). More hydrophobic esters were produced due to presence of hydrophobic environment in active catalyst pore which encouraged partition of succinic acid molecules [222]. The ethanol being an excess reactant occupied the majority of the surplus active sites owing to competitive adsorption. This resulted in the conversion of the monoester to more valuable diester. The final yield of diester increased to 96% with usage of UZeoY. Fig. 4.22 showed the consecutive decrease in the concentration of monoester with increase in diester concentration with time. The yield of the diester is furthermore compared with other catalysts as reported in literature. The performance of UZeoY as a catalyst is very encouraging as it could obtain a very high yield of diester at moderate reaction conditions. Furthermore, the catalyst could be easily recovered from the aqueous reaction mixture by filtration and subsequently regenerated and reused.

Table 4.16 Esterification of succinic acid with ethanol using H form of synthesized zeolites as catalyst.

Catalyst (H form of zeolites)	% Conversion of Succinic acid	Yield of Esters	
		Monoester	Diester
CZeoY	79	12	88
RZeoY	76	20	80
UZeoY	82	4	96

Reaction condition: mole ratio of succinic acid to ethanol: 1:3, amount of catalyst: 1g, reaction time: 12h, reaction temperature: 72^{o}C

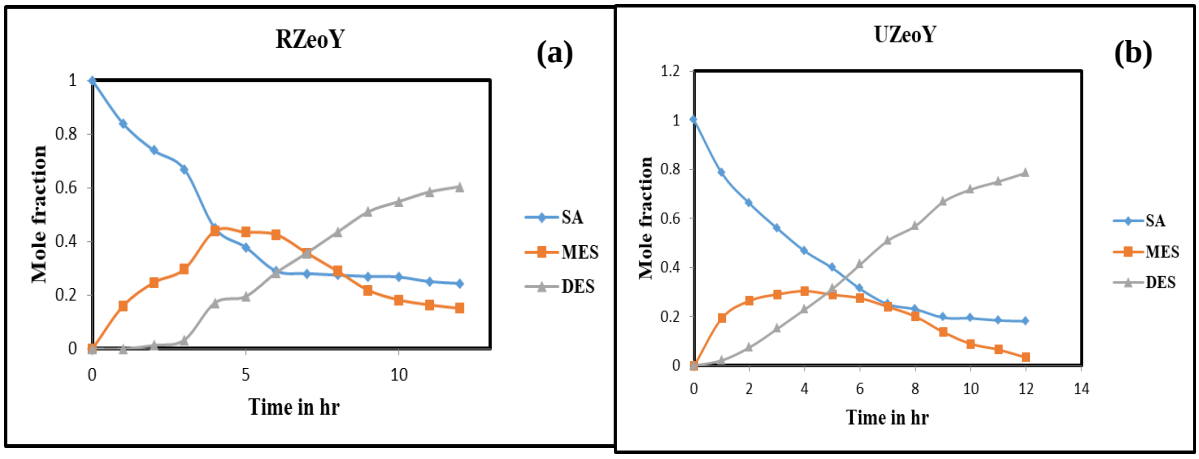

SA: Succinic acid; MES: Monoester; DES: Diester

Fig. 4.22 Catalytic activity of Y zeolites [(a) RZeoY and (b) UZeoY] with time on stream

4.5.3 Kinetic and rate constant study

Esterification of succinic acid takes place in presence of ethanol with the help of all zeolite catalyst. Eq. (5) represents rate expression.

$$-d[SA]/dt = k*[SA]^{n}*[EtOH]^{m} \quad \ldots\ldots\ldots (5)$$

Where, [SA] = Succinic acid concentration, [EtOH] = Ethanol concentration, k = reaction rate constant

Theoretically, one mole of succinic acid reacts with one mole of ethanol. In the kinetic study, due to excess ethanol concentration, the reaction rate is not affected by the ethanol concentration.

The rate expression presented in Eq. (5) is pseudo-order for the ethanol concentration. It is expressed as

$$-d\,[SA]/\,dt = k * [\,SA\,]^{n} \quad \text{……..(6)}$$

The above rate expression with separation of variables gives

$$-d\,[SA]\,/[SA]^{n} = k * dt \quad \text{……..(7)}$$

Eq. (7) on integration yield

$$(\,[SA]^{-n+1} - [\,SA0]^{-n+1})/\,1 - n = k * t$$

$$[SA] = [SA0] * (\,1 - X_A\,)$$

$$[SA0]^{-n+1}\,((\,1 - X_A\,)^{-n+1} - 1\,)\,/1 - n = k * t$$

First-order kinetics

$$1\text{-}X_A = e^{-k*t} \quad \text{…….. (8)}$$

The linearized form $-\ln(1 - X_A) = k * t$

Where, X_A = fractional conversion of SA,k = rate constant, min^{-1}

The expression for first-order kinetics as shown in eq. (8) was used to fit the experimental data. Fig. 4.23 presents the plot of –ln (1-Xa) versus t for KZeoY and UZeoY, considering the first-order kinetics. The assumed reaction order is best fitted with the experimental data if the R^2 value is greater than 0.9. All cases used for the determination of the order of the reaction are straight lines passing almost through the origin. The linear fit expression gives the value of the rate constant. It reveals that for succinic acid esterification, the reaction rate varies

linearly with the concentration of succinic acid. The linear fit expression for first-order kinetics in Fig. 4.23 is summarized in Table 4.17. A plot of −ln(1−conversion) versus reaction time for reactions carried out at 72°C is shown in Fig. 4.23 for both zeolites (KZeoY and UZeoY) . This plot shows a near linear character for both the zeolites. This suggests a first-order dependence of the rate of the reaction on succinic acid concentration [226]. The initial assumption of irreversible first order reaction thus matched with result. The rate constants for RZeoY and CZeoY is also calculated and given in Table 4.17. The value of rate constant is different in both cases. The rate constants are 0.52×10^{-4} s^{-1} and 0.39×10^{-4} s^{-1} for UZeoY and KZeoY respectively. Even though the mechanism of the reaction for the two zeolites may be the same, the differences in their activity can be attributed to their difference in surface area, active site distribution, well-dispersed morphology and the highest crystallinity of UZeoY.

Table 4.17: Rate constant, K for the all the zeolites

Zeolite	**Rate constant, K value in s^{-1}**
UZeoY	0.52×10^{-4}
KZeoY	0.39×10^{-4}
CZeoY	0.47×10^{-4}
RZeoY	0.45×10^{-4}

(a)

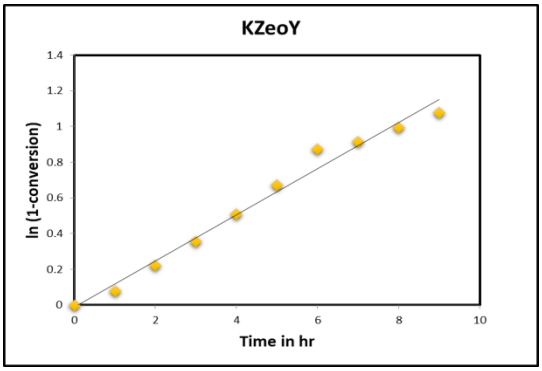

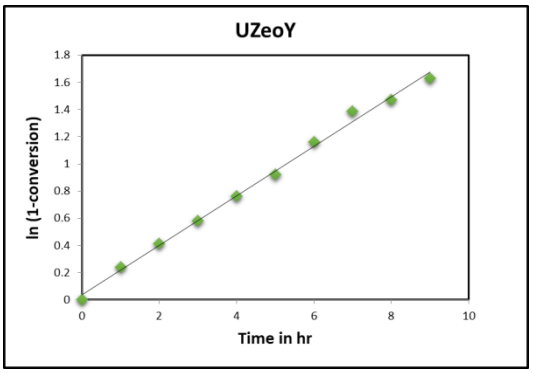

(b)

Fig. 4.23. Plot of the conversion of succinic acid with time for (a) KZeoY and (b) UZeoY

CHAPTER - 5

Conclusions and future scope

There is a growing interest in finding alternate promising avenues for the synthesis of zeolite Y to supplement, if not substitute, the existing conventional hydrothermal processes using organic chemical sources. Also a lot of in-depth research is undergoing to explore the real potential of this technology in the current zeolite Y market for catalytic and other applications. In this final chapter of the dissertation, major conclusions are drawn, based on the extensive research work carried out and some lights have been shed on the scope and directions of future research work.

5.1. Major Conclusion

Zeolite Y is successfully synthesized by using a novel material and also by a novel technique. Kachchh kaolin clay proves to be a sustainable environmental friendly precursor for synthesis of zeolite Y. This clay can be used as an alternate indigenous and inexpensive source of silica and alumina. The abundant availability and low cost of kaolin clay in the Kachchh district of Gujarat makes it a potential and untapped raw material for synthesis of zeolites. The alternate novel green way of synthesis of zeolite was attempted by using ultrasonication. This synthesis method demonstrated a very simple, fast, efficient and ecologically responsive route to obtain zeolite Y. The detailed characterization of all the synthesized zeolites and comparison with international standard samples indicated proper formation of zeolite Y with required structural properties. The synthesized zeolite Y was applied as a catalyst in esterification of succinic acid with ethanol which showed good conversion and selectivity generating very good yield of diethyl succinate at moderate reaction conditions. Overall the synthesized zeolites proved to be an inexpensive and simple way of preparation of environmentally benign catalysts, which has a good potential for application in various chemical industries.

The major findings are as follows:

- A zeolite Y (RZeoY) was synthesized in the laboratory by standard hydrothermal method as prescribed in literature using standard chemicals for reference purpose. The RZeoY was compared with a commercial zeolite Y from Zeolyst international

(CZeoY). Both RZeoY and CZeoY were characterized using standard methods and used as a reference benchmark.

- The kaolin clay from the Kachchh region of Gujarat, India was used as an ecological novel raw material for zeolite Y synthesis due to their lower costs and abundant availability compared to traditional precursors.
- The kaolin clay was leached with H_2SO_4 to remove impurities and attain the required silica-alumina ratio for zeolite synthesis. Acid leaching revealed reduction in Al_2O_3 content from 41% to 21%, and increase in silica–alumina ratio from 1.3 to 2.4 which were favorable for the synthesis of zeolite. Detailed examination revealed that the BET surface area increased from 10.322 to 54.193 m^2g^{-1} and pore volume from 0.041 to 0.152 cm^3g^{-1} showed that the leached clay itself has the potential to be used as a catalyst. When applied as a catalyst in esterification it showed the formation of diester. These proved inert structures of Si-O and Al-O are now active and ready for zeolitation. This method demonstrated a low cost (~ $0.6/kg) and efficient way of preparing porous kaolin clay having required active sites and high silica-alumina ratio. This activated kaolin clay proved to be a base material for zeolite Y synthesis.
- Similarly, bentonite clay from the same region was also attempted as a source of silica. Acid leaching with 5M H_2SO_4 increased the Si/Al ratio up to 4.04 with an increase in surface area and pore volume revealing a highly porous structure. This also revealed an economical and effective way of preparing low cost (~ $0.4/Kg) porous activated bentonite clay. When applied as a catalyst in esterification it showed the formation of diester. However, when used as a potential raw material for zeolite Y synthesis, the results were not as expected.
- The activated kaolin clay was used as a precursor (acted as an alternate natural source of silica-alumina) for synthesis of zeolite Y (KZeoY). Detailed characterizations and matching with reference (RZeoY) and commercial (CZeoY) sample confirmed the formation of zeolite Y having SiO_2/Al_2O_3 ratio of 3.09, specific surface area 320 m^2g^{-1}, pore volume 0.22 cm^3g^{-1} and average pore diameter 2.89 nm. The crystallinity was 76% having lattice parameter 24.65 Å.
- An alternative green method was applied for synthesis of zeolite Y (UZeoY) which was performed in two stages that included ageing step applying ultrasound

pretreatment combined with hydrothermal treatment. Detailed characterizations and matching with RZeoY and CZeoY sample confirmed the formation of zeolite Y with 98.01% crystallinity, 24.67 Å lattice parameter, BET surface area 751 m^2g^{-1}, pore volume 0.33 cm^3g^{-1} and average pore diameter of 1.8 nm. The ultrasonication influences the UZeoY properties. Average crystal size, particle size distribution decreased and the textural properties changed slightly. This fact is attributed to the contribution of the sonication process energy that induces the formation of a greater number of nuclei favoring the crystallization stage. The synthesis method was a very simple, fast, efficient and environmentally friendly route to obtain zeolite Y.

- Treatment of the zeolite Y with ammonium nitrate revealed that Na-cations from KZeoY were detached and replaced with NH_4^+ which subsequently became H^+ after calcination and confirmed the formation of active acid sights required for reaction.
- The H form of all synthesized zeolites was applied as a catalyst in the esterification reaction of succinic acid with ethanol. The reaction was carried out at 72^oC. The acid to alcohol ratio was 1: 3, reaction time was 12 h and the amount of catalyst was kept 1 g for all experiments. The same reaction was carried out with raw kaolin clay also.
- The conversion of succinic acid by using raw kaolin clay is only 28% but the same kaolin clay base zeolite (KZeoY) gave 72% conversion, which is even at par with 76% result of reference Zeolite Y (RZeoY). No significant difference was observed in conversion between both zeolites even though the difference in S_{BET} existed. BET study showed that both KZeoY and RZeoY had comparable S_{BJH} and V_{BJH} even though S_{BET} was less for KZeoY. KZeoY is showing more mesoporosity with high value of d_{BJH} and d_{Avg} than RZeoY, which increased molecular diffusion rates; overall pore accessibility, enhanced transport characteristics and reduced transportation lag of molecules. Wide-pore zeolites increased the catalyst effectiveness by attaining higher intra crystalline diffusivity.
- The ethanol being an excess reactant occupied the majority of the surplus active sites owing to competitive adsorption. This resulted in the conversion of the monoester to a more valuable diester. The final yield of diester increased to 60% with usage of KZeoY. The consecutive decrease in the concentration of monoester with increase in diester concentration with time is noted. A plot of −ln(1−conversion) versus reaction

time for reactions carried out at 72°C for KZeoY. This plot shows near linear straight line characteristics and passing through origin. This suggests a first-order dependence of the rate of the reaction on succinic acid concentration and rate constant of 0.39×10^{-4} s^{-1}.

- The performance of synthesized KZeoY catalyst is also at par by obtaining reasonably good yield of diester at moderate reaction conditions. Furthermore, the solid catalyst could be easily recovered from the aqueous reaction mixture by filtration and subsequently regenerated and reused.
- The H form of ultrasonicated Zeolite UZeoY was applied as a catalyst in esterification reaction of succinic acid. The reaction conditions are kept same as discussed in KZeoY. The UZeoY showed highest 82 % conversion compared to 79% for commercial CZeoY respectively.
- The UZeoY presented a high BET surface, leading more cell crystals and more pore mouths exposed and resulting in an external and BET surface area increase. This is consistent with a reduction in particle size with the highest crystallinity with smaller crystal size; minimize the diffusion length of reactant molecules into the pores and correspondingly the products out of zeolites. This increased molecular diffusion rates; overall pore accessibility, enhanced transport characteristics and reduced transportation lag of molecules.
- The ethanol being an excess reactant occupied the majority of the surplus active sites owing to competitive adsorption. This resulted in the conversion of the monoester to a more valuable diester. The final yield of diester increased to 96% with usage of UZeoY. The consecutive decrease in the concentration of monoester with increase in diester concentration with time is noted. A plot of −ln(1−conversion) versus reaction time for reactions carried out at 72°C for UZeoY. This plot shows near linear straight line characteristics and passing through origin. This suggests a first-order dependence of the rate of the reaction on succinic acid concentration and rate constant of 0.52×10^{-4} s^{-1}.
- The RZeoY and CZeoY catalysts are also showing the same first order behavior with rate constant 0.45×10^{-4} $s^{-1}$and 0.47×10^{-4} s^{-1} respectively.

- The performance of present synthesized UZeoY catalyst is worthy by obtaining a very high yield of diester at moderate reaction conditions. Furthermore, the catalyst could be easily recovered from the aqueous reaction mixture by filtration and subsequently regenerated and reused.

5.2 Original contribution by the thesis

The research work provides a feasible method to prepare zeolite Y using kaolin clay of Kachchh region of Gujarat, India as an indigenous and inexpensive source of silica and alumina by hydrothermal method. Another environmentally benign synthesis method is demonstrated by using chemical route but using ultrasonic technique. All the samples were characterized and formation of zeolite Y was confirmed. The research work also provides a comprehensive structural analysis of synthesized zeolite Y accompanied by comparison with commercial samples. The synthesized zeolite Y was applied as a catalyst and an effective way of production of valuable diethyl succinate was demonstrated by esterification of succinic acid with ethanol. This research work provides valuable insights to an effective way of synthesizing environmentally benign porous zeolite Y having high surface area and pore volume that is useful for catalytic applications.

5.3 Future scope of work

Kachchh Kaolin clay proves to be a good raw material for the synthesis of zeolite Y which can be subsequently used as a catalyst for esterification reaction. The synthesized zeolite Y possessed good structural properties. However, for the commercialization and full-scale implementation of the zeolite Y further research work needs to be carried out to make the overall process more energy efficient and economical. The focus of the future research should be on further improvement of the zeolite properties by incorporating green synthesis techniques and exploring other potential applications.

Kachchh kaolin clay which is inexpensive, abundantly available and a good source of silica indicated to be an excellent raw material to synthesize zeolite Y. The synthesized zeolite Y possessed the required porosity and other required structural properties. The bentonite clay of

the Kachchh region is also tested for zeolite Y synthesis. The result was not as per the requirement. In future, advanced experimentation can be carried out and this work can be taken up employing some new idea and synthesis of zeolite Y can be attempted. Other types of clay like Montmorillonite, Ball etc. which are abundantly available in the Kachchh region can be checked for their suitability as a raw material for zeolite synthesis. The process conditions for the synthesis like temperature and time of reaction can be further fine-tuned or changed to produce better quality of zeolite Y with improved surface area and pore volume. Other mineral acids apart from sulfuric acid can be checked for their effectiveness in removing metal impurities. Kaolin as the source of silica can be tried for the synthesis of other types of zeolites using the same hydrothermal method. Required and necessary modifications in the process conditions can be attempted for the synthesis of other types of zeolites. Scale up of the manufacturing process to a pilot plant scale and then to the commercial scale may be attempted after doing due efficacy and economy check.

Application of ultrasound proved to be very advantageous in terms of simplicity, rapid reaction, no requirement of any complex facilities, high crystal growth rate, good product quality in terms of particle size distribution and morphology. The process is also a step towards green synthesis. The ultrasonication effect can be varied and optimized as per the demand of quality of zeolite. The combination of Kachchh kaolin and ultrasonication can be tried for the synthesis of zeolite Y for complete green synthesis.

The prepared zeolite Y was used for esterification of succinic acid to produce diethyl succinate. Understanding of the esterification reaction mechanism with elaborated kinetic study is required to improve the yield of diethyl succinate. The same zeolite Y can be used as a catalyst in other reactions also mainly in the petroleum industry. Also the performance of the zeolite Y as adsorbent, catalyst support and similar application may be explored.

Reference:

[1] Zeolites Market by Type (Natural, Synthetic), Function (Ion-Exchange, Catalyst, Molecular Sieve), Synthetic Zeolites Application (Detergents, Absorbent, Catalysts), Natural Zeolites Application, and Region - Global Forecast to 2026, Mark. Mark. (2022). www.marketsandmarkets.com/Market-Reports/zeolites-market-76442083.html.

[2] Z.A. Alothman, A review: Fundamental aspects of silicate mesoporous materials, Materials (Basel). 5 (2012) 2874–2902. doi:10.3390/ma5122874.

[3] B. Kwakye-Awuah, E. Von-Kiti, R. Buamah, I. Nkrumah, C. Williams, Effect of crystallization time on the hydrothermal synthesis of zeolites from kaolin and bauxite, Int. J. Sci. Eng. Res. 5 (2014) 734–741.

[4] Henry E. Mgbemere, Ikenna C. Ekpe, Ganiyu I. Lawal, Zeolite Synthesis, Characterization and Application Areas: A Review, Int. Res. J. Environ. Sci. 6 (2017) 45–59.

[5] V. Brahmkhatri, A. Patel, Esterification of bioplatform molecules over 12-tungstophosphoric acid anchored to MCM-41, J. Porous Mater. 20 (2013) 209–217. doi:10.1007/s10934-012-9590-1.

[6] S.R. Kirumakki, N. Nagaraju, K. V. Murthy, S. Narayanan, Esterification of salicylic acid over zeolites using dimethyl carbonate, Appl. Catal. A Gen. 226 (2002) 175–182. doi:10.1016/S0926-860X(01)00900-0.

[7] N. Gokulakrishnan, A. Pandurangan, P.K. Sinha, Esterification of acetic acid with propanol isomers under autogeneous pressure: A catalytic activity study of Al-MCM-41 molecular sieves, J. Mol. Catal. A Chem. 263 (2007) 55–61. doi:10.1016/j.molcata.2006.08.005.

[8] Ammar S. Abbas, Rowaida N. Abbas, Preparation and Characterization of Nay Zeolite for Biodiesel Production, Iraqi J. Chem. Pet. Eng. 16 (2015) 19–29. http://www.iasj.net/iasj?func=fulltext&aId=102642.

[9] Y. Li, W. Yang, Microwave synthesis of zeolite membranes: A review, J. Memb. Sci. 316 (2008) 3–17. doi:https://doi.org/10.1016/j.memsci.2007.08.054.

[10] Y. Hasegawa, C. Abe, F. Mizukami, Y. Kowata, T. Hanaoka, Application of a CHA-type zeolite membrane to the esterification of adipic acid with isopropyl alcohol using sulfuric acid catalyst, J. Memb. Sci. 415–416 (2012) 368–374. doi:10.1016/j.memsci.2012.05.021.

[11] X.C. Xu, W. Yang, J. Liu, L.W. Lin, Synthesis of a High-Permeance NaA Zeolite Membrane by Microwave Heating, Adv. Mater.12 (2000) 195–198. doi:10.1002/(SICI)1521-4095(200002)12:3<195.

[12] N. Kosinov, J. Gascon, F. Kapteijn, E.J.M. Hensen, Recent developments in zeolite membranes for gas separation, J. Memb. Sci. 499 (2016) 65–79. doi:https://doi.org/10.1016/j.memsci.2015.10.049.

[13] N. Caponi, G.C. Collazzo, S.L. Jahn, G.L. Dotto, M.A. Mazutti, E.L. Foletto, Use of brazilian kaolin as a potential low-cost adsorbent for the removal of malachite green from colored effluents, Mater. Res. 20 (2017) 14–22. doi:10.1590/1980-5373-mr-2016-0673.

[14] F.O. Nwosu, O.J. Ajala, R.M. Owoyemi, B.G. Raheem, Preparation and characterization of adsorbents derived from bentonite and kaolin clays, Appl. Water Sci. 8 (2018) 1–10. doi:10.1007/s13201-018-0827-2.

[15] J.A. Alexander, M.A. Ahmad Zaini, A. Surajudeen, E.N.U. Aliyu, A.U. Omeiza, Surface modification of low-cost bentonite adsorbents—A review, Part. Sci. Technol. 37 (2019) 534–545. doi:10.1080/02726351.2018.1438548.

[16] A. Primo, H. Garcia, Zeolites as catalysts in oil refining., Chem. Soc. Rev. 43 (2014) 7548–7561. doi:10.1039/c3cs60394f.

[17] I. Publication, C. Engineering, Synthesis of Faujasite Zeolites from Kankara Kaolin Clay, J. Appl. Sci. 3 (2007) 1017–1021.

[18] E.B.G.. Johnson, S.E.. Arshad, J. Asik, Hydrothermal Synthesis of Zeolite A Using Natural Kaolin from KG. Gading Bongawan Sabah, J. Appl. Sci. 14 (2014) 3282–3287. doi:10.3923/jas.2014.3282.3287.

[19] E.B.G. Johnson;, S.E. Arshad;, J. Asik, Hydrothermal Synthesis of Zeolite A Using Natural Kaolin from KG. Gading Bongawan Sabah, J. Appl. Sci. 14 (2014) 3282–3287. doi:10.3923/jas.2014.3282.3287.

[20] X. Liu, Z. Yan, H. Wang, Y. Luo, In Situ Synthesis of NaY Zeolite with Coal-Based Kaolin, J. Nat. Gas Chem. 12 (2003) 63–70. doi:10.1016/S1003-9953-2003-12-1-63-73.

[21] H. Faghihian, N. Godazandeha, Synthesis of nano crystalline zeolite Y from bentonite, J. Porous Mater. 16 (2009) 331–335. doi:10.1007/s10934-008-9204-0.

[22] M.A. Ismail, M.A.Z. Eltayeb, S.A.A. Maged, Synthesis of Zeolite A from Sudanese Montmorillonite Clay to remove Nickel and Copper ions from Aqueous Solutions, Int. J. Chem. Biochem. Sci. 4 (2013) 46–56.

[23] Z. Zhang, X. Zhang, F. Ling, W. Sun, Growth of nano-zeolite Beta on Montmorillonite: Preparation, characterization and catalytic performance, Stud. Surf. Sci. Catal. 174 (2008) 889–892. doi:10.1016/S0167-2991(08)80031-6.

[24] X.S. Zhao, G.Q. Lu, H.Y. Zhu, Effects of Ageing and Seeding on the Formation of Zeolite Y from Coal Fly Ash, J. Porous Mater. 4 (1997) 245–251. doi:10.1023/A:1009669104923.

[25] C. Belviso, F. Cavalcante, A. Lettino, S. Fiore, Effects of ultrasonic treatment on zeolite synthesized from coal fly ash, Ultrason. Sonochem. 18 (2011) 661–668. doi:10.1016/j.ultsonch.2010.08.011.

[26] K.D. Pandiangan, W. Simanjuntak, E. Pratiwi, M. Rilyanti, Characteristics and catalytic activity of zeolite-a synthesized from rice husk silica and aluminium metal by sol-gel method, J. Phys. Conf. Ser. 1338 (2019). doi:10.1088/1742-6596/1338/1/012015.

[27] J.J.F. Saceda, R.L. De Leon, K. Rintramee, S. Prayoonpokarach, J. Wittayakun, Properties of silica from rice husk and rice husk ash and their utilization for zeolite y synthesis, Quim. Nova. 34 (2011) 1394–1397. doi:10.1590/S0100-40422011000800018.

[28] Y. Sugano, R. Sahara, T. Murakami, T. Narushima, Y. Iguchi, C. Ouchi, Hydrothermal synthesis of zeolite a using blast furnace slag, ISIJ Int. 45 (2005) 937–945. doi:10.2355/isijinternational.45.937.

[29] P. Krongkrachang, P. Thungngern, P. Asawaworarit, N. Houngkamhang, A. Eiad-Ua, Synthesis of Zeolite Y from Kaolin via hydrothermal method, Mater. Today Proc. 17 (2019) 1431–1436. doi:10.1016/j.matpr.2019.06.164.

[30] W. Gao, S. Zhao, H. Wu, W. Deligeer, S. Asuha, Direct acid activation of kaolinite and its effects on the adsorption of methylene blue, Appl. Clay Sci. 126 (2016) 98–106. doi:10.1016/j.clay.2016.03.006.

[31] K.G. Bhattacharyya, S. Sen Gupta, Adsorption of a few heavy metals on natural and modified kaolinite and montmorillonite: A review, Adv. Colloid Interface Sci. 140 (2008) 114–131. doi:https://doi.org/10.1016/j.cis.2007.12.008.

[32] Prajitha Prabhakaran M K and Pushpaletha P, Catalyst Preparation , Characterization and Catalytic Activity of Kaolinite Clay from Nileswar , Kerala, Int. J. Appl. Chem. 13 (2017) 461–475.

[33] T.N. Don, T.N. Hung, P.T. Huyen, T.X. Bai, H.T.T. Huong, N.T. Linh, L. Van Duong, M.H. Pham, Synthesis, characterization and catalytic activity of nano-zeolite Y for the alkylation of benzene with isopropanol, Indian J. Chem. Technol. 23 (2016) 392–399.

[34] K.R. Sabu, R. Sukumar, R. Rekha, M. Lalithambika, A comparative study on H2SO4, HNO3 and HClO4 treated metakaolinite of a natural kaolinite as Friedel-Crafts alkylation catalyst, Catal. Today. 49 (1999) 321–326. doi:10.1016/S0920-5861(98)00439-8.

[35] E. Sri Rahayu, G. Subiyanto, A. Imanuddin, Wiranto, S. Nadina, R. Ristiani, Suhermina, E. Yuniarti, Kaolin as a Source of Silica and Alumina for Synthesis of Zeolite y and Amorphous Silica Alumina, MATEC Web Conf. 156 (2018) 1–6. doi:10.1051/matecconf/201815605002.

[36] J. Liu, Z. Yun, X. Gui, CE/Kaolin clay as an active catalyst for fatty acid methyl esters production from cottonseed oil in a new integrated apparatus, Brazilian J. Chem. Eng. 35 (2018) 147–154. doi:10.1590/0104-6632.20180351s20160504.

[37] C.H. Zhou, An overview on strategies towards clay-based designer catalysts for green and sustainable catalysis, Appl. Clay Sci. 53 (2011) 87–96. doi:10.1016/j.clay.2011.04.016.

[38] E.B.G. Johnson, S.E. Arshad, Hydrothermally synthesized zeolites based on kaolinite: A review, Appl. Clay Sci. 97–98 (2014) 215–221. doi:10.1016/j.clay.2014.06.005.

[39] H. Ramirez Mendoza, J. Jordens, M. Valdez Lancinha Pereira, C. Lutz, T. Van Gerven, Effects of ultrasonic irradiation on crystallization kinetics, morphological and structural properties of zeolite FAU, Ultrason. Sonochem. 64 (2020) 105010. doi:10.1016/j.ultsonch.2020.105010.

[40] D. Reinoso, M. Adrover, M. Pedernera, Green synthesis of nanocrystalline faujasite zeolite, Ultrason. Sonochem. 42 (2018) 303–309. doi:10.1016/j.ultsonch.2017.11.034.

[41] X. Meng, F.S. Xiao, Green routes for synthesis of zeolites, Chem. Rev. 114 (2014) 1521–1543. doi:10.1021/cr4001513.

[42] S.E. Lehman, S.C. Larsen, Zeolite and mesoporous silica nanomaterials: Greener syntheses, environmental applications and biological toxicity, Environ. Sci. Nano. 1 (2014) 200–213. doi:10.1039/c4en00031e.

[43] A. Khaleque, M.M. Alam, M. Hoque, S. Mondal, J. Bin Haider, B. Xu, M.A.H. Johir, A.K. Karmakar, J.L. Zhou, M.B. Ahmed, M.A. Moni, Zeolite synthesis from low-cost materials and environmental applications: A review, Environ. Adv. 2 (2020). doi:10.1016/j.envadv.2020.100019.

[44] K. Li, J. Valla, J. Garcia-Martinez, Realizing the commercial potential of hierarchical zeolites: New opportunities in catalytic cracking, ChemCatChem. 6 (2014) 46–66. doi:10.1002/cctc.201300345.

[45] J. Shi, Y. Wang, W. Yang, Y. Tang, Z. Xie, Recent advances of pore system construction in zeolite-catalyzed chemical industry processes, Chem. Soc. Rev. 44 (2015) 8877–8903. doi:10.1039/C5CS00626K.

[46] K.P. De Jong, J. Zečević, H. Friedrich, P.E. De Jongh, M. Bulut, S. Van Donk, R. Kenmogne, A. Finiels, V. Hulea, F. Fajula, Zeolite y crystals with trimodal porosity as ideal hydrocracking catalysts, Angew. Chemie - Int. Ed. 49 (2010) 10074–10078. doi:10.1002/anie.201004360.

[47] W. Li, J. Zheng, Y. Luo, Z. Da, Effect of hierarchical porosity and phosphorus modification on the catalytic properties of zeolite Y, Appl. Surf. Sci. 382 (2016) 302–308. doi:10.1016/j.apsusc.2016.04.146.

[48] W. Li, J. Zheng, Y. Luo, C. Tu, Y. Zhang, Z. Da, Hierarchical Zeolite Y with Full Crystallinity: Formation Mechanism and Catalytic Cracking Performance, Energy and Fuels. 31 (2017) 3804–3811. doi:10.1021/acs.energyfuels.6b03421.

[49] J. Thomas F. Degnan, Applications of zeolites in petroleum refining, Top. Catal. 13 (2000) 349–356. doi:10.1023/A.

[50] W. Vermeiren, J.P. Gilson, Impact of Zeolites on the Refining and Petrochemical Industry, Top. Catal. 52 (2009) 1131–1161. doi:10.13140/2.1.3726.8164.

[51] J.Q. Wang, Y.X. Huang, Y. Pan, J.X. Mi, New hydrothermal route for the synthesis of high purity nanoparticles of zeolite y from kaolin and quartz, Microporous Mesoporous Mater. 232 (2016) 77–85. doi:10.1016/j.micromeso.2016.06.010.

[52] W. Vermeiren, J.P. Gilson, Impact of zeolites on the petroleum and petrochemical industry, Top. Catal. 52 (2009) 1131–1161. doi:10.1007/s11244-009-9271-8.

[53] R. Millini, G. Bellussi, Chapter 1 Zeolite Science and Perspectives, in: Zeolites Catal. Prop. Appl., The Royal Society of Chemistry, 2017: pp. 1–36. doi:10.1039/9781788010610-00001.

[54] E.M. Flanigen, R.W. Broach, S.T. Wilson, Introduction, Zeolites Ind. Sep. Catal. (2010) 1–26. doi:10.1002/9783527629565.ch1.

[55] Z. Huang, J.-F. Su, Y.-H. Guo, X.-Q. Su, L.-J. Teng, Synthesis of well-crystallized zeolite beta at large scale and its incorporation into polysulfone matrix for gas separation, Chem. Eng. Commun. 196 (2009) 969–986. doi:10.1080/00986440902797824.

[56] L.B. McCusker, D.H. Olson, C. Baerlocher, Atlas of Zeolite Framework Types, 2007. doi:10.1016/B978-0-444-53064-6.X5186-X.

[57] A.M. Doyle, T.M. Albayati, Encyclopedia of Membranes, Appl. Catal. A Gen. 19 (2016) 87–91. doi:10.1016/j.apcata.2012.10.009.

[58] A. Corma, F. Rey, S. Valencia, J.L. Jordá, J. Rius, A zeolite with interconnected 8-, 10- and 12-ring pores and its unique catalytic selectivity, Nat. Mater. 2 (2003) 493–497. doi:10.1038/nmat921.

[59] W.O. Haag, R.M. Lago, P.B. Weisz, The active site of acidic aluminosilicate catalysts, Nature. 309 (1984) 589–591. doi:10.1038/309589a0.

[60] B. Bogdanov, D. Georgiev, K. Angelova, I. Markovska, Y. Hristov, International Science conference 4, Int. Sci. Conf. 4th - 5th June 2009, Stara Zagor. Bulg. “Economics Soc. Dev. Base Knowledge.” VII (2009) 1–5.

[61] E.M. Flanigen, Plenary Paper—Technology: Molecular sieve zeolite technology - the first twenty-five years, Pure Appl. Chem. 52 (1980) 2191–2211. doi:10.1351/pac198052092191.

[62] Y. Tai, Lignin Fast Pyrolysis_Towards Enhanced Product Selectivities by Varying Particle Sizes of HZSM5 Zeolites, 2017.

[63] C.F. Ren, G. Coudurier, C. Naccache, Alkylation of Chlorobenzene over H-Mordenite and H-ZSM-5: Effect of Si/AI Ratio, in: Y. Murakami, A. Iijima, J.W. Ward (Eds.), New Dev. Zeolite Sci. Technol., Elsevier, 1986: pp. 733–738. doi:https://doi.org/10.1016/S0167-2991(09)60941-1.

[64] K. Gołąbek, A.E. Palomares, J. Martínez-Triguero, K.A. Tarach, K. Kruczała, V. Girman, K. Góra-Marek, Ce-modified zeolite BEA catalysts for the trichloroethylene oxidation. The role of the different and necessary active sites, Appl. Catal. B Environ. 259 (2019). doi:10.1016/j.apcatb.2019.118022.

[65] G. Perot, M. Guisnet, Advantages and disadvantages of zeolites as catalysts in organic chemistry, J. Mol. Catal. 61 (1990) 173–196. doi:https://doi.org/10.1016/0304-5102(90)85154-A.

[66] P.B. Weisz, V.J. Frilette, Intracrystalline and Molecular-shape-selective Catalysis BY Zeolite Salts, J. Phys. Chem. 64 (1960) 382. doi:10.1021/j100832a513.

[67] P.H. Espeel, B. Janssens, P.A. Jacobs, Functional selectivity in Friedel-Crafts alkylations with polyfunctional reactants over acid zeolites, J. Org. Chem. 58 (1993) 7688–7693. doi:10.1021/jo00079a012.

[68] S.M. Csicsery, The cause of shape selectivity of transalkylation in mordenite, J. Catal. 23 (1971) 124–130. doi:https://doi.org/10.1016/0021-9517(71)90032-7.

[69] B. Yilmaz, U. Müller, Catalytic applications of zeolites in chemical industry, Top. Catal. 52 (2009) 888–895. doi:10.1007/s11244-009-9226-0.

[70] N.-Q. Feng, G.-F. Peng, Applications of natural zeolite to construction and building materials in China, Constr. Build. Mater. 19 (2005) 579–584. doi:https://doi.org/10.1016/j.conbuildmat.2005.01.013.

[71] Ž.Z. Tasić, G.D. Bogdanović, M.M. Antonijević, Application of natural zeolite in wastewater treatment: A review, J. Min. Metall. A Min. 55 (2019) 67–79. doi:10.5937/jmma1901067t.

[72] T.F. Degnan, Jr., Applications of zeolites in petroleum refing, Top. Catal. 13 (2000) 349–356. doi:10.1023/A:1009054905137.

[73] A. Malekpour, M. Edrisi, S. Hajialigol, S. Shirzadi, Solid phase extraction–inductively coupled plasma spectrometry for adsorption of Co(II) and Ni(II) from radioactive wastewaters by natural and modified zeolites, J. Radioanal. Nucl. Chem. 288 (2011) 663–669. doi:10.1007/s10967-011-1013-2.

[74] X. Fan, Y. Jiao, Porous materials for catalysis: Toward sustainable synthesis and applications of zeolites, Elsevier Inc., 2019. doi:10.1016/B978-0-12-814681-1.00005-9.

[75] Y. Shu, A. Travert, R. Schiller, M. Ziebarth, R. Wormsbecher, W.-C. Cheng, Effect of Ionic Radius of Rare Earth on USY Zeolite in Fluid Catalytic Cracking: Fundamentals and Commercial Application, Top. Catal. 58 (2015) 334–342. doi:10.1007/s11244-015-0374-0.

[76] E.T.C. Vogt, B.M. Weckhuysen, Fluid catalytic cracking: recent developments on the grand old lady of zeolite catalysis, Chem. Soc. Rev. 44 (2015) 7342–7370. doi:10.1039/C5CS00376H.

[77] U. Olsbye, S. Svelle, K.P. Lillerud, Z.H. Wei, Y.Y. Chen, J.F. Li, J.G. Wang, W.B. Fan, The formation and degradation of active species during methanol conversion over protonated zeotype catalysts, Chem. Soc. Rev. 44 (2015) 7155–7176. doi:10.1039/C5CS00304K.

[78] M.M. Rahman, R. Liu, J. Cai, Catalytic fast pyrolysis of biomass over zeolites for high quality bio-oil – A review, Fuel Process. Technol. 180 (2018) 32–46. doi:https://doi.org/10.1016/j.fuproc.2018.08.002.

[79] Y. Akdeniz, Cation Exchange in Zeolites, Structure Modification, (1999).https://hdl.handle.net/11147/3915.

[80] J. Wen, H. Dong, G. Zeng, Application of zeolite in removing salinity/sodicity from wastewater: A review of mechanisms, challenges and opportunities, J. Clean. Prod. 197 (2018) 1435–1446. doi:https://doi.org/10.1016/j.jclepro.2018.06.270.

[81] Y. Zhang, N. Ren, Y. Tang, Chapter 17 - Zeolite Nanocrystals: Hierarchical Assembly and Applications, Ordered Porous Solids. (2009) 441–475. doi:https://doi.org/10.1016/B978-0-444-53189-6.00017-2.

[82] M. Ansari, A. Aroujalian, A. Raisi, B. Dabir, M. Fathizadeh, Preparation and characterization of nano-NaX zeolite by microwave assisted hydrothermal method, Adv. Powder Technol. 25 (2014) 722–727. doi:10.1016/j.apt.2013.10.021.

[83] O. Muraza, A. Abdul-Lateef, T. Tago, A.B.D. Nandiyanto, H. Konno, Y. Nakasaka, Z.H. Yamani, T. Masuda, Microwave-assisted hydrothermal synthesis of submicron ZSM-22 zeolites and their applications in light olefin production, Microporous Mesoporous Mater. 206 (2015) 136–143. doi:10.1016/j.micromeso.2014.12.025.

[84] C.G. Sangeetha, P. Baskar, Zeolite and its potential uses in agriculture : A critical review, Agric. Rev. 37 (2016) 101–108.doi: 10.18805/ar.v0iof.9627.

[85] A.K. Jamil, O. Muraza, A.M. Al-Amer, Microwave-assisted solvothermal synthesis of ZSM-22 zeolite with controllable crystal lengths, Particuology. 24 (2016) 138–141. doi:https://doi.org/10.1016/j.partic.2015.09.002.

[86] X.J. Wang, C.L. Yan, Synthesis of nano-sized NaY zeolite composite from metakaolin by ionothermal method with microwave assisted, Inorg. Mater. 46 (2010) 517–521. doi:10.1134/S0020168510050146.

[87] L. Han, X. Yan, L. Guo, Y. Duan, Z. Wang, T. Lu, J. Xu, Y. Zhan, J. Wang, Ionothermal synthesis of triclinic sapo-34 zeolites, Catalysts. 11 (2021). doi:10.3390/catal11050616.

[88] Y. Wu, X. Ren, J. Wang, Facile synthesis and morphology control of zeolite MCM-22 via a two-step sol–gel route with tetraethyl orthosilicate as silica source, Mater. Chem. Phys. 113 (2009) 773–779. doi:https://doi.org/10.1016/j.matchemphys.2008.08.008.

[89] M. Sathupunya, E. Gulari, S. Wongkasemjit, Na-A (LTA) zeolite synthesis directly from alumatrane and silatrane by sol-gel microwave techniques, J. Eur. Ceram. Soc. 23 (2003) 1293–1303. doi:https://doi.org/10.1016/S0955-2219(02)00287-X.

[90] K.J. Rao, B. Vaidhyanathan, M. Ganguli, P.A. Ramakrishnan, Synthesis of Inorganic Solids Using Microwaves, Chem. Mater. 11 (1999) 882–895. doi:10.1021/cm9803859.

[91] N. Sapawe, A.A. Jalil, S. Triwahyono, M.I.A. Shah, R. Jusoh, N.F.M. Salleh, B.H. Hameed, A.H. Karim, Cost-effective microwave rapid synthesis of zeolite NaA for removal of methylene blue, Chem. Eng. J. 229 (2013) 388–398. doi:https://doi.org/10.1016/j.cej.2013.06.005.

[92] T. Le, Q. Wang, B. Pan, A. V Ravindra, S. Ju, J. Peng, Process regulation of microwave intensified synthesis of Y-type zeolite, Microporous Mesoporous Mater. 284 (2019) 476–485. doi:https://doi.org/10.1016/j.micromeso.2019.04.029.

[93] Y. Li, W. Yang, Microwave synthesis of zeolite membranes: A review, J. Memb. Sci. 316 (2008) 3–17. doi:https://doi.org/10.1016/j.memsci.2007.08.054.

[94] S. Abbasian, M. Taghizadeh, Effects of microwave and ultrasonic-assisted aging on the synthesis of H-ZSM-5 nanozeolite and its catalytic performance in methanol dehydration, Int. J. Chem. React. Eng. 12 (2014) 355–362. doi:10.1515/ijcre-2014-0021.

[95] T.J. Mason, J.P. Lorimer, An introduction to sonochemistry, Endeavour. 13 (1989) 123–128. doi:https://doi.org/10.1016/0160-9327(89)90086-0.

[96] Ö. Andaç, M. Tatlıer, A. Sirkecioğlu, I. Ece, A. Erdem-Şenatalar, Effects of ultrasound on zeolite A synthesis, Microporous Mesoporous Mater. 79 (2005) 225–233. doi:https://doi.org/10.1016/j.micromeso.2004.11.007.

[97] L. Boels, R.M. Wagterveld, M.J. Mayer, G.J. Witkamp, Seeded calcite sonocrystallization, J. Cryst. Growth. 312 (2010) 961–966. doi:https://doi.org/10.1016/j.jcrysgro.2010.01.016.

[98] J.H. Bang, K.S. Suslick, Applications of ultrasound to the synthesis of nanostructured materials, Adv. Mater. 22 (2010) 1039–1059. doi:10.1002/adma.200904093.

[99] P. Pal, J.K. Das, N. Das, S. Bandyopadhyay, Synthesis of NaP zeolite at room temperature and short crystallization time by sonochemical method, Ultrason. Sonochem. 20 (2013) 314–321. doi:https://doi.org/10.1016/j.ultsonch.2012.07.012.

[100] L. Huang, F. Qin, Z. Huang, Y. Zhuang, J. Ma, H. Xu, W. Shen, Hierarchical ZSM-5 Zeolite Synthesized by an Ultrasound-Assisted Method as a Long-Life Catalyst for Dehydration of Glycerol to Acrolein, Ind. Eng. Chem. Res. 55 (2016) 7318–7327. doi:10.1021/acs.iecr.6b01140.

[101] S. Inagaki, S. Shinoda, S. Hayashi, T. Wakihara, H. Yamazaki, J.N. Kondo, Y. Kubota, Improvement in the catalytic properties of ZSM-5 zeolite nanoparticles via mechanochemical and chemical modifications, Catal. Sci. Technol. 6 (2016) 2598–2604. doi:10.1039/C5CY01644D.

[102] M. Abrishamkar, S.N. Azizi, H. Kazemian, The Effects of Various Sources and Templates on the Microwave-assisted Synthesis of BZSM-5 Zeolite, Zeitschrift Für Anorg. Und Allg. Chemie. 637 (2011) 312–316. doi:10.1002/zaac.201000309.

[103] X. Fu, X. Sheng, Y. Zhou, Z. Fu, S. Zhao, Z. Zhang, Y. Zhang, Ultrasonic/microwave synergistic synthesis of well-dispersed hierarchical zeolite Y with improved alkylation catalytic activity, Korean J. Chem. Eng. 33 (2016) 1931–1937. doi:10.1007/s11814-016-0022-9.

[104] J. Kong, X. Sheng, Y. Zhou, Y. Zhang, S. Zhou, Z. Zhang, Ultrasound-assisted synthesis of nanosized hierarchical ZSM-5 and its catalytic performance as the support for heteropolyacid, J. Porous Mater. 21 (2014) 241–249. doi:10.1007/s10934-013-9769-0.

[105] S. Oruji, R. Khoshbin, R. Karimzadeh, Preparation of hierarchical structure of Y zeolite with ultrasonic-assisted alkaline treatment method used in catalytic cracking of middle distillate cut: The effect of irradiation time, Fuel Process. Technol. 176 (2018) 283–295. doi:10.1016/j.fuproc.2018.03.035.

[106] W. Kim, D. Choi, S. Kim, Sonochemical synthesis of zeolite a from metakaolinite in NaOH solution, Mater. Trans. 51 (2010) 1694–1698. doi:10.2320/matertrans.M2010191.

[107] Y. Mu, Y. Zhang, J. Fan, C. Guo, Effect of ultrasound pretreatment on the hydrothermal synthesis of SSZ-13 zeolite, Ultrason. Sonochem. 38 (2017) 430–436. doi:https://doi.org/10.1016/j.ultsonch.2017.03.043.

[108] N.M. Musyoka, L.F. Petrik, E. Hums, H. Baser, W. Schwieger, In situ ultrasonic monitoring of zeolite A crystallization from coal fly ash, Catal. Today. 190 (2012) 38–46. doi:10.1016/j.cattod.2012.03.023.

[109] T. Pan, Z. Wu, A.C.K. Yip, Advances in the green synthesis of microporous and hierarchical zeolites: A short review, Catalysts. 9 (2019) 1–18. doi:10.3390/catal9030274.

[110] T. Abdullahi, Z. Harun, M.H.D. Othman, A review on sustainable synthesis of zeolite from kaolinite resources via hydrothermal process, Adv. Powder Technol. 28 (2017) 1827–1840. doi:10.1016/j.apt.2017.04.028.

[111] M. Hosseini, M.A. Zanjanchi, B. Ghalami-Choobar, H. Golmojdeh, Ultrasound-assisted dealumination of zeolite y, J. Chem. Sci. 127 (2015) 25–31. doi:10.1007/s12039-014-0745-2.

[112] R. Zhang, P. Zhong, H. Arandiyan, Y. Guan, J. Liu, N. Wang, Y. Jiao, X. Fan, Using ultrasound to improve the sequential post-synthesis modification method for making mesoporous Y zeolites, Front. Chem. Sci. Eng. 14 (2020) 275–287. doi:10.1007/s11705-019-1905-1.

[113] A. Tadjarodi, M. Dehghani, M. Imani, Green synthesis and characterization of palladium nanoparticles supported on zeolite Y by sonochemical method, powerful and efficient catalyst for Suzuki-Miyaura coupling of aryl halides with phenylboronic acid, Appl. Organomet. Chem. 32 (2018) 1–10. doi:10.1002/aoc.4594.

[114] B. WANG, J. WU, N. LI, Z. YUAN, S. XIANG, Rapid Synthesis of MCM-36 Zeolite under Ultrasonic Treatment, Chinese J. Catal. 28 (2007) 398–400. doi:10.1016/s1872-2067(07)60035-7.

[115] S.K. Nayak, S.R. Mohanty, Zeolite Synthesis from Waste and its Applications: A Retrospective, Int. J. Innov. Sci. Res. Technol. 4 (2019) 408–423. www.ijisrt.com.

[116] M. Meftah, W. Oueslati, N. Chorfi, A. Ben Haj Amara, Effect of the raw material type and the reaction time on the synthesis of halloysite based Zeolite Na-P1, Results Phys. 7 (2017) 1475–1484. doi:10.1016/j.rinp.2017.04.013.

[117] G.E. Christidis, H. Papantoni, Synthesis of FAU Type Zeolite Y from Natural Raw Materials: Hydrothermal SiO2-Sinter and Perlite Glass, Open Mineral. J. 2 (2008) 1–5. doi:10.2174/1874456700802010001.

[118] O.A. Ajayi, S.S. Adefila, M.T. Ityokumbul, Monitoring zeolite NaY formation from potassium-rich Nigerian kaolinite clay, Ain Shams Eng. J. 9 (2018) 1653–1661. doi:10.1016/j.asej.2016.10.008.

[119] M.K. Prajitha Prabhakaran, P. Pushpaletha, Preparation of solid acid catalyst from modified Kaolinite and its characterization and catalytic activity, Indian J. Chem. Technol. 24 (2017) 637–643.

[120] S. Kumar, A.K. Panda, R.K. Singh, Preparation and characterization of acids and alkali treated kaolin clay, Bull. Chem. React. Eng. Catal. 8 (2013) 61–69. doi:10.9767/bcrec.8.1.4530.61-69.

[121] L.B. McCusker, D.H. Olson, C. Baerlocher, Atlas of Zeolite Framework Types, 2007. doi:10.1016/B978-0-444-53064-6.X5186-X.

[122] M. Salavati-Niasari, F. Mohandes, From Zeolite to Host-Guest Nanocomposite Materials, Adv. Divers. Ind. Appl. Nanocomposites. (2011). doi:10.5772/15042.

[123] N. Taufiqurrahmi, A.R. Mohamed, S. Bhatia, Nanocrystalline zeolite Y: Synthesis and characterization, IOP Conf. Ser. Mater. Sci. Eng. 17 (2011). doi:10.1088/1757-899X/17/1/012030.

[124] N. V. Choudary, B.L. Newalkar, Use of zeolites in petroleum refining and petrochemical processes: Recent advances, J. Porous Mater. 18 (2011) 685–692. doi:10.1007/s10934-010-9427-8.

[125] A.M. Doyle, T.M. Albayati, A.S. Abbas, Z.T. Alismaeel, Biodiesel production by esterification of oleic acid over zeolite Y prepared from kaolin, Renew. Energy. 97 (2016) 19–23. doi:10.1016/j.renene.2016.05.067.

[126] Y. Bai, W. Wu, X. Bian, Dynamic synthesis route of zeolite y with kaolin to improve yield, Green Process. Synth. 7 (2018) 23–29. doi:10.1515/gps-2016-0172.

[127] M. Warzybok, J. Warchoł, Synthesis of kaolin-based zeolite Y and its application for adsorption of two carbonyl compound gases, Czas. Inżynierii Lądowej, Środowiska i Archit. 65 (2018) 13–26. doi:10.7862/rb.2018.2.

[128] M. Tavasoli, H. Kazemian, S. Sadjadi, M. Tamizifar, Synthesis and characterization of zeolite nay using kaolin with different synthesis methods, Clays Clay Miner. 62 (2014) 508–518. doi:10.1346/CCMN.2014.0620605.

[129] S. Subagjo, E.S. Rahayu, T.W. Samadhi, M.L. Gunawan, Synthesis of NaY zeolite using mixed Calcined Kaolins, J. Eng. Technol. Sci. 47 (2015) 633–639. doi:10.5614/j.eng.technol.sci.2015.47.6.4.

[130] A.K. Panda, B.G. Mishra, D.K. Mishra, R.K. Singh, Effect of sulphuric acid treatment on the physico-chemical characteristics of kaolin clay, Colloids Surfaces A Physicochem. Eng. Asp. 363 (2010) 98–104. doi:10.1016/j.colsurfa.2010.04.022.

[131] F. Pan, X. Lu, Q. Zhu, Z. Zhang, Y. Yan, T. Wang, S. Chen, A fast route for synthesizing nano-sized ZSM-5 aggregates, J. Mater. Chem. A. 2 (2014) 20667–20675. doi:10.1039/c4ta04073b.

[132] A.A. Al-Zahrani, M.H. Abdul-Majid, Extraction of Alumina from Local Clays by Hydrochloric Acid Process, JKAU Eng. Sci. 20 (2009) 29–41. https://www.kau.edu.sa/Files/320/Researches/54693_25008.pdf.

[133] J.B. Adeoye, J.A. Omoleye, M.E. Ojewumi, R. Babalola, Synthesis of zeolite y from kaolin using novel method of dealumination, Int. J. Appl. Eng. Res. 12 (2017) 755–760.

[134] L.A.S. Do Nascimento, R.S. Angélica, C.E.F. da Costa, J.R. Zamian, G.N. da Rocha Filho, Comparative study between catalysts for esterification prepared from kaolins, Appl. Clay Sci. 51 (2011) 267–273. doi:10.1016/j.clay.2010.11.030.

[135] M.A. Uzair, A. Waqas, A. Afzal, S.H. Ansari, M.A. Ur Rehman, Application of acid treated kaolin clay for conversion of polymeric waste material into pyrolysis diesel fuel, 2014 Int. Conf. Energy Syst. Policies, ICESP 2014. (2015). doi:10.1109/ICESP.2014.7346979.

[136] C. Belver, M.A. Bañares Muñoz, M.A. Vicente, Chemical Activation of a Kaolinite under Acid and Alkaline Conditions, Chem. Mater. 14 (2002) 2033–2043. doi:10.1021/cm0111736.

[137] J.A. Parmar, D.R. Gandhi, L. V Chopda, P.H. Rana, Esterification of bioplatform molecule succinic acid using ZSM-5 and HZSM-5 catalysts, Indian Chem. Eng. 0 (2019) 1–9. doi:10.1080/00194506.2019.1699872.

[138] É. Makó, Z. Senkár, J. Kristóf, V. Vágvölgyi, Surface modification of mechanochemically activated kaolinites by selective leaching, J. Colloid Interface Sci. 294 (2006) 362–370. doi:https://doi.org/10.1016/j.jcis.2005.07.033.

[139] A. Hattab, M. Bagane, M. Chlendi, Characterization of Tataouines Raw and Activated Clay, J. Chem. Eng. Process Technol. 04 (2013) 2–5. doi:10.4172/2157-7048.1000155.

[140] G. of India, Indian Minerals Yearbook 2016 (Part- III : Mineral Reviews), 2018. doi:10.2759/061731.

[141] F.E. Soetaredjo, A. Ayucitra, S. Ismadji, A.L. Maukar, KOH/bentonite catalysts for transesterification of palm oil to biodiesel, Appl. Clay Sci. 53 (2011) 341–346. doi:10.1016/j.clay.2010.12.018.

[142] R. Sirsam, G. Usmani, Use of Surface Modified Bentonite Clay Catalyst for Esterification of Maleic Acid With Ethanol, Int. J. Res. Eng. Technol. 04 (2015) 144–150. doi:10.15623/ijret.2015.0404025.

[143] J.A. Melero, L.F. Bautista, J. Iglesias, G. Morales, R. Sánchez-Vazquez, Production of biodiesel from waste cooking oil in a continuous packed bed reactor with an agglomerated Zr-SBA-15/bentonite catalyst, Appl. Catal. B Environ. 145 (2014) 197–204. doi:10.1016/j.apcatb.2013.02.050.

[144] L. Wu, T.Y. Wei, Z.F. Tong, Y. Zou, Z.J. Lin, J.H. Sun, Bentonite-enhanced biodiesel production by NaOH-catalyzed transesterification of soybean oil with methanol, Fuel Process. Technol. 144 (2016) 334–340. doi:10.1016/j.fuproc.2015.12.017.

[145] B. Vijayakumar, C. Ravindra Reddy, P. Iyengar, G. Nagendrappa, B.S. Jai Prakash, Synthesis of p-tolyl stearate catalyzed by acid activated Indian bentonite, Indian J. Chem. Technol. 12 (2005) 316–321.

[146] W. Wang, X. Wang, C. Song, X. Wei, J. Ding, J. Xiao, Sulfuric acid modified bentonite as the support of tetraethylenepentamine for CO2 capture, Energy and Fuels. 27 (2013) 1538–1546. doi:10.1021/ef3021816.

[147] Z. Darvishi, A. Morsali, Synthesis and characterization of Nano-bentonite by sonochemical method, Ultrason. Sonochem. 18 (2011) 238–242. doi:10.1016/j.ultsonch.2010.05.012.

[148] W.K. Mekhamer, The colloidal stability of raw bentonite deformed mechanically by ultrasound, J. Saudi Chem. Soc. 14 (2010) 301–306. doi:10.1016/j.jscs.2010.04.013.

[149] B.S. Surendra, M. Veerabhadraswamy, H.G. Anil Kumar, B.K. Kendagannaswamy, H.P. Nagaswarupa, S.C. Prashanth, Microwave assisted physico-chemical modification of Bentonite clay: Characterization and photocatalytic activity, Mater. Today Proc. 4 (2017) 11727–11736. doi:10.1016/j.matpr.2017.09.089.

[150] E.L. Foletto, D.S. Paz, A. Gündel, Acid-activation assisted by microwave of a brazilian bentonite and its activity in the bleaching of soybean oil, Appl. Clay Sci. 83–84 (2013) 63–67. doi:10.1016/j.clay.2013.08.017.

[151] S.C. Motshekga, S.S. Ray, M.S. Onyango, M.N.B. Momba, Microwave-assisted synthesis, characterization and antibacterial activity of Ag/ZnO nanoparticles supported bentonite clay, J. Hazard. Mater. 262 (2013) 439–446. doi:10.1016/j.jhazmat.2013.08.074.

[152] D. Gandhi, R. Bandyopadhyay, S. Parikh, Structural and composition enhancement of Indian Kachchh kaolin clay: characterisation and application as low-cost catalyst, Indian Chem. Eng. 0 (2020) 1–11. doi:10.1080/00194506.2020.1828191.

[153] Z. Vuković, A. Milutonović, L. Rožić, A. Rosić, Z. Nedić, D. Jovanović, The influence of acid treatment on the composition of bentonite, Clays Clay Miner. 54 (2006) 697–702. doi:10.1346/CCMN.2006.0540605.

[154] K. Al-Essa, Activation of Jordanian Bentonite by Hydrochloric Acid and Its Potential for Olive Mill Wastewater Enhanced Treatment, J. Chem. 2018 (2018). doi:10.1155/2018/8385692.

[155] N. Yildiz, Z. Aktas, A. Calimli, Sulphuric Acid Activation of a Calcium Bentonite, Part. Sci. Technol. 22 (2004) 21–33. doi:10.1080/02726350490422392.

[156] S. Balcı, Structural property improvements of bentonite with sulfuric acid activation, J. Turkish Chem. Soc. 1 (2018) 201–212. doi:https://doi.org/10.1515/ijcre-2018-0167.

[157] S. Pande, A. Lagashetty, C.D. Madhusoodana, Acid Activation and its Characterisation of Gulbarga City Bentonite Clay, Mater. Sci. Res. India. 8 (2011) 283–288.

[158] A.M. Elfadly, I.F. Zeid, F.Z. Yehia, M.M. Abouelela, A.M. Rabie, Production of aromatic hydrocarbons from catalytic pyrolysis of lignin over acid-activated bentonite clay, Fuel Process. Technol. 163 (2017) 1–7. doi:10.1016/j.fuproc.2017.03.033.

[159] E.E. Bulent Caglar, Beytullah Afsin, Engin Koksal, Ahmet Tabak, Characterization of Unye bentonite after treatment with sulfuric acid, Quim. Nov. 36 (2013) 955–959.

[160] K. Motlagh, A.A. Youzbashi, Z.A. Rigi, Effect of acid activation on structural and bleaching properties of a bentonite, Iran. J. Mater. Sci. Eng. 8 (2011) 50–56.

[161] H. Zhao, C.H. Zhou, L.M. Wu, J.Y. Lou, N. Li, H.M. Yang, D.S. Tong, W.H. Yu, Catalytic dehydration of glycerol to acrolein over sulfuric acid-activated montmorillonite catalysts, Appl. Clay Sci. 74 (2013) 154–162. doi:10.1016/j.clay.2012.09.011.

[162] E.G. Garrido-Ramírez, B.K.G. Theng, M.L. Mora, Clays and oxide minerals as catalysts and nanocatalysts in Fenton-like reactions - A review, Appl. Clay Sci. 47 (2010) 182–192. doi:10.1016/j.clay.2009.11.044.

[163] J. Feng, X. Hu, P.L. Yue, Novel Bentonite Clay-Based Fe - Nanocomposite as a Heterogeneous Catalyst for Photo-Fenton Discoloration and Mineralization of Orange II, Environ. Sci. Technol. 38 (2004) 269–275. doi:10.1021/es034515c.

[164] E. Emam, G. Centi, S. Perathoner, a. Vaccari, Clays as Catalysts in Petroleum Refining Industry, Appl. Clay Sci. 3 (2008) 161–198. doi:10.1016/S0169-1317(98)00058-1.

[165] M. Ghiaci, M. Mostajeran, A. Gil, Synthesis and characterization of Co-Mn nanoparticles immobilized on a modified bentonite and its application for oxidation of p -xylene to terephthalic acid, Ind. Eng. Chem. Res. 51 (2012) 15821–15831. doi:10.1021/ie3021939.

[166] G. García, W. Aguilar-Mamani, I. Carabante, S. Cabrera, J. Hedlund, J. Mouzon, Preparation of zeolite A with excellent optical properties from clay, J. Alloys Compd. 619 (2015) 771–777. doi:10.1016/j.jallcom.2014.09.080.

[167] H. Ma, Q. Ya, Y. Fu, C. Ma, X. Dong, Synthesis of zeolite of type a from bentonite by alkali fusion activation using na2co3, Ind. Eng. Chem. Res. 49 (2010) 454–458. doi:10.1021/ie901205y.

[168] H. Faghihian, N. Godazandeha, Synthesis of nano crystalline zeolite Y from bentonite, J. Porous Mater. 16 (2009) 331–335. doi:10.1007/s10934-008-9204-0.

[169] S.R. Kirumakki, N. Nagaraju, K.V.R. Chary, Esterification of alcohols with acetic acid over zeolites Hβ, HY and HZSM5, Appl. Catal. A Gen. 299 (2006) 185–192. doi:10.1016/j.apcata.2005.10.033.

[170] S. Induri, S. Sengupta, J.K. Basu, A kinetic approach to the esterification of maleic anhydride with methanol on H-Y zeolite, J. Ind. Eng. Chem. 16 (2010) 467–473. doi:10.1016/j.jiec.2010.01.053.

[171] C. Baroi, A.K. Dalai, Esterification of free fatty acids (FFA) of Green Seed Canola (GSC) oil using H-Y zeolite supported 12-Tungstophosphoric acid (TPA), Appl. Catal. A Gen. 485 (2014) 99–107. doi:10.1016/j.apcata.2014.07.033.

[172] Z.T. Alismaeel, A.S. Abbas, T.M. Albayati, A.M. Doyle, Biodiesel from batch and continuous oleic acid esterification using zeolite catalysts, Fuel. 234 (2018) 170–176. doi:10.1016/j.fuel.2018.07.025.

[173] A. Corma, H. Garcia, S. Iborra, J. Primo, Modified faujasite zeolites as catalysts in organic reactions: Esterification of carboxylic acids in the presence of HY zeolites, J. Catal. 120 (1989) 78–87. doi:10.1016/0021-9517(89)90252-2.

[174] G.J. Gomes, D.M. Dal Pozzo, M.F. Zalazar, M.B. Costa, P.A. Arroyo, P.R.S. Bittencourt, Oleic Acid Esterification Catalyzed by Zeolite Y-Model of the Biomass Conversion, Top. Catal. 62 (2019) 874–883. doi:10.1007/s11244-019-01172-3.

[175] A. Osatiashtiani, B. Puértolas, C.C.S. Oliveira, J.C. Manayil, B. Barbero, M. Isaacs, C. Michailof, E. Heracleous, J. Pérez-Ramírez, A.F. Lee, K. Wilson, On the influence of Si:Al ratio and hierarchical porosity of FAU zeolites in solid acid catalysed esterification pretreatment of bio-oil, Biomass Convers. Biorefinery. 7 (2017) 331–342. doi:10.1007/s13399-017-0254-x.

[176] L.E. Safitri, U.K. Zuryati, H.N. Rohma, Y.L. Ni'Mah, D. Prasetyoko, Synthesis zeolite y from kaolin bangka belitung: Activation of metakaolin with various concentration of sulfuric acid, J. Phys. Conf. Ser. 1567 (2020). doi:10.1088/1742-6596/1567/3/032099.

[177] E. Santacesaria, D. Gelosa, P. Danise, S. Carrà, Vapor-phase esterification catalyzed by decationized Y zeolites, J. Catal. 80 (1983) 427–436. doi:10.1016/0021-9517(83)90266-X.

[178] A.M. Doyle, Z.T. Alismaeel, T.M. Albayati, A.S. Abbas, High purity FAU-type zeolite catalysts from shale rock for biodiesel production, Fuel. 199 (2017) 394–402. doi:10.1016/j.fuel.2017.02.098.

[179] G. Kuriakose, N. Nagaraju, Selective synthesis of phenyl salicylate (salol) by esterification reaction over solid acid catalysts, J. Mol. Catal. A Chem. 223 (2004) 155–159. doi:10.1016/j.molcata.2004.03.057.

[180] L.D. Borges, N.N. Moura, A.A. Costa, P.R.S. Braga, J.A. Dias, S.C.L. Dias, J.L. De MacEdo, G.F. Ghesti, Investigation of biodiesel production by HUSY and Ce/HUSY zeolites: Influence of structural and acidity parameters, Appl. Catal. A Gen. 450 (2013) 114–119. doi:10.1016/j.apcata.2012.10.009.

[181] J. Aracil, M. Martinez, N. Sa´nchez, A. Corma, Formation of a jojoba oil analog by esterification of oleic acid using zeolites as catalyst, Zeolites. 12 (1992) 233–236. doi:10.1016/S0144-2449(05)80288-X.

[182] W. Liu, P. Yin, J. Zhang, Q. Tang, R. Qu, Biodiesel production from esterification of free fatty acid over PA/NaY solid catalyst, Energy Convers. Manag. 82 (2014) 83–91. doi:10.1016/j.enconman.2014.02.062.

[183] G. Nagendrappa, Organic synthesis using clay and clay-supported catalysts, Appl. Clay Sci. 53 (2011) 106–138. doi:10.1016/j.clay.2010.09.016.

[184] H. Robson, Verified Syntheses of Zeolitic Materials, 3rd ed., (2016) ISBN: 978-0-692-68539-6, 221-222

[185] A.O. Ajayi, A.Y. Atta, B.O. Aderemi, S.S. Adefila, Novel method of metakaolin dealumination - preliminary investigation, J. Appl. Sci. Res. 6 (2010) 1539–1546.

[186] H.G. Karge, Characterization by IR spectroscopy, (2001) 69–71.

[187] H.N. Southworth, Scanning Electron Microscopy and Microanalysis, Physicochem. Methods Miner. Anal. (1975) 421–450. doi:10.1007/978-1-4684-2046-3_11.

[188] N.J. Saikia, D.J. Bharali, P. Sengupta, D. Bordoloi, R.L. Goswamee, P.C. Saikia, P.C. Borthakur, Characterization, beneficiation and utilization of a kaolinite clay from Assam, India, Appl. Clay Sci. 24 (2003) 93–103. doi:10.1016/S0169-1317(03)00151-0.

[189] R. Vijayragavan, S. Mullainathan, M. Balachandramohan, N. Krishnamoorthy, S. Nithiyanantham, S. Murugesan, V. Vanathi, Mineralogical Characterization Studies on Unburnt Ceramic Product Made From Rock Residue Additives By Ft-Ir Spectroscopic Technique, Int. J. Mod. Phys. Conf. Ser. 22 (2013) 62–70. doi:10.1142/s2010194513009938.

[190] H. Cheng, J. Yang, Q. Liu, J. Zhang, R.L. Frost, A spectroscopic comparison of selected Chinese kaolinite, coal bearing kaolinite and halloysite - A mid-infrared and near-infrared study, Spectrochim. Acta - Part A Mol. Biomol. Spectrosc. 77 (2010) 856–861. doi:10.1016/j.saa.2010.08.018.

[191] B. Plešingerová, G. Súčik, M. Fabián, Surface area change of kaolin causing annealing, Acta Metall. Slovaca. 17 (2011) 169–176.

[192] S. Bawa, A. Ahmed, P. Okonkwo, the Study of Thermal Effect on the Surface Properties of Gamma-Alumina Synthesied From Kankara Kaolin., Niger. J. Technol. 35 (2015) 66. doi:10.4314/njt.v35i1.11.

[193] G. Varga, The structure of kaolinite and metakaolinite, Epa. - J. Silic. Based Compos. Mater. 59 (2007) 6–9. doi:10.14382/epitoanyag-jsbcm.2007.2.

[194] S.L. Abdullahi, A.A. Audu, Comparative analysis on chemical composition of bentonite clays obtained from Ashaka and tango deposits in Gombe State, Nigeria, ChemSearch J. 8 (2017) 35–40.

[195] F.R. V Días, S.P. Santos, Studies on the acid activation of brazilian smectitic clays, Quim. Nova. 24 (2001) 345–353.

[196] N. Venkatathri, Characterization and catalytic properties of a naturally occurring clay , Bentonite, Bull. Catal. Soc. India. 5 (2006) 61–72.

[197] S. Korichi, A. Elias, A. Mefti, Characterization of smectite after acid activation with microwave irradiation, Appl. Clay Sci. 42 (2009) 432–438. doi:10.1016/j.clay.2008.04.014.

[198] L. Andrini, R. Moreira Toja, M.R. Gauna, M.S. Conconi, F.G. Requejo, N.M. Rendtorff, Extended and local structural characterization of a natural and 800 °C fired Na-montmorillonite–Patagonian bentonite by XRD and Al/Si XANES, Appl. Clay Sci. 137 (2017) 233–240. doi:10.1016/j.clay.2016.12.030.

[199] W.P. Gates, J.S. Anderson, M.D. Raven, G.J. Churchman, Mineralogy of a bentonite from Miles, Queensland, Australia and characterisation of its acid activation products, Appl. Clay Sci. 20 (2002) 189–197. doi:10.1016/S0169-1317(01)00072-2.

[200] M.A. Mekewi, A.S. Darwish, M.S. Amin, G. Eshaq, H.A. Bourazan, Copper nanoparticles supported onto montmorillonite clays as efficient catalyst for methylene blue dye degradation, Egypt. J. Pet. 25 (2016) 269–279. doi:10.1016/j.ejpe.2015.06.011.

[201] P. Komadel, M. Janek, J. Madejová, A. Weekes, C. Breen, Acidity and catalytic activity of mildly acid-treated Mg-rich montmorillonite and hectorite, J. Chem. Soc. - Faraday Trans. 93 (1997) 4207–4210. doi:10.1039/a705227h.

[202] I.S.S. Pinto, S.M. Sadeghi, N.E. Izatt, H.M.V.M. Soares, Recovery of metals from an acid leachate of spent hydrodesulphurization catalyst using molecular recognition technology, Chem. Eng. Sci. 138 (2015) 353–362. doi:https://doi.org/10.1016/j.ces.2015.08.018.

[203] M. Regel-Rosocka, A review on methods of regeneration of spent pickling solutions from steel processing, J. Hazard. Mater. 177 (2010) 57–69. doi:https://doi.org/10.1016/j.jhazmat.2009.12.043.

[204] S. Chandrasekhar, P.N. Pramada, Kaolin-based zeolite Y, a precursor for cordierite ceramics, Appl. Clay Sci. 27 (2004) 187–198. doi:10.1016/j.clay.2004.07.001.

[205] M.M.J. Treacy, J.B. Higgins, Collection of Simulated XRD Powder Patterns for Zeolites Fifth (5th) Revised Edition, 2007. doi:10.1016/B978-0-444-53067-7.X5470-7.

[206] N. Salahudeen, A.S. Ahmed, Synthesis of hexagonal zeolite Y from Kankara kaolin using a split technique, J. Incl. Phenom. Macrocycl. Chem. 87 (2017) 149–156. doi:10.1007/s10847-016-0686-0.

[207] J.K.M. Ernest Kentsa, Horace Manga Ngomo, Charles Fon Abi, Julius Sami Ndi, Sary Awad, Divine Dingka, Synthesis and characterization of zeolite Y from akilbenza clay: effect of crystallization time, J. Chem. Inf. Model. 8 (2019) 1–22. doi:10.1017/CBO9781107415324.004.

[208] Y.K. Krisnandi, I.R. Saragi, R. Sihombing, R. Ekananda, I.P. Sari, B.E. Griffith, J. V Hanna, Synthesis and characterization of crystalline NaY-Zeolite from Belitung Kaolin as catalyst for n-Hexadecane cracking, Crystals. 9 (2019) 1–14. doi:10.3390/cryst9080404.

[209] B. Liu, F. Chen, L. Zheng, J. Ge, H. Xi, Y. Qian, Synthesis and structural properties of hierarchically structured aluminosilicates with zeolite y (FAU) frameworks, RSC Adv. 3 (2013) 15075–15084. doi:10.1039/c3ra41862f.

[210] H.N. Kim, K.S. Suslick, The effects of ultrasound on crystals: Sonocrystallization and sonofragmentation, Crystals. 8 (2018). doi:10.3390/cryst8070280.

[211] T.S. Ćeranić, V.M. Radak, T.M. Lukić, D. Nikolić, Properties of (Na,K) exchanged forms of NH4□Y zeolite thermally treated at 873 K, Zeolites. 5 (1985) 42–44. doi:https://doi.org/10.1016/0144-2449(85)90010-7.

[212] T. Alam, Y.K. Krisnandi, W. Wibowo, D.A. Nurani, D.U.C. Rahayu, H. Haerudin, Synthesis and characterization hierarchical HY zeolite using template and non template methods, AIP Conf. Proc. 2023 (2018). doi:10.1063/1.5064091.

[213] G.S. Nikolaidis, Preferential oxidation of carbon monoxide in microchannels – development of catalysts for the low temperature regime and kinetic study, Distribution. (2007).

[214] W. Lutz, Zeolite Y: Synthesis, modification, and properties - A case revisited, Adv. Mater. Sci. Eng. 2014 (2014). doi:10.1155/2014/724248.

[215] D.J. Benedict, S.J. Parulekar, S.P. Tsai, Pervaporation-assisted esterification of lactic and succinic acids with downstream ester recovery, J. Memb. Sci. 281 (2006) 435–445. doi:10.1016/j.memsci.2006.04.012.

[216] I.G. Hakeem, F. Aberuagba, U. Musa, Catalytic pyrolysis of waste polypropylene using Ahoko kaolin from Nigeria, Appl. Petrochemical Res. 8 (2018) 203–210. doi:10.1007/s13203-018-0207-8.

[217] N. Bizaia, E.H. De Faria, G.P. Ricci, P.S. Calefi, E.J. Nassar, K.A.D.F. Castro, S. Nakagaki, K.J. Ciuffi, R. Trujillano, M.A. Vicente, A. Gil, S.A. Korili, Porphyrin-kaolinite as efficient catalyst for oxidation reactions, ACS Appl. Mater. Interfaces. 1 (2009) 2667–2678. doi:10.1021/am900556b.

[218] J. Ramirez-Ortiz, M. Martinez, H. Flores, Metakaolinite as a catalyst for biodiesel production from waste cooking oil, Front. Chem. Sci. Eng. 6 (2012) 403–409. doi:10.1007/s11705-012-1224-2.

[219] C.H. Zhou, G.L. Li, X.Y. Zhuang, P.P. Wang, D.S. Tong, H.M. Yang, C.X. Lin, L. Li, H. Zhang, S.F. Ji, W.H. Yu, Roles of texture and acidity of acid-activated sepiolite catalysts in gas-phase catalytic dehydration of glycerol to acrolein, Mol. Catal. 434 (2017) 219–231. doi:10.1016/j.mcat.2016.12.022.

[220] Ravichandran, J., Sivasankar, B. Properties and Catalytic Activity of Acid-Modified Montmorillonite and Vermiculite. Clays Clay Miner. 45, 854–858 (1997). https://doi.org/10.1346/CCMN.1997.0450609.

[221] J. Pérez-Ramírez, C.H. Christensen, K. Egeblad, C.H. Christensen, J.C. Groen, Hierarchical zeolites: enhanced utilisation of microporous crystals in catalysis by advances in materials design, Chem. Soc. Rev. 37 (2008) 2530–2542. doi:10.1039/B809030K.

[222] J.H. Clark, V. Budarin, T. Dugmore, R. Luque, D.J. Macquarrie, V. Strelko, Catalytic performance of carbonaceous materials in the esterification of succinic acid, Catal. Commun. 9 (2008) 1709–1714. doi:https://doi.org/10.1016/j.catcom.2008.01.037.

[223] A.K. Kolah, N.S. Asthana, D.T. Vu, C.T. Lira, D.J. Miller, Reaction kinetics for the heterogeneously catalyzed esterification of succinic acid with ethanol, Ind. Eng. Chem. Res. 47 (2008) 5313–5317. doi:10.1021/ie0706616.

[224] C.R. Reddy, B. Vijayakumar, P. Iyengar, G. Nagendrappa, B.S. Jai Prakash, Synthesis of phenylacetates using aluminium-exchanged montmorillonite clay catalyst, J. Mol. Catal. A Chem. 223 (2004) 117–122. doi:10.1016/j.molcata.2003.11.039.

[225] K.U. Nandhini, B. Arabindoo, M. Palanichamy, V. Murugesan, Al-MCM-41 supported phosphotungstic acid: Application to symmetrical and unsymmetrical ring opening of succinic anhydride, J. Mol. Catal. A Chem. 243 (2006) 183–193. doi:10.1016/j.molcata.2005.08.028.

[226] S.R. Kirumakki, N. Nagaraju, K.V.R. Chary, S. Narayanan, Kinetics of esterification of aromatic carboxylic acids over zeolites Hβ and HZSM5 using dimethyl carbonate, Appl. Catal. A Gen. 248 (2003) 161–167. doi:10.1016/S0926-860X(03)00152-2.

Research Publications

List of publications

Journal

1. D. Gandhi, R. Bandyopadhyay, S. Parikh, Structural and composition enhancement of Indian Kachchh kaolin clay: characterisation and application as low-cost catalyst, Indian Chem. Eng. 0 (2020) 1–11. **doi:10.1080/00194506.2020.1828191**, Taylor & Francis publication.

2. D. Gandhi, R. Bandyopadhyay, B. Soni, Zeolite Y from kaolin clay of Kachchh, India: Synthesis, characterization and catalytic application, J. Indian Chem. Soc. 98 (2021) 100246. **doi:10.1016/j.jics.2021.100246**, Elsevier publication.

3. D. Gandhi, R. Bandyopadhyay, B. Soni, Naturally occurring bentonite clay: Structural augmentation, characterization and application as catalyst, Materials Today: Proceedings (2022). **doi.org/10.1016/j.matpr.2022.02.346**, Elsevier publication.

Conference:

1. Recent development in zeolite catalysis for refinery applications at International Conference on Paradigm shift in Chemical engineering education, processes and technology, 16-17 September, 2017, Ahmedabad Organized by The Institution of Engineers. **ISBN: 978-93-5281-401-5.**

2. Exploring the Potential of Acid Treated Bentonite Clay for Various Catalytic Applications (February 5, 2020). Proceedings of the International Conference on Advances in Chemical Engineering (AdChE) 2020, Published in **Elsevier** SSRN: **doi:10.2139/ssrn.3707320**

3. Naturally Occurring Bentonite Clay: Structural Augmentation, Characterization and Application as Catalyst. 19-21 November 2021, International Symposium on Materials of the Millennium: Emerging Trends and Future Prospects (MMETFP-2021) organized by Pandit Deendayal Energy University (PDEU), Gandhinagar, Gujarat and Material Research Society of India (MRSI).

****

APPENDIX

APPENDIX–A

Crystallinity

&

Lattice parameter calculation

Crystallinity calculation

Method:

- The 2 θ versus intensity plot from a diffractometer is generated for all samples.
- To calculate the crystallinity, need intensity data of main peaks. (as tabulated below)
- **Sample Name: UZeoY**

	Intensity value	
Sample name	**CZeoY**	**UZeoY**
Common peak		
6.11	1535	3137
10.14	914	708
11.88	993	513
15.62	2075	1677
18.6	1117	750
20.3	1548	1297
22.8	573	392
23.7	2610	2817
25.8	382	296

$$\text{Crystallinity} = \frac{\text{Sum of the intensity of the characteristic XRD peak of product}}{\text{Sum of the intensity of the characteristic XRD peak of reference sample}}$$

$$\text{Crystallinity} = \frac{3137+708+513+1677+750+1297+392+2817+296}{1535+914+993+2075+1117+1548+573+2610+382}$$

$$= \frac{11587}{11747} = 0.9863 = \mathbf{98.63\%}$$

The crystallinity of the synthesized zeolite Y were evaluated by using above formula. The XRD pattern of commercial zeolite Y sample obtained from Zeolyst international as a reference, the crystallinity of UZeoY was evaluated 98.63%.

Lattice parameter calculation

Method:

- Recorded diffraction pattern over as wide a range of 2θ as possible.
- Calculated the value of $\sin^2\theta$ for each diffraction line.

Bragg's Law

$$\lambda = 2d\ Sin\theta$$

$$\lambda^2 = 4d^2 \sin^2\theta$$

$$\sin^2\theta = \frac{\lambda^2}{4d^2}$$

- Obtain interplanar spacing, d_{hkl}, from the plane spacing equation

$$d_{hkl\ Cubic} = \frac{a}{\sqrt{h^2+k^2+l^2}}$$

- Substitute plane-spacing equation into Bragg'slaw

$$\sin^2\theta = \frac{\lambda^2}{4a^2}(h^2+k^2+l^2)$$

- For any single diffraction pattern

$$C = \frac{\lambda^2}{4a^2} \equiv Cons$$

Hence

$$\sin^2\theta\ \alpha\ (h^2+k^2+l^2)$$

- The method is based upon of Bragg's law and the plane-spacing equations.
  - For any two different reflections/planes,θ_1 and θ_2

$$\frac{\sin^2\theta_1}{\sin^2\theta_2} = \frac{h_1^2+k_1^2+l_1^2}{h_2^2+k_2^2+l_2^2} = \frac{k_1}{k_2}$$

Both the numerator and denominator are integers that scale with *h k l*

  - Obtain $h^2 + k^2 + l^2$ for a given reflection by dividing the $\sin^2\theta$ values for each reflection with that for the first (i.e., minimum) one.

- Multiply by the appropriate number to obtain an integer (usually 1, 2 or 3).
- Subsequent integers represent the quadratic form of the Miller indices.
- Take λ=1.54Å

- For all samples follow the given procedures and finally calculated lattice parameter.
    - Identify the peaks.
    - Determine $\sin^2\theta$.
    - Calculate the ratio $\sin^2\theta/\sin^2\theta_{min}$ and multiply by the appropriate integers.
    - Select the result from (3) that yields $h^2+k^2+l^2$ as an integer.
    - Compare results with the sequences of $h^2+k^2+l^2$ values to identify the Bravais lattice.
    - Calculate lattice parameters.

- **Sample Name: UZeoY**

Peak	2Θ	Θ	RAD	sinΘ	$sin^2Θ$	$sin^2Θ/sin^2Θmin$	$1*sin^2Θ/sin^2Θmin$	$2*sin^2Θ/sin^2Θmin$	$3*sin^2Θ/sin^2Θmin$	$h^2+k^2+l^2$	hkl	$λ^2*h^2+k^2+l^2$	$(λ^2*h^2+k^2+l^2)/sin^2Θ$	$((λ^2*h^2+k^2+l^2)/sin^2Θ)/4$	a= avg lattice parameter
1	6.2	3.1	0.05	0.05	0.00	0.99	0.99	1.99	2.98	3	111	7.11	2432.81	608.20	24.66
2	10.09	5.045	0.09	0.09	0.01	2.63	2.63	5.26	7.88	8	220	18.97	2453.45	613.36	24.77
3	11.83	5.915	0.10	0.10	0.01	3.61	3.61	7.22	10.83	11	311	26.09	2456.48	614.12	24.78
4	12.43	6.215	0.11	0.11	0.01	3.98	3.98	7.96	11.95	12	222	28.46	2428.23	607.06	24.64
5	15.6	7.8	0.14	0.14	0.02	6.26	6.26	12.52	18.78	19	331	45.06	2446.45	611.61	24.73
6	18.59	9.295	0.16	0.16	0.03	8.86	8.86	17.73	26.59	27	511	64.03	2454.51	613.63	24.77
7	20.24	10.12	0.18	0.18	0.03	10.49	10.49	20.98	31.47	32	440	75.89	2458.08	614.52	24.79
8	21.62	10.81	0.19	0.19	0.04	11.95	11.95	23.90	35.86	35	531	83.01	2359.73	589.93	24.29
9	23.5	11.75	0.21	0.20	0.04	14.09	14.09	28.18	42.27	43	533	101.98	2459.10	614.78	24.79
10	26.9	13.45	0.23	0.23	0.05	18.38	18.38	36.77	55.15	55	642	130.44	2411.00	602.75	24.55
															246.77
														Average	**24.68**

- **Sample Name: KZeoY**

Peak	2Θ	Θ	RAD	sinΘ	$\sin^2\Theta$	$\sin^2\Theta/\sin^2\Theta_{min}$	$1*\sin^2\Theta/\sin^2\Theta_{min}$	$2*\sin^2\Theta/\sin^2\Theta_{min}$	$3*\sin^2\Theta/\sin^2\Theta_{min}$	$h^2+k^2+l^2$	hkl	$\lambda^2*h^2+k^2+l^2$	$(\lambda^2*h^2+k^2+l^2)/\sin^2\Theta$	$((\lambda^2*h^2+k^2+l^2)/\sin^2\Theta)/4$	a= avg lattice parameter
1	6.22	3.11	0.05	0.05	0.00	1.00	1.00	2.00	3.00	3	111	7.11	2417.21	604.30	24.58
2	10.14	5.07	0.09	0.09	0.01	2.65	2.65	5.31	7.96	8	220	18.97	2429.38	607.34	24.64
3	11.88	5.94	0.10	0.10	0.01	3.64	3.64	7.28	10.92	11	311	26.09	2435.92	608.98	24.68
4	12.43	6.215	0.11	0.11	0.01	3.98	3.98	7.96	11.95	12	222	28.46	2428.23	607.06	24.64
5	15.62	7.81	0.14	0.14	0.02	6.27	6.27	12.55	18.82	19	331	45.06	2440.22	610.06	24.70
6	18.64	9.32	0.16	0.16	0.03	8.91	8.91	17.82	26.74	27	511	64.03	2441.48	610.37	24.71
7	20.31	10.16	0.18	0.18	0.03	10.56	10.56	21.13	31.69	32	440	75.89	2441.34	610.34	24.70
8	21.3	10.65	0.19	0.18	0.03	11.61	11.61	23.21	34.82	35	531	83.01	2430.32	607.58	24.65
9	23.6	11.8	0.21	0.20	0.04	14.21	14.21	28.42	42.63	43	533	101.98	2438.60	609.65	24.69
10	24.92	12.46	0.22	0.22	0.05	15.82	15.82	31.64	47.45	47	444	111.47	2394.45	598.61	24.47
															246.46
														Average	**24.65**

- **Sample Name: RZeoY**

Peak	2Θ	Θ	RAD	sinΘ	$\sin^2\Theta$	$\sin^2\Theta/\sin^2\Theta_{min}$	$1*\sin^2\Theta/\sin^2\Theta_{min}$	$2*\sin^2\Theta/\sin^2\Theta_{min}$	$3*\sin^2\Theta/\sin^2\Theta_{min}$	$h^2+k^2+l^2$	hkl	$\lambda^2*h^2+k^2+l^2$	$(\lambda^2*h^2+k^2+l^2)/\sin^2\Theta$	$((\lambda^2*h^2+k^2+l^2)/\sin^2\Theta)/4$	a= avg lattice parameter
1	6.15	3.08	0.05	0.05	0.00	1.00	1.00	2.00	3.00	3	111	7.11	2472.49	618.12	24.86
2	10.09	5.05	0.09	0.09	0.01	2.69	2.69	5.37	8.06	8	220	18.97	2453.45	613.36	24.77
3	11.9	5.95	0.10	0.10	0.01	3.73	3.73	7.47	11.20	11	311	26.09	2427.77	606.94	24.64
4	15.58	7.79	0.14	0.14	0.02	6.38	6.38	12.77	19.15	19	331	45.06	2452.69	613.17	24.76
5	18.62	9.31	0.16	0.16	0.03	9.09	9.09	18.19	27.28	27	511	64.03	2446.68	611.67	24.73
6	20.28	10.14	0.18	0.18	0.03	10.77	10.77	21.54	32.31	32	440	75.89	2448.50	612.12	24.74
7	22.71	11.36	0.20	0.20	0.04	13.47	13.47	26.94	40.41	40	620	94.86	2447.18	611.79	24.73
8	23.57	11.79	0.21	0.20	0.04	14.49	14.49	28.99	43.48	43	533	101.98	2444.72	611.18	24.72
9	25.69	12.85	0.22	0.22	0.05	17.17	17.17	34.35	51.52	51	551	120.95	2447.24	611.81	24.73
10	31.3	15.65	0.27	0.27	0.07	25.29	25.29	50.57	75.86	76	822	180.24	2476.85	619.21	24.88
															247.535
														Average	**24.75**

APPENDIX–B

Sample batch calculation

Sample batch calculation

Zeolite Y Synthesis:

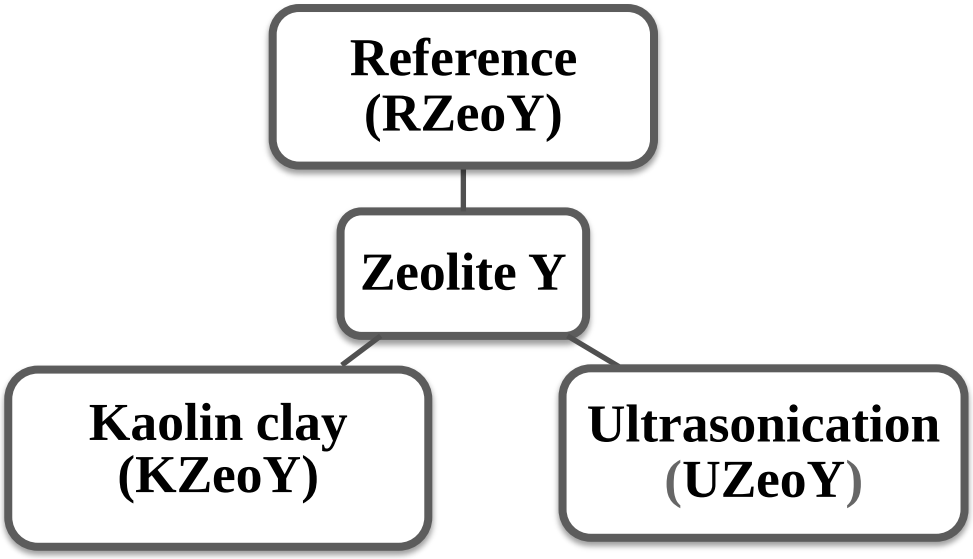

- **Chemicals:**

♣ **Sodium silicate synthesis process:-**

- Sodium silicate glass also known water glass is received from manufacturer.
- Water glass is taken in large container and heated at 60 – 70^{o}C.
- No extra water is added in this process.

SiO_2 = 21.44 % Na_2O = 6.76 %

♣ **Sodium aluminate synthesis process:-**

- Sodium aluminate is directly received from manufacturer.
- Bauxite is added (in very less amount) to increase alumina content.

Al_2O_3 = 17.60 % Na_2O = 15.80 %

♣ DM Water

♣ Sodium Hydroxide 99% pure

♣ **Kaolinite clay 10 M H_2SO_4 treated XRF result:-**

SiO_2	Al_2O_3	Na_2O	TiO_2	Fe_2O_3	K_2O	CaO	MnO	MgO
67.985	28.613	0.044	2.408	0.292	0.197	0.017	0.007	0.011

1) Synthesis of reference zeolite Y (RZeoY) and zeolite by Ultrasonication (UZeoY):-

Batch Composition

Seed Gel: 10.67 Na_2O : 1 Al_2O_3 : 10 SiO_2 : 180 H_2O

Overall Gel: 4.70 Na_2O : 1 Al_2O_3 : 10 SiO_2 : 180 H_2O

Source materials:

1) DM Water
2) Sodium silicate solution (Na_2O 6.76%, SiO_2 21.44%)
3) Sodium aluminate solution (Al_2O_3 17.60%, Na_2O 15.80%)
4) Sodium Hydroxide 98% pure

Batch preparation

Preparation of Seed gel

Seed Gel: 10.67 Na_2O : 1 Al_2O_3 : 10 SiO_2 : 180 H_2O

1) Sodium silicate (**Na_2SiO_3**) solution (Na_2O 6.76%, SiO_2 21.44%)
2) Sodium aluminate(**$Na_2Al_2O_4$**) solution (Al_2O_3 17.60%, Na_2O 15.80%)

Reactant	**Mol. Wt.**	**Molar composition**	**Molar composition × Mol. Wt.**
Al_2O_3	101.96	1	101.96
SiO_2	60.08	10	600.8
Na_2O	61.97	10.67	661.2199
H_2O	18.02	180	3243.6
		Total	**4607.5799**

For Al_2O_3 :

$$\frac{101.96\times100}{4607.5799} = 2.2128g$$

Amount of $Na_2Al_2O_4$:

$$\frac{2.2188\times100}{17.60} = 12.5727\ g$$

For SiO_2 :

$$\frac{600.8\times100}{4607.5799} = 13.0394g$$

Amount of Na_2SiO_3:

$$\frac{13.0394\times100}{21.44} = 60.81809g$$

For Na_2O :

$$\frac{661.2199\times100}{4607.5799} = 14.3507g$$

Amount of Na_2O with Na_2SiO_3:

$$\frac{6.76\times60.81809}{100} = 4.113g$$

Amount of Na_2O with $Na_2Al_2O_4$:

$$\frac{12.5727\times15.80}{100} = 1.9865g$$

Total Na_2O :

$$1.9865g + 4.113g = 6.0978g$$

Amount of Na_2O to be added:

$$14.3507g - 6.0978\ g = 8.2529g$$

For NaOH :

1 Na_2O = 2 NaOH

$$\frac{8.2529\times2\times39.997}{61.97} = 10.6533g$$

For H_2O :

$$\frac{3243.6\times100}{4607.5799} = 70.3971g$$

Amount of chemicals to be added in seed gel:

Name of chemicals	Amount in g
Na_2SiO_3	60.81809
$Na_2Al_2O_4$	12.5727
NaOH	10.6533
H_2O	70.3971
Total	154.4419

Procedure:

- Add 70.3971 g water , 10.6533 g sodium hydroxide , 12.5727 g sodium aluminate and stir in 250 mL plastic bottle until dissolved.
- Add drop wise 60.8181 g sodium silicate solution in above mixture and stir moderately for at least 1 hr. Cap the bottle and keep the solution for aging at room temperature for 1 day.

Preparation of Overall Gel

Overall Gel: 4.70 Na_2O : 1 Al_2O_3 : 10 SiO_2 : 180 H_2O

1) Sodium silicate (**Na_2SiO_3**) solution (Na_2O 6.76%, SiO_2 21.44%)
2) Sodium aluminate(**$Na_2Al_2O_4$**) solution (Al_2O_3 17.60%, Na_2O 15.80%)

Reactant	Mol. Wt.	Molar composition	Molar composition × Mol. Wt.
Al_2O_3	101.96	1	101.96
SiO_2	60.08	10	600.8
Na_2O	61.97	4.70	291.259
H_2O	18.02	180	3243.6
		Total	**4273.619**

For Al_2O_3 :

$$\frac{101.96\times100}{4237.619} = 2.4061g$$

Amount of $Na_2Al_2O_4$:

$$\frac{2.4061\times100}{17.60} = 13.6711\ g$$

For SiO_2 :

$$\frac{600.8\times100}{4237.619} = 14.1778g$$

Amount of Na_2SiO_3:

$$\frac{141778\times100}{21.44} = 66.1278g$$

For Na_2O :

$$\frac{291.259\times100}{4237.619} = 6.8732g$$

Amount of Na_2O with Na_2SiO_3:

$$\frac{6.76\times66.1278}{100} = 4.4703g$$

Amount of Na_2O with $Na_2Al_2O_4$:

$$\frac{13.6711\times15.80}{100} = 2.1601g$$

Total Na_2O :

$$4.4703g + 2.16013g = 6.6304g$$

Amount of Na_2O to be added:

$$6.8732g - 6.6304\ g = 0.2428g$$

For NaOH :

1 Na_2O = 2 NaOH

$$\frac{0.2428\times2\times39.997}{61.97} = 0.3135g$$

For H_2O :

$$\frac{3243.6\times100}{4237.619} = 76.5429g$$

Amount of chemicals to be added in overall gel:

Name of chemicals	Amount in g
Na_2SiO_3	66.1278
$Na_2Al_2O_4$	13.6711
NaOH	0.3135
H_2O	76.5429
Total	156.6553

Procedure:

- Add 76.5429g water , 0.3135g sodium hydroxide , 13.6711g sodium aluminate and stir in 250 mL plastic bottle until dissolved.
- Add drop wise 66.1278g sodium silicate solution in above mixture and stir moderately for at least 20 min.

2) Synthesis of zeolite from Kaolin clay(KZeoY):-

Batch Composition

Seed Gel: 10.67 Na_2O : 1 Al_2O_3 : 10 SiO_2 : 180 H_2O

Overall Gel: 4.70 Na_2O : 1 Al_2O_3 : 10 SiO_2 : 180 H_2O

Batch preparation

Preparation of Seed gel

Seed Gel: 10.67 Na_2O : 1 Al_2O_3 : 10 SiO_2 : 180 H_2O

1) Sodium silicate (**Na_2SiO_3)** solution (Na_2O 6.76%, SiO_2 21.44%)
2) Sodium aluminate(**$Na_2Al_2O_4$**) solution (Al_2O_3 17.60%, Na_2O 15.80%)

Reactant	Mol. Wt.	Molar composition	Molar composition × Mol. Wt.
Al_2O_3	101.96	1	101.96
SiO_2	60.08	10	600.8
Na_2O	61.97	10.67	661.2199
H_2O	18.02	180	3243.6
		Total	**4607.5799**

For Al_2O_3 :

$$\frac{101.96\times100}{4607.5799} = 2.2128g$$

Amount of $Na_2Al_2O_4$:

$$\frac{2.2188\times100}{17.60} = 12.5727\ g$$

For SiO_2 :

$$\frac{600.8\times100}{4607.5799} = 13.0394g$$

Amount of Na_2SiO_3:

$$\frac{13.0394\times100}{21.44} = 60.81809g$$

For Na_2O :

$$\frac{661.2199\times100}{4607.5799} = 14.3507g$$

Amount of Na_2O with Na_2SiO_3:

$$\frac{6.76\times60.81809}{100} = 4.113g$$

Amount of Na_2O with $Na_2Al_2O_4$:

$$\frac{12.5727 \times 15.80}{100} = 1.9865g$$

Total Na_2O :

$$1.9865g + 4.113g = 6.0978g$$

Amount of Na_2O to be added:

$$14.3507g - 6.0978\ g = 8.2529g$$

For NaOH:

1 Na_2O = 2 NaOH

$$\frac{8.2529 \times 2 \times 39.997}{61.97} = 10.6533g$$

For H_2O:

$$\frac{3243.6 \times 100}{4607.5799} = 70.3971g$$

Amount of chemicals to be added in seed gel:

Name of chemicals	Amount in g
Na_2SiO_3	60.81809
$Na_2Al_2O_4$	12.5727
NaOH	10.6533
H_2O	70.3971
Total	154.4419

Procedure:

- Add 70.3971 g water , 10.6533 g sodium hydroxide , 12.5727 g sodium aluminate and stir in 250 mL plastic bottle until dissolved.

- Add drop wise 60.8181 g sodium silicate solution in above mixture and stir moderately for at least 1 hr. Cap the bottle and keep the solution for aging at room temperature for 1 day.

Preparation of Overall Gel

Overall Gel: 4.70 Na_2O : 1 Al_2O_3 : 10 SiO_2 : 180 H_2O

Reactant	Mol. Wt.	Molar composition	Molar composition × Mol. Wt.
Al_2O_3	101.96	1	101.96
SiO_2	60.08	10	600.8
Na_2O	61.97	4.70	291.259
H_2O	18.02	180	3243.6
		Total	**4273.619**

For Al_2O_3 :

$$\frac{101.96\times100}{4237.619} = 2.4061g$$

Amount of modified kaolin clay:

$$\frac{2.4061\times100}{28.61} = 8.41\ g$$

For SiO_2 :

$$\frac{600.8\times100}{4237.619} = 14.1778g$$

Amount of SiO_2 from **modified kaolin clay:**

$$\frac{8.41\times67.98}{100} = 5.72g$$

Remaining amount of SiO_2 :

$$14.1778g - 5.72g = 8.4578g$$

Amount of Na_2SiO_3:

$$\frac{8.4578 \times 100}{21.44} = 39.4487g$$

For Na_2O :

$$\frac{291.259 \times 100}{4237.619} = 6.8732g$$

Amount of Na_2O with Na_2SiO_3:

$$\frac{6.76 \times 39.4487}{100} = 2.6667g$$

Amount of Na_2O with modified kaolin clay:

$$\frac{8.81 \times 0.044}{100} = 0.0037004g$$

Total Na_2O :

$$2.6667g + 0.0037004g = 2.6704g$$

Amount of Na_2O to be added:

$$6.8732g - 2.6704\ g = 4.2028g$$

For NaOH :

1 Na_2O = 2 NaOH

$$\frac{4.2028 \times 2 \times 39.997}{61.97} = 5.4252g$$

For H_2O :

$$\frac{3243.6 \times 100}{4237.619} = 76.5429g$$

Amount of chemicals to be added in overall gel:

Name of chemicals	Amount in g
Na_2SiO_3	39.4487
Modified Kaolin clay	8.41
NaOH	5.4252
H_2O	76.5429
Total	128.6044

Procedure:

- Add 8.41g of modified Kaolin clay with 5.4252g sodium hydroxide and fused and crushed in powder form. 76.5429g of water is added to powder.
- Dispersed drop wise 39.4487g sodium silicate solution in above mixture and stir moderately for at least 20 min.

-_

APPENDIX–C

Research publications

&

Conferences

Journal of the Indian Chemical Society 98 (2021) 100246

Contents lists available at ScienceDirect

Journal of the Indian Chemical Society

journal homepage: www.editorialmanager.com/JINCS/default.aspx

Zeolite Y from kaolin clay of Kachchh, India: Synthesis, characterization and catalytic application

Dolly Gandhi [a,*], Rajib Bandyopadhyay [b], Bhavna Soni [c]

[a] Department of Chemical Engineering, Vishwakarma Government Engineering College, 382424, India and Gujarat Technological University, Ahmedabad, India
[b] Department of Chemistry, School of Technology, Pandit Deendayal Energy University, Gandhinagar, 382007, India
[c] Department of Chemical Engineering, SAL College of Engineering, Ahmedabad, 380060, India

ARTICLE INFO

Keywords:
Zeolite Y
Kaolin clay
Hydrothermal synthesis
Catalyst
Fluid catalytic cracking

ABSTRACT

Kaolin clay obtained from Kachchh, Gujarat was used as alumina and silica source to synthesize zeolite Y by hydrothermal method. The synthesis route comprised of the following steps: sulfuric acid treatment at 110 °C (4 h) for impurity removal followed by calcination at 600 °C for 4 h, thermal activation of kaolin into metakaolin by NaOH fusion at 850 °C (8 h); aging of reaction mixtures at 50 °C (24 h); crystallization (24 h) followed by washing and drying. The synthesized zeolite Y was examined by multiple characterization techniques which revealed a pore volume of 0.22 cm^3/g with pore size of 2.89 nm having essential surface area of 320 m^2/g, indicating a porous material having majority of micropores and remaining mesopores. The zeolite exhibited good catalytic activity for succinic acid esterification using ethanol to produce monoethyl and diethyl succinate. The conversion of SA (72%) and yield (60%) of valuable diester indicated good conversion rate and selectivity at moderate reaction conditions. Detailed structural comparison with zeolite Y synthesized using standard chemical route is also carried out. This work demonstrated an effective way of preparing environmentally benign porous zeolite Y having high surface area and pore volume that can be useful for catalytic applications.

1. Introduction

The district of Kachchh in Gujarat, India is endowed with huge reserves of minerals like Lignite, Gypsum, Bauxite, Kaolin, Bentonite etc. Of these, kaolin clay or China clay which mainly comprises of kaolinite ($Al_2Si_2O_5(OH)_4$) is commercially valuable as it is inexpensive and has numerous applications owing to its favorable properties. Kaolinite, a 1:1 structurally layered mineral comprised of silica (SiO_4) tetrahedral sheet and alumina (AlO_6) octahedral sheet has the required SiO_2/Al_2O_3 ratio which makes the kaolin clay a desirable and low-priced raw material for synthesis of zeolites. This clay can withstand physico-chemical treatments, even under strong acid and alkali conditions which make it easy to transform. Hence, kaolin clay is gaining importance and becoming a valuable raw material to synthesize zeolites for application as adsorbents, ion-exchangers, catalysts and components of catalyst [1]. As natural zeolites possess inherent disadvantages like presence of impurities, inconsistent pore size and low cation exchange capacity, they are not preferred for critical catalytic application where product consistency is important. Compared to natural zeolites, synthetic zeolites are favored as catalysts owing to high purity of the crystalline products and uniformity in the particle size [2]. Out of all the zeolites, zeolite Y which falls under faujasite class of zeolites has gained importance as catalyst. Zeolite Y has faujasite (FAU) framework structure, having an internally connected complex network of micropores. The pores, which are formed by 12 Si or Al atoms which are linked through O atoms forming a tetrahedral structure. The pores have a moderately large diameter of 7.4 Å forming a porous structure. 10 sodalite cages surround the inner cavity with diameter of 12 Å. The unit cell of the zeolite has a cubic structure having high thermal stability and good Brønsted acidity [3,4]. Due to the porous structure with large void space and interconnectivity, large sized molecules can easily access the interior active sites resulting in high reaction rates and enhanced selectivity. The catalytic activity depends on the strong network of macropores and mesopores for mass transfer from the surface of the crystal to the internal mesopores for subsequent diffusion into the micropores where reaction occurs [5,6]. However, to synthesize zeolite Y with proper hierarchical structure with required mesoporosity simultaneously maintaining its crystallinity is still a challenge [7]. Hence, this hierarchical structure is generated synthetically by various forms of acid treatment or a combination of acid and base treatment. Zeolites find important strategic applications in the petroleum refining and

* Corresponding author.
E-mail address: drgandhi@vgecg.ac.in (D. Gandhi).

https://doi.org/10.1016/j.jics.2021.100246
Received 12 September 2021; Received in revised form 24 October 2021; Accepted 4 November 2021

ARTICLE IN PRESS

Materials Today: Proceedings xxx (xxxx) xxx

Contents lists available at ScienceDirect

Materials Today: Proceedings

journal homepage: www.elsevier.com/locate/matpr

Naturally occurring bentonite clay: Structural augmentation, characterization and application as catalyst

Dolly Gandhi [a,b,*], Rajib Bandyopadhyay [c], Bhavna Soni [d]

[a] Department of Chemical Engineering,Vishwakarma Government Engineering College, Ahmedabad 382424, India
[b] Gujarat Technological University, Ahmedabad, India
[c] Department of Chemistry, School of Technology, Pandit Deendayal Energy University, Gandhinagar 382007, India
[d] Department of Chemical Engineering, SAL College of Engineering, Ahmedabad 380060, India

ARTICLE INFO

Article history:
Available online xxxx

Keywords:
Bentonite clay
Acid activation
Characterization
Low cost catalyst
Esterification

ABSTRACT

Locally available Bentonite clay is structurally augmented by acid activation to enhance the catalytic properties. Bentonite sample post beneficiation was treated with sulfuric acid followed by calcination. The structural augmentation of the acid-treated bentonite was examined by characterization techniques comprising of XRF, FTIR, XRD, DTA, SEM and BET. Detailed characterization revealed substantial removal of metal oxides along with structural water causing significant structural disorderliness resulting in amorphous structure. Disaggregation and reduction in magnitude of the clay structure resulted in a highly porous structure with improved silica-alumina ratio (4.08) combined with increased pore volume (0.113 cm^3/g) and surface area (305.56 m^2/g). The bentonite clay after acid activation was used as a catalyst for diester preparation using succinic acid and ethanol. The conversion of succinic acid was 62% with high yield (73%) of valuable diester demonstrating high activity and selectivity. It was confirmed that acid treatment is an economical (~ $400/t) and effective way of preparing environmentally benign porous activated clay having high surface area, pore volume and mesoporosity that can be applied as catalyst, adsorbent, catalyst support and high grade, low cost base material for zeolite synthesis.

Selection and peer-review under responsibility of the scientific committee of the International Symposium on Materials of the Millennium: Emerging Trends and Future Prospects.

1. Introduction

Bentonite clay is available in abundance in the Kachchh region in Gujarat, India with an estimated reserve of 144 million tons [1]. The reserves are rich in both sodium and calcium based bentonite. Bentonite clay is industrially valued due to its favorable physico-chemical properties such as high plasticity, lubricity, dry bonding strength, shear and compressive strength and low permeability and compressibility. These makes it extremely suitable for variety of applications such as drilling fluid for mining activities, foundry sand binding, iron ore pelletization, water proofing and sealing agent, etc. However, additional positive textural properties like high specific surface area and pore volume, highly organized layered structure, excellent cation exchange capacity coupled with chemical and mechanical stability makes bentonite clay appropriate for application as catalyst as well as adsorbents in a wide range of chemical process industries [2–6]. Being a green, nontoxic and low-cost raw material, additional treatment of raw bentonite clay can modify the structure of clay and augment the required textural properties making it a valuable material for catalytic and adsorbent applications. The structural transformation and properties modification can be done by different treatment methods like chemical activation, mechano-chemical activation, intercalation, thermo-chemical activation etc [7]. Other advanced methods like ultrasonic irradiation [8,9] and microwave irradiation [10–12] for structural enhancement are also reported in literature. Acid treatment of clay creates more acidic sites along with greater surface areas compared to the pristine clay which is promising for application as a catalyst [13]. Greater emphasis on green catalysis makes acid activated bentonite clay a potential candidate for environmental friendly applications. Acid activated and ion exchanged bentonite clay based designer catalysts are suitable for organic synthesis. Moreover, impregnation of the acidified bentonite clay with additives like Lewis or Brønsted acid compounds, pure metals and/or

* Corresponding author.
E-mail address: dollydutta.75@gmail.com (D. Gandhi).

https://doi.org/10.1016/j.matpr.2022.02.346
2214-7853/
Selection and peer-review under responsibility of the scientific committee of the International Symposium on Materials of the Millennium: Emerging Trends and Future Prospects.

Please cite this article as: D. Gandhi, R. Bandyopadhyay and B. Soni, Naturally occurring bentonite clay: Structural augmentation, characterization and application as catalyst, Materials Today: Proceedings, https://doi.org/10.1016/j.matpr.2022.02.346

INDIAN CHEMICAL ENGINEER
https://doi.org/10.1080/00194506.2020.1828191

Structural and composition enhancement of Indian Kachchh kaolin clay: characterisation and application as low-cost catalyst

Dolly Gandhi[a,b], Rajib Bandyopadhyay[c] and Sachin Parikh[d]

[a]Department of Chemical Engineering, Vishwakarma Government Engineering College, Ahmedabad, India; [b]Gujarat Technological University, Ahmedabad, India; [c]Department of Science, School of Technology, Pandit Deendayal Petroleum University, Gandhinagar, India; [d]Department of Chemical Engineering, L. D. College of Engineering, Ahmedabad, India

ABSTRACT

The effect of acid treatment on kaolin clay from the Kachchh region of Gujarat, India, was explored to prepare a low-cost (−$0.6/kg) catalyst. The clay was treated with 10 M H_2SO_4 which increased the Si/Al ratio from 1.3 to 2.4, surface area from 10.322 to 54.193 m^2/g and pore volume from 0.041 to 0.152 cm^3/g. The XRF analysis indicated that the metal oxides in treated clay decreased with increasing acid strength; consequently increasing the SiO_2 content. SEM micrographs displayed gradual disaggregation and decrease in the size of clay structure with an increase in acid strength. TG-DTA study confirmed the removal of structural water. FTIR and X-ray diffraction analysis indicated metal removal creating a large degree of structural disorder resulting in reduced crystallinity and leading towards the amorphous phase. BET study confirmed the formation of additional mesopores. The acid-treated clay was applied as a catalyst for the esterification of succinic acid (SA) with ethanol. The conversion of SA increased from 27% to 56% revealing higher activity and selectivity in terms of higher yield (96%) of valuable diester. The catalyst was reused up to three cycles with a slight loss of catalytic activity.

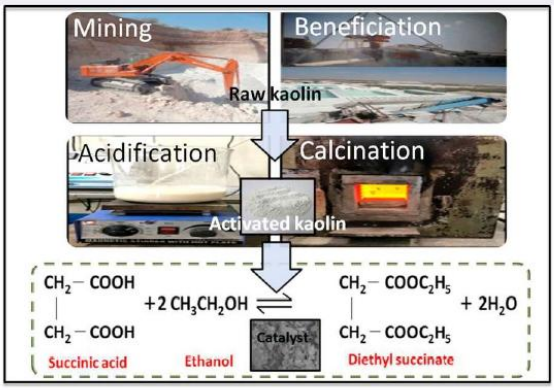

KEYWORDS
Kaolin clay; beneficiation; sulphuric acid; low-cost catalyst; esterification

CONTACT Dolly Gandhi drgandhi@vgecg.ac.in Department of Chemical Engineering, Vishwakarma Government Engineering College, 382424 Ahmedabad, India; Gujarat Technological University, Ahmedabad, India

The Institution of Engineers (India)
GUJARAT STATE CENTRE
Under the Aegis of Chemical Engineering Division Board, IEI

In collaboration with

Gujarat Narmada Valley Fertilizers & Chemicals Ltd.

GUJARAT STATE FERTILIZERS & CHEMICALS LTD.

In association with

Committee on Information and Communication Technology (ICT)

FEISCA Federation of Engineering Institution of South Central Asia (FEISCA)

Certificate

International Conference
(Part of Centenary Celebration)
on

"Paradigm shift in Chemical engineering education, processes and technology"

September 16-17, 2017, Ahmedabad

This is to certify that

Mr./Ms./Prof./Dr. DOLLY RAJNIKANT GANDHI

of V. G. E. C., Chandkheda has attended the

International Conference on

"Paradigm Shift in Chemical Engineering Education,

Processes and Technology" organized by

Institution of Engineers (India),

Gujarat State Centre (Chemical Division Board), Ahmedabad

and presented a paper

which has been published in the proceedings released on this occasion .

Er. S. B. Vasava
Chairman

Er. H. U. Kalyani
Hon. Secretary

UPES
UNIVERSITY WITH A PURPOSE

INTERNATIONAL CONFERENCE ON
ADVANCES IN CHEMICAL ENGINEERING-2020 (AdChE-2020)

Certificate of Participation

This is to certify that

Dolly Gandhi

has presented a Paper titled

Exploring the potential of acid treated Bentonite clay for various Catalytic applications

under the theme

Chemical Reaction and Reactor Engineering

at the **"International Conference on Advances in Chemical Engineering-2020 (AdChE-2020)"**

organized by the **Department of Chemical Engineering, UPES, Dehradun, India**

between February 5-7, 2020.

Dr. P. VIJAY
Convener, AdChE-2020

SERB INDIA

UPES UNIVERSITY WITH A PURPOSE | RESEARCH & DEVELOPMENT

SSRN

Dr. J.K. PANDEY
Convener, AdChE-2020

SOT
SCHOOL OF TECHNOLOGY

PDEU
PANDIT DEENDAYAL ENERGY UNIVERSITY
Formerly Pandit Deendayal Petroleum University (PDPU)

CERTIFICATE OF PARTICIPATION

This certificate is awarded to

Ms. Dolly Gandhi

for poster presentation at

"INTERNATIONAL SYMPOSIUM ON MATERIALS OF THE MILLENNIUM: EMERGING TRENDS AND FUTURE PROSPECTS (MMETFP-2021)"

held at

School of Technology, Pandit Deendayal Energy University, Gujarat on November 19-21, 2021.

Prof. Rajib Bandyopadhyay
Chairman, MMETFP-2021
Head, Dept. of Chemistry, PDEU

Prof. A.R. Jani
Chairman, MMETFP-2021
Chairman, MRSI Gujarat Chapter

Dr. Kalisadhan Mukherjee
Convener MMETFP-2021
Dept. of Chemistry, PDEU

Organized by

DEPARTMENT OF CHEMISTRY & PHYSICS, SCHOOL OF TECHNOLOGY
PANDIT DEENDAYAL ENERGY UNIVERSITY, GANDHINAGAR, GUJARAT, INDIA
in collaboration with
MATERIALS RESEARCH SOCIETY OF INDIA (MRSI)